

Quivers as Calculators: Counting, Correlators and Riemann Surfaces

Jurgis Pasukonis¹ and Sanjaye Ramgoolam²

School of Physics and Astronomy
Queen Mary, University of London
Mile End Road
London E1 4NS UK

Abstract

The spectrum of chiral operators in supersymmetric quiver gauge theories is typically much larger in the free limit, where the superpotential terms vanish. We find that the finite N counting of operators in any free quiver theory, with a product of unitary gauge groups, can be described by associating Young diagrams and Littlewood-Richardson multiplicities to a simple modification of the quiver, which we call the split-node quiver. The large N limit leads to a surprisingly simple infinite product formula for counting gauge invariant operators, valid for any quiver with bifundamental fields. An orthogonal basis for the operators, in the finite N CFT inner product, is given in terms of *quiver characters*. These are constructed by inserting permutations in the split-node quivers and interpreting the resulting diagrams in terms of symmetric group matrix elements and branching coefficients. The fusion coefficients in the chiral ring - valid both in the UV and in the IR - are computed at finite N . The derivation follows simple diagrammatic moves on the quiver. The large N counting and correlators are expressed in terms of topological field theories on Riemann surfaces obtained by thickening the quiver. The TFTs are based on symmetric groups and defect observables associated with subgroups play an important role. We outline the application of the free field results to the construction of BPS operators in the case of non-zero super-potential.

¹j.pasukonis@qmul.ac.uk

²s.ramgoolam@qmul.ac.uk

Contents

1	Introduction and Summary	4
2	Counting operators	10
2.1	The group integral formula	12
2.2	Infinite product generating functions	19
3	Construction of free orthogonal basis	23
3.1	Review of \mathbb{C}^3	23
3.2	Generalized restricted Schur basis	28
3.3	Two-point function	33
3.4	Covariant basis	34
3.5	Examples	36
3.5.1	Conifold	37
3.5.2	$\mathbb{C}^3/\mathbb{Z}_2$	41
3.5.3	dP_0	41
3.5.4	$\mathbb{C}^2/\mathbb{Z}_n \times \mathbb{C}$	44
4	Chiral ring structure constants	45
4.1	Restricted Schur basis	46
4.2	Covariant basis	50
5	Quivers and topological field theories on Riemann surfaces	57
5.1	S_n topological lattice gauge theory and defect operators	57
5.2	Counting, correlators and defects in S_n TFT	62
5.3	Fundamental groups, covering spaces and worldsheets	68
5.4	Young diagram basis and TFT constructions	70
6	Interacting chiral ring	71
6.1	Review of the chiral ring	71
6.2	Chiral ring from operators	74

6.3	Giant gravitons in the conifold	75
7	The case with fundamental matter	77
8	Discussion and future avenues	81
8.1	IR fixed point	81
8.2	Directions for the future	82
A	Symmetric group formulae	85
A.1	General	85
A.2	Branching coefficients	86
A.3	Clebsch-Gordan coefficients	88
A.4	Multiplicities	89
B	Quiver characters	90
B.1	Symmetric group characters	90
B.2	Restricted quiver characters	91
B.3	Covariant quiver characters	92
C	General basis from invariance	93
C.1	Review of \mathbb{C}	93
C.2	Review of \mathbb{C}^3	94
C.3	General quiver	97
D	Proofs	99
D.1	Proof of large N counting	99
D.2	Proofs of quiver character identities	100
D.3	Derivation of two-point function	104
D.4	Derivation of chiral ring structure constants	106
D.5	Finite N chiral ring with superpotential, using explicit operators	109

1 Introduction and Summary

In the AdS/CFT correspondence [1–3], the Hamiltonian for translations of the global time in the AdS side corresponds to the scaling operator on the CFT side. Classifying the states of a given energy and computing their interactions allows comparisons between the two sides. States in CFT are related to local operators through radial quantization. This paper is primarily concerned with the counting of states and computation of correlators in a large class of free theories, parametrized by quivers. A quiver is a directed graph used to describe the gauge group and matter content of the theory [4]. The nodes correspond to gauge groups which we will take to be unitary groups, so that the gauge group is $\prod_a U(N_a)$ where a is an index running over labels $\{1, 2, \dots\}$ for the nodes. Each directed edge starting from a and ending at b correspond to a bifundamental field (N_a, \bar{N}_b) transforming in the fundamental of $U(N_a)$ and anti-fundamental of $U(N_b)$. Our results show that the quiver diagram itself becomes a powerful computational tool. Counting of gauge invariant operators can be expressed using the operation of splitting each node into a pair called the plus (or incoming) node and the minus (or outgoing) node. The plus node has all the incoming lines of the original quiver and the minus node has all the outgoing line. A new line is introduced for each pair, going from plus to minus. This modified quiver is called the *split-node* quiver. In going from counting of operators to their correlators, the split-node quiver is used to define *quiver characters* which encode representation theory data associated with permutation groups and their representations. These are generalizations of symmetric group characters, parametrized by quivers, and obey analogous identities. They are constructed by inserting permutations in the split-node quiver and interpreting the resulting diagram in terms of matrix elements of permutations and branching coefficients for symmetric group reductions. This reprises the theme that there is a close connection between the counting and construction of operators, when we use the right group theoretic framework [5, 6]. The quiver diagram thus gives elegant expressions for the counting of chiral operators, the two point functions between chiral and anti-chiral operators, the chiral ring fusion coefficients, both for finite rank N_a as well as at large N_a . The combinatorial data related to counting and correlators is also shown to have an interpretation in terms topological field theories on surfaces which are obtained by thickening the quiver. At large N_a , the combinatorics can be expressed in terms of the counting of covering spaces of these surfaces.

Before explaining some of these results in more detail, we will describe some of the background to this work, with particular attention to the significance of finite N results

in AdS/CFT. The canonical example of AdS/CFT is the duality between type IIB on $AdS_5 \times S^5$ and $\mathcal{N} = 4$ SYM with $U(N)$ gauge group. The half-BPS sector of gauge theory operators contains duals to a rich variety of space-time objects including perturbative Kaluza-Klein states, giant gravitons and LLM geometries [2, 3, 7–10]. Thanks to non-renormalization theorems (see the review [11] for the references on this) the counting and extremal correlators of BPS states do not change from the zero coupling answer. The lowest weights of the half-BPS representations are holomorphic traces and products of traces of a complex matrix, such as $tr Z, tr Z^2, (tr Z)^2$. The two-point correlators between holomorphic and anti-holomorphic operators is diagonalized by Schur Polynomial operators [9]

$$\chi_R(Z) = \frac{1}{n!} \sum_{\sigma \in S_n} \chi_R(\sigma) Z_{i_{\sigma(1)}}^{i_1} \cdots Z_{i_{\sigma(n)}}^{i_n} \quad (1.1)$$

so that

$$\langle \chi_R(Z) \chi_S(Z^\dagger) \rangle = \delta_{RS} f_R \quad (1.2)$$

where R is a Young diagram with n boxes, $\chi_R(\sigma)$ is a character of the S_n group element σ in the irreducible representation (irrep) R of S_n , f_R is a polynomial in N . In the leading large N limit, the trace basis is also an orthogonal basis - this is large N factorization - but this does not hold at finite N . Finite N effects are nicely encoded in the Young diagram R , which does not have more than N rows. Giant gravitons are particularly interesting since their semiclassical properties are sensitive to finite N cutoffs [7]. The three-point functions of the Schur Polynomial operators are computed in terms of Littlewood-Richardson coefficients [12]. They have recently been tested using semiclassical methods in spacetime [13–15]. The Young diagram description of operators dual to giants forms the starting point for modifications of the operators which correspond to strings attached to giants [16].

There has been a lot of work on the extension of the dictionary between giants and operators, to the case of quarter and eighth BPS giants. The story is substantially more complicated in this case. The spectrum of BPS operators now jumps in going from zero coupling to weak coupling and is conjectured to remain unchanged from weak to strong coupling [17, 18]. At zero coupling, we have holomorphic operators constructed from two complex matrices X, Y of size N for the quarter BPS sector and three complex matrices X, Y, Z for the eighth-BPS sector (There are also additional eighth-BPS operators where the lowest weights are constructed with fermions [19], but they will not be our concern here). Diagonal bases for the free field CFT inner product on these spaces of multi-matrix gauge invariant operators at finite N have been constructed [20–23]. Not all of these

operators are annihilated by the one-loop dilatation operator [24]. These operators which get anomalous dimensions are descendants and contain commutators e.g. $[X, Y]$ [25, 26].

The correct BPS operators at weak coupling, annihilated by the 1-loop dilatation operator, can also be characterized as those that are orthogonal to the descendants in the zero-coupling inner product. This illustrates the usefulness of the zero coupling inner product for physics at weak coupling. Another remarkable example of the power of zero coupling, is that bases constructed to diagonalize the free field inner product by exploiting the enhanced symmetries of this limit [22, 27, 28], notably Brauer algebra symmetries, have been shown to give a large subset of quarter BPS operators to all orders in $1/N$ [29] with a proposed matching to states from LLM geometries [30].

The limit of zero coupling is of intrinsic interest, beyond the application to semiclassical giants at strong coupling. In this limit, there is a huge amount of data from the gauge theory Ideas for the dual string theory can be tested. Aspects related to higher spin symmetries have been explored in [31]. One approach to the construction of the dual string theories for the free limit is to follow the example of low dimensional example of two dimensional Yang Mills theory [32]. In this solvable model, the large N expansion can be computed in terms of symmetric groups and a topological string model can be derived. Much the same strategy can be applied to study the combinatoric aspects of correlators in the free limit of CFTs in any dimension. For two and three-point functions, the space-time dependence is determined by conformal invariance, so all the non-triviality is in this combinatorics. In the simplest case of half-BPS operators, it is indeed known [9, 33, 34] that two point functions are related to Belyi maps (holomorphic maps with three branch points) with sphere as target space. In this paper, we will find a generalization of this fact to any free quiver gauge theory, where the target space is constructed by starting with a thickening of the quiver to a surface, and then cutting the surface to insert some conditions on the monodromies of branched covers over the cuts (see section 5). A version of the connection between correlators and Belyi maps also holds for hermitian Matrix models (involving so-called clean Belyi maps) [34]. This has been used to relate hermitian Matrix Model correlators to the A -model topological string with \mathbb{P}^1 target [35].

Beyond the standard example of AdS/CFT which involves the near-horizon geometry of branes at a point in \mathbb{C}^3 , there are several closely related generalizations. One infinite class comes from orbifolds [36]. An infinite class comes from toric non-compact Calabi-Yaus, which may not be orbifolds [37]. Among the examples we will use to illustrate the general counting and correlator formulae, we will use a \mathbb{C}^3/Z_2 orbifold and a \mathbb{C}^3/Z_3 orbifold. As a simple example of toric CY we will use the conifold, where the AdS/CFT dictionary was

established in [38]. The combinatorics of free field correlators in the conifold theory is the same as in the ABJM model [39], where calculations using Young diagram techniques have been studied in [40]. It should be noted that our results apply to the free field limit of any quiver, even those which are not related to conformal field theories in the infrared. If the theory is asymptotically free, the free limit is the same as the deep UV limit, so this is a restriction that may be useful to keep in mind. We focus on the correlators of complex scalars, which can exist even in non-supersymmetric theories. However, the discussion is particularly meaningful for the case of $\mathcal{N} = 1$ supersymmetric theories, where these are the scalar components of a chiral superfield and the chiral gauge invariant operators form part of the chiral ring. Our results on the chiral ring of free gauge theories may be useful more generally beyond the context of ADS/CFT. For example the detailed study of chiral rings [41] was valuable in understanding connections between 4D dynamics of $\mathcal{N} = 1$ SUSY gauge theory and matrix models [42]. While the generic gauge theories have non-zero superpotential, the limit of zero superpotential is a special point of the moduli space with enhanced symmetries, which can be of higher spin type involving higher derivative currents (e.g as in [31]) or of standard type in terms of derivatives but involving the matrix structure of fields in a non-trivial way [28]). Chiral rings give the ring of functions on the vacuum moduli space and the study of this space for vanishing superpotential terms and at finite N should be of interest from a purely gauge theoretic perspective.

The key qualitative result of this paper is that the quiver diagram, which is initially introduced to describe the matter content of a gauge theory with product gauge group, comes to life as a powerful tool for the computation of counting and correlators of chiral operators. The explicit formulae in the bulk of the paper covers the cases with any number of $U(N_a)$ gauge groups and any number of bifundamentals (which includes adjoints). Section 2 starts from the known counting formula in terms of group integrals to arrive at an expression in terms of Young diagrams. Specifically the result is expressed in terms of Littlewood-Richardson (LR) coefficients, which are known to given in terms of efficient combinatoric rules for combining Young diagrams, familiar from tensor products of $U(N)$ irreps. The finite N constraints are simply $l(R_a) \leq N_a$, requiring the lengths $l(R_a)$ of the first column to be less than N . The form of the LR coefficients can be read off by a simple manipulations on the quiver diagram. The general equation is 2.12 and the diagrammatic rules are stated after the equation. The rules involve the application of a move we call *splitting-the-nodes*, the appropriateness of which is immediately visible from an inspection of the Figures 2, 3, 4. The quiver obtained by thus splitting the nodes of the quiver defining the gauge theory, is called the *split-node quiver*. When there are multiple flavours M_{ab} of

fields for the same initial and end-points of the quiver, we can organize the counting in terms of representations these flavour groups $U(M_{ab})$. This covariant counting is given in eqn. (2.22). In addition to LR coefficients, it involves the Kronecker product coefficients, which are multiplicities depending on a triple of Young diagrams all with the same number of boxes. In section 2.2 we turn to the simplifications which arise when we consider operators containing a total number of fields which is less than the N_a . This allows us to derive an infinite product generating function 2.39, of somewhat surprising simplicity, containing terms which have a simple description in terms of loops in the quiver.

In section 3 we show that the effectiveness of the quiver diagrams continues when we consider the two point functions in the quiver theory. In particular we compute the 2-point functions involving gauge-invariants constructed from holomorphic functions of the chiral matter fields inserted at one point, and anti-holomorphic operators at another point. By taking one point to zero and the other to infinity, this defines an inner product for the operators. We find, for a general quiver Q , the analogs of the equations (1.1) and (1.2).

To motivate our strategy for arriving at the quiver analogs of these, we note that permutation group characters appearing in (1.1) obey some orthogonality and invariance properties e.g. which are useful in considering the correlators of the half-BPS sector in $\mathcal{N} = 4$ SYM

$$\begin{aligned} \chi_R(\sigma) &= \chi_R(\alpha\sigma\alpha^{-1}) \\ \sum_{\sigma \in S_n} \chi_R(\sigma)\chi_S(\sigma) &= n!\delta_{RS} \end{aligned} \tag{1.3}$$

A more complete list of the identities is in Appendix B.1. For a general quiver Q , we choose integers $n_{ab} \geq 0$ for each directed edge of the quiver, which determine integers n_a for each node according to $n_a = \sum_b n_{ba} = \sum_b n_{ab}$. In addition we choose irreducible representation labels R_a of S_{n_a} for each node, i.e Young diagrams with n_a boxes (restricted to $l(R_a) \leq N$), i.e no more than N_a rows). We choose irreps r_{ab} of $S_{n_{ab}}$ for each edge. Finally ν_a^+ is a choice from the multiplicity of the irrep $\otimes_b r_{ba}$ of $\times_b S_{n_{ba}}$ in the restriction of irrep R_a of S_{n_a} to the subgroup $\times_b S_{n_{ba}}$; ν_a^- is a choice from the multiplicity of the irrep $\otimes_b r_{ab}$ of $\times_b S_{n_{ab}}$ in the restriction of irreps R_a of S_{n_a} to the subgroup $\times_b S_{n_{ab}}$. These multiplicities are given by Littlewood-Richardson coefficients. We use the label \mathbf{L} for the whole set $\{R_a, r_{ab}, \nu_a^-, \nu_a^+\}$ of representation theoretic labels. Given this data, we define *quiver characters*,

$$\chi_Q(\mathbf{L}, \sigma_a) \tag{1.4}$$

which obey analogs of the above 1.3. There is one permutation σ_a for each node. These properties are stated in equations B.10B.12B.13 and proved in Appendix D.2. The standard

symmetric group identities can be viewed as a special case of these quiver character identities, when the quiver consists of one edge connecting a node to itself. This simple quiver is the one relevant to the half-BPS sector of $N = 4$ SYM.

The quiver characters are written in terms of matrix elements of the permutations σ_a in irreps R_a , contracted with branching coefficients of symmetric groups. In terms of split-node quiver, the formulae for the quiver characters can be written down by inserting the σ_a in the lines introduced in the splitting of the nodes, which join the ν_a^+ node to the ν_a^- node. Branching coefficients are associated with these nodes. The contractions of these branching coefficients and matrix elements are most clearly understood by looking at a few examples. We recommend to the reader a casual look at Figures 3.17, 3.70, 3.49 which are relevant for $\mathbb{C}^3, \mathcal{C}, \mathbb{C}^3/Z_2$ respectively, before delving into the detailed formulae for the quiver characters. The precise rules for associating formulae to these diagrams are explained in Section 3 and Appendix A.

Bases diagonalizing the CFT inner product for chiral operators are not unique. This is well known already in studies of the eighth-BPS sector of $\mathcal{N} = 4$ SYM. We have the restricted Schur basis, where there are Young diagram labels for each type of chiral field. This basis is not covariant under the global symmetries mixing the different types of arrows with the same start and end points. The basis described above, labelled by \mathbf{L} is the generalization to any quiver of the restricted Schur basis. We will, not surprisingly, call it the restricted Schur basis for general quivers. We also develop the covariant basis for general quivers. There are again generalized characters for any quiver Q , with representation labels \mathbf{K} . Analogous character identities are derived and used to prove the orthogonality of the corresponding operators.

Section 4 gives the structure constants of the chiral ring both in the restricted Schur basis and the covariant basis. The Littlewood-Richardson coefficients

$$g(R_1, R_2, R_3) = \frac{1}{n_1! n_2!} \sum_{\sigma_1 \in S_{n_1}} \sum_{\sigma_2 \in S_{n_2}} \chi_{R_1}(\sigma_1) \chi_{R_2}(\sigma_2) \chi_{R_3}(\sigma_1 \circ \sigma_2) \quad (1.5)$$

have a generalization

$$g^Q(\mathbf{L}^{(1)}, \mathbf{L}^{(2)}, \mathbf{L}^{(3)}) = \sum_{\sigma_1, \sigma_2} \chi_Q(\mathbf{L}^{(1)}, \sigma^{(1)}) \chi_Q(\mathbf{L}^{(2)}, \sigma^{(2)}) \chi^Q(\mathbf{L}^{(3)}, \sigma^{(1)} \circ \sigma^{(2)}) \quad (1.6)$$

These are the chiral ring structure constants for the free quiver theories. By studying these structure constants, we obtain selection rules for the r_{ab}, R_a in the restricted Schur basis, as stated in equation (4.13). The result is expressed in a factorized form : there is a product over the gauge groups, and for each gauge group there is product with the ν^+

and ν^- multiplicity labels appearing in separate factors (see equation 4.11). Analogous selection rules are derived for the covariant basis (4.24). There is a factorization over the gauge groups with ν^- labels again separated from ν^+ factors, while there are also factors for the directed edges (4.27). Even for the case of \mathbb{C}^3 , all these selection rules controlling the chiral ring structure constants at finite N have not been made explicit before.

Section 5 observes that the counting and correlators of the gauge invariant operators can be interpreted in terms of observables in topological field theory on Riemann surfaces, with S_n gauge group. The integer n depends on the $n_{ab;\alpha}$. The Riemann surface is obtained by thickening the quiver. See Figures 20, 22, 24 for the Riemann surfaces arising in the case of $\mathbb{C}^3, \mathcal{C}, \mathbb{C}^3/\mathbb{Z}_2$ respectively. The S_n topological field theory on the thickened quiver is related to counting of covers of this Riemann surface. The covering spaces can be interpreted as string worldsheets following an analogous logic which lead to the development of the string theory of large N two dimensional Yang Mills [32]. It will be interesting to clarify the role of this thickened quiver Riemann surface in the context of Sasaki-Einstein geometries arising in AdS/CFT for quiver gauge theories in the toric cases [37].

Section 6 explains how the results on free chiral operators developed here can be used to approach the construction of the chiral ring when a non-zero superpotential is turned on. This allows us to make some comments on our original motivating interest, the connection between giant gravitons and operators. Section 7 starts the discussion of how to extend the results for general theories with bi-fundamental fields (which may include adjoints), to the case where there are fundamentals or anti-fundamentals. For the case of SQCD, we describe counting formulae in terms of Young diagrams, making contact with recent literature, and we give a corresponding orthogonal basis of operators. Restricting for concreteness to the conifold case, Section 8.1 recalls the difference between the UV and IR fixed points (both in the limit of zero super-potential) and explains the fact that the chiral ring structure constants calculated at the free UV fixed point are the same as at the IR fixed point with vanishing superpotential. This section concludes with some avenues for future research.

2 Counting operators

In this section we derive counting formulas for chiral gauge invariant operators in a general quiver gauge theory. We find that counting is neatly expressed in terms of the *split-node quiver*, which is a simple modification of the quiver diagram, with Young diagram labels on the edges, and Littlewood-Richardson multiplicities associated with the nodes. In the case

of the covariant basis, we will also need Kronecker product multiplicities for the symmetric groups.

An $\mathcal{N} = 1$ supersymmetric quiver gauge theory is defined by a directed graph, called quiver, a gauge group factor associated to each quiver node, and a superpotential. For most of this paper we consider a free theory, with vanishing superpotential. We take the gauge group to be $\prod_{a=1}^G U(N_a)$, where a runs over G nodes. Each arrow in the quiver between nodes a and b denotes a chiral multiplet transforming as (N_a, \bar{N}_b) . We denote the number of directed arrows from a to b by M_{ab} . The free theory has a global symmetry $\prod_{a,b} U(M_{ab})$. The full matter content is denoted by

$$\Phi = \{ \Phi_{ab;\alpha} : \alpha \in \{1, \dots, M_{ab}\} \} \quad (2.1)$$

An example that we will often use is the quiver for $\mathbb{C}^3/\mathbb{Z}_2$ theory, with a gauge group generalized to $U(N_1) \times U(N_2)$ shown in Figure 1. It is rich enough to demonstrate the different ingredients we will need to deal with the most general quiver.

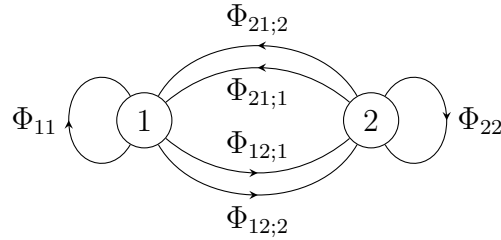


Figure 1: $\mathbb{C}^3/\mathbb{Z}_2$ quiver

Here we consider counting of chiral gauge invariant operators, such as, for the $\mathbb{C}^3/\mathbb{Z}_2$ example:

$$\text{tr}(\Phi_{11}\Phi_{11}), \text{tr}(\Phi_{12;1}\Phi_{21;2}), \text{tr}(\Phi_{11}\Phi_{12;1}\Phi_{22}\Phi_{21;1}), \dots \quad (2.2)$$

graded by the number of times $\{n_{ab;\alpha}\}$ each field appears in the operator. The numbers $n_{ab;\alpha}$ determine the numbers of indices in the fundamental and anti-fundamental of each gauge group $U(N_a)$. These have to be equal by gauge invariance and they are denoted by n_a

$$n_a = \sum_b \sum_{\alpha=1}^{M_{ba}} n_{ba;\alpha} = \sum_b \sum_{\alpha=1}^{M_{ab}} n_{ab;\alpha} \quad (2.3)$$

Note that in the limit $N_a \rightarrow \infty$ gauge invariant operators are in one-to-one correspondence with closed cycles in the quiver, but for finite N_a there are non-trivial identifications

between operators. In Section 2.1 we use group integral formula to directly derive finite N_a results, which will be our main focus in this paper. Furthermore, in Section 2.2 we also show how in the $N_a \rightarrow \infty$ limit our results lead to particularly nice formulas for counting closed cycles in a directed graph.

2.1 The group integral formula

There is a group integral formula for the counting of gauge-invariant operators [43–46]. It has been useful in the context of computation of indices recently. We will use the group integral formula to show that the finite N counting can be expressed in terms of Young diagrams R_a at the nodes with n_a boxes (i.e. $R_a \vdash n_a$), $r_{ab;\alpha} \vdash n_{ab;\alpha}$ at the edges and Littlewood-Richardson coefficients $\prod_a g(\cup_{b,\alpha} r_{ab;\alpha}; R_a) g(\cup_{b,\alpha} r_{ba;\alpha}; R_a)$ at the edges. The index α always appears on symbols carrying subscripts a, b which run over the pairs of gauge groups and range over $1 \leq \alpha \leq M_{ab}$. When $M_{ab} = 0$, all symbols carrying the corresponding α are dropped from the formulae.

The partition function for counting operators in any quiver is:

$$\mathcal{N}(\{t_{ab;\alpha}\}; \{N_a\}, \{M_{ab}\}) = \int \prod_a dU_a \quad e^{\sum_n \sum_{a,b,\alpha} \frac{(t_{ab;\alpha})^n}{n} \text{tr} U_a^n \text{tr} (U_b^\dagger)^n} \quad (2.4)$$

where $t_{ab;\alpha}$ are fugacities associated with $n_{ab;\alpha}$. That is, if $\mathcal{N}(\{n_{ab;\alpha}\}; \{N_a\}, \{M_{ab}\})$ is the number of operators with charges $\{n_{ab;\alpha}\}$ then the partition function is

$$\mathcal{N}(\{t_{ab;\alpha}\}; \{N_a\}, \{M_{ab}\}) \equiv \sum_{\{n_{ab;\alpha}\}} \left(\prod_{a,b,\alpha} (t_{ab;\alpha})^{n_{ab;\alpha}} \right) \mathcal{N}(\{n_{ab;\alpha}\}; \{N_a\}, \{M_{ab}\}) \quad (2.5)$$

We will henceforth write \int for $\int \prod_a dU_a$. Writing the exponential as a product and

expanding in series

$$\begin{aligned}
& \mathcal{N}(\{t_{ab;\alpha}\}; \{N_a\}, \{M_{ab}\}) \\
&= \sum_{\{k_{ab;\alpha}^{(n)}\}=0}^{\infty} \int \prod_{a,b,\alpha,n} (t_{ab;\alpha})^{nk_{ab;\alpha}^{(n)}} \frac{(\text{tr } U_a^n)^{k_{ab;\alpha}^{(n)}} (\text{tr } U_b^\dagger)^{k_{ab;\alpha}^{(n)}}}{n^{k_{ab;\alpha}^{(n)}} k_{ab;\alpha}^{(n)}!} \\
&= \int \sum_{\{k_{ab;\alpha}^{(n)}\}=0}^{\infty} \prod_{a,b,\alpha} (t_{ab;\alpha})^{\sum_n nk_{ab;\alpha}^{(n)}} \prod_n \prod_{a,b,\alpha} \frac{(\text{tr } U_a^n)^{k_{ab;\alpha}^{(n)}} (\text{tr } U_b^\dagger)^{k_{ab;\alpha}^{(n)}}}{n^{k_{ab;\alpha}^{(n)}} k_{ab;\alpha}^{(n)}!} \quad (2.6) \\
&= \int \sum_{\{n_{ab;\alpha}\}=0}^{\infty} \prod_{a,b,\alpha} \frac{(t_{ab;\alpha})^{n_{ab;\alpha}}}{n_{ab;\alpha}!} \\
&\quad \times \sum_{\sigma_{ab;\alpha} \in S_{n_{ab;\alpha}}} \prod_a \sum_{R_a \vdash n_a} \chi_{R_a}(\cup_{b,\alpha} \sigma_{ab;\alpha}) \chi_{R_a}(U_a) \sum_{S_a \vdash n_a} \chi_{S_a}(\cup_{b,\alpha} \sigma_{ba;\alpha}) \chi_{S_a}(U_a^\dagger)
\end{aligned}$$

We have factored the powers $(t_{ab;\alpha})^{n_{ab;\alpha}}$, recognized that for fixed $n_{ab;\alpha}$, the sums over $k_{ab;\alpha}^{(n)}$ run over partitions of $n_{ab;\alpha}$, which correspond to conjugacy classes in $S_{n_{ab;\alpha}}$. We observe that

$$\prod_n \prod_{a,b,\alpha} (\text{tr } U_a^n)^{k_{ab;\alpha}^{(n)}} = \sum_{\substack{R_a \vdash n_a \\ l(R_a) \leq N_a}} \chi_{R_a}(\cup_{a,b,\alpha} \sigma_{ab;\alpha}) \chi_{R_a}(U_a) \quad (2.7)$$

for $\sigma_{ab;\alpha}$ being a permutation in the conjugacy class of $n_{ab;\alpha}$ specified by $k_{ab;\alpha}^{(n)}$. Since the number of permutations in the specified conjugacy class is precisely

$$\frac{n_{ab;\alpha}!}{\prod_n n^{k_{ab;\alpha}^{(n)}} k_{ab;\alpha}^{(n)}!} \quad (2.8)$$

we have converted the sums over partitions to sums over permutations. We have also recognized that the traces can be expanded in terms of Schur Polynomials with coefficients given by the characters of these permutations. Note, crucially, the height of the Young diagram R_a is at most N_a , this fully captures the effect of finite N_a . Using the orthogonality of the Schur Polynomials under group integration

$$\int dU_a \chi_{R_a}(U_a) \chi_{S_a}(U_a^\dagger) = \delta_{R_a S_a} \quad (2.9)$$

we can expand characters in irreps R_a of S_{n_a} into characters of $\prod_{b,\alpha} r_{ab;\alpha}$ with expansion coefficients which are Littlewood-Richardson numbers

$$\chi_{R_a}(\cup_{b,\alpha} \sigma_{ab;\alpha}) = \sum_{r_{ab;\alpha} \vdash n_{ab;\alpha}} g(\cup_{b,\alpha} r_{ab;\alpha}; R_a) \prod_{b,\alpha} \chi_{r_{ab;\alpha}}(\sigma_{ab;\alpha}) \quad (2.10)$$

This leads to

$$\begin{aligned}
& \mathcal{N}(\{t_{ab;\alpha}\}; \{N_a\}, \{M_{ab}\}) \\
&= \sum_{\{n_{ab;\alpha}\}} \prod_{a,b,\alpha} \frac{(t_{ab;\alpha})^{n_{ab;\alpha}}}{n_{ab;\alpha}!} \sum_{\sigma_{ab;\alpha} \in S_{n_{ab;\alpha}}} \sum_{\substack{R_a \vdash n_a \\ l(R_a) \leq N_a}} \sum_{r_{ab;\alpha} \vdash n_{ab;\alpha}} \sum_{s_{ab;\alpha} \vdash n_{ab;\alpha}} \\
& \quad \prod_a g(\cup_{b,\alpha} r_{ab;\alpha}; R_a) g(\cup_{b,\alpha} s_{ba;\alpha}; R_a) \prod_{a,b,\alpha} \chi_{r_{ab;\alpha}}(\sigma_{ab;\alpha}) \chi_{s_{ab;\alpha}}(\sigma_{ab;\alpha}) \\
&= \sum_{\{n_{ab;\alpha}\}} \prod_{a,b,\alpha} (t_{ab;\alpha})^{n_{ab;\alpha}} \sum_{\substack{R_a \vdash n_a \\ l(R_a) \leq N_a}} \sum_{r_{ab;\alpha} \vdash n_{ab;\alpha}} \prod_a g(\cup_{b,\alpha} r_{ab;\alpha}; R_a) g(\cup_{b,\alpha} r_{ba;\alpha}; R_a)
\end{aligned} \tag{2.11}$$

In the second line we used orthogonality of characters $\sum_{\sigma} \chi_r(\sigma) \chi_s(\sigma) = n! \delta_{rs}$. This form of the partition function, comparing with (2.5), gives explicit counting for each choice of charges $\{n_{ab;\alpha}\}$

$$\boxed{\mathcal{N}(\{n_{ab;\alpha}\}; \{N_a\}, \{M_{ab}\}) = \sum_{\substack{R_a \vdash n_a \\ l(R_a) \leq N_a}} \sum_{r_{ab;\alpha} \vdash n_{ab;\alpha}} \prod_a g(\cup_{b,\alpha} r_{ab;\alpha}; R_a) g(\cup_{b,\alpha} r_{ba;\alpha}; R_a)} \tag{2.12}$$

There is a simple diagrammatic description of this formula, deriving directly from the quiver itself:

Diagrammatic Rules for counting local operators in the quiver theory

- Choose integers $n_{ab;\alpha} \geq 0$ for all the edges of the quiver Q , subject to $n_a = \sum_b n_{ba}$.
- Replace each node with a pair of nodes, joined by a line labelled by a Young diagram R_a with n_a boxes. One of these two nodes, called the plus node, has all incoming lines and the other, called the minus node, has all outgoing lines. The resulting diagram is the *split-mode quiver*.
- To all the previously existing edges, attach Young diagrams $r_{ab;\alpha}$ with $n_{ab;\alpha}$ boxes.
- To each minus node attach a Littlewood-Richardson multiplicity $g(\cup_b \cup_{\alpha=1}^{M_{ab}} r_{ab;\alpha}; R_a)$ which couples all the incoming lines to R_a . To each plus node attach the LR multiplicity $g(\cup_b \cup_{\alpha=1}^{M_{ba}} r_{ba;\alpha}; R_a)$
- Take the product of LR-coefficients over all the nodes. This is the counting of free chiral operators with numbers $\{n_{ba;\alpha}\}$ of fields of type α transforming as (N_a, \bar{N}_b) .

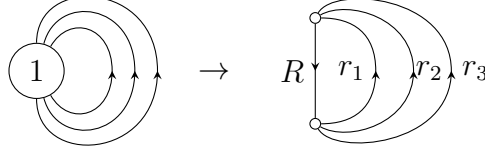


Figure 2: Split-node quiver for \mathbb{C}^3 .

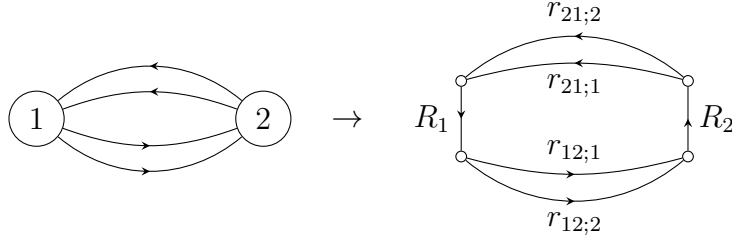


Figure 3: Split-node quiver for the conifold.

These steps are illustrated for \mathbb{C}^3 in Figure 2. We have suppressed the a, b indices labeling the nodes of the quiver, since there is only one node in this case.

$$\mathcal{N}_{\mathbb{C}^3}(n_1, n_2, n_3; N) = \sum_{\substack{R \vdash n \\ l(R) \leq N}} g(r_1, r_2, r_3; R) g(r_1, r_2, r_3; R) \quad (2.13)$$

This equation was given in [23, 47]. For \mathcal{C} , we read off the counting from (2.12) or by following the steps in Figure 3.

$$\begin{aligned} \mathcal{N}_{\mathcal{C}}(n_{12;1}, n_{12;2}, n_{21;1}, n_{21;2}; N_1, N_2) &= \sum_{\substack{R_1 \vdash n_1 \\ l(R_1) \leq N_1}} \sum_{\substack{R_2 \vdash n_2 \\ l(R_2) \leq N_2}} \sum_{r_{12;1} \vdash n_{12;1}} \sum_{r_{12;2} \vdash n_{12;2}} \sum_{r_{21;1} \vdash n_{21;1}} \sum_{r_{21;2} \vdash n_{21;2}} \\ &g(r_{12;1}, r_{12;2}; R_1) g(r_{12;1}, r_{12;2}; R_2) g(r_{21;1}, r_{21;2}; R_1) g(r_{21;1}, r_{21;2}; R_2) \end{aligned} \quad (2.14)$$

This counting for the free conifold operators has not been given before. For $\mathbb{C}^3/\mathbb{Z}_2$, again following the steps above shown in Figure 4 or specializing (2.12), we get

$$\begin{aligned} \mathcal{N}_{\mathbb{C}^3/\mathbb{Z}_2}(n_{11}, n_{22}, n_{12;1}, n_{12;2}, n_{21;1}, n_{21;2}; N_1, N_2) \\ = \sum_{\substack{R_1 \vdash n_1 \\ l(R_1) \leq N_1}} \sum_{\substack{R_2 \vdash n_2 \\ l(R_2) \leq N_2}} \sum_{r_{11} \vdash n_{11}} \sum_{r_{22} \vdash n_{22}} \sum_{r_{12;1} \vdash n_{12;1}} \sum_{r_{12;2} \vdash n_{12;2}} \sum_{r_{21;1} \vdash n_{21;1}} \sum_{r_{21;2} \vdash n_{21;2}} \\ g(r_{11}, r_{12;1}, r_{12;2}; R_1) g(r_{22}, r_{12;1}, r_{12;2}; R_2) g(r_{11}, r_{21;1}, r_{21;2}; R_1) g(r_{22}, r_{21;1}, r_{21;2}; R_2) \end{aligned} \quad (2.15)$$

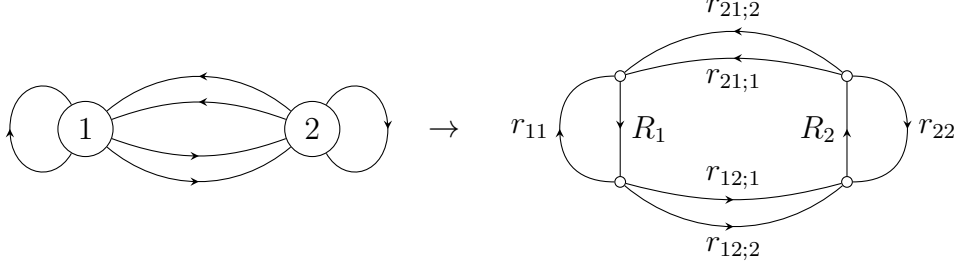


Figure 4: Split-node quiver for $\mathbb{C}^3/\mathbb{Z}_2$.

There is another useful form of the counting formula where we do not specify $\{n_{ab;\alpha}\}$ but only $\{n_{ab}\}$

$$n_{ab} = \sum_{\alpha} n_{ab;\alpha} \quad (2.16)$$

that is, the total number of fields transforming under $U(M_{ab})$ global symmetry group. This will be related to the covariant basis, where we can count states according to representations of the global symmetry group $\prod_{ab} U(M_{ab})$. We group together representations $\cup_{\alpha} r_{ab;\alpha}$ corresponding to the same pair (a, b) , and expand the multiplicities in (2.12) as

$$\begin{aligned} g(\cup_{b,\alpha} r_{ab;\alpha}; R_a) &= \sum_{\{s_{ab}^-\}} g(\cup_b s_{ab}^-; R_a) \prod_b g(\cup_{\alpha} r_{ab;\alpha}; s_{ab}^-) \\ g(\cup_{b,\alpha} r_{ba;\alpha}; R_a) &= \sum_{\{s_{ba}^+\}} g(\cup_b s_{ba}^+; R_a) \prod_b g(\cup_{\alpha} r_{ba;\alpha}; s_{ba}^+) \end{aligned} \quad (2.17)$$

s_{ab}^{\pm} are intermediate representations in the reductions $R_a \rightarrow \{\cup_b s_{ab}^-\} \rightarrow \{\cup_{b,\alpha} r_{ab;\alpha}\}$ and $R_a \rightarrow \{\cup_b s_{ba}^+\} \rightarrow \{\cup_{b,\alpha} r_{ba;\alpha}\}$. Next, we apply (A.40) for fixed (a, b) :

$$\sum_{\{r_{ab;\alpha}\}} g(\cup_{\alpha} r_{ab;\alpha}; s_{ab}^+) g(\cup_{\alpha} r_{ab;\alpha}; s_{ab}^-) = \sum_{\Lambda_{ab}} C(s_{ab}^+, s_{ab}^-, \Lambda_{ab}) g(\cup_{\alpha} [n_{ab;\alpha}]; \Lambda_{ab}) \quad (2.18)$$

where $\cup_{\alpha} [n_{ab;\alpha}]$ is the irrep of $\times_{\alpha} S_{n_{ab;\alpha}}$ consisting of the single row symmetric irreps $[n_{ab;\alpha}]$ for each factor. We find

$$\begin{aligned} \mathcal{N}(\{n_{ab;\alpha}\}; \{N_a\}, \{M_{ab}\}) &= \sum_{\substack{R_a \vdash n_a \\ l(R_a) \leq N_a}} \sum_{\substack{s_{ab}^+ \vdash n_{ab} \\ s_{ab}^- \vdash n_{ab}}} \sum_{\substack{\Lambda_{ab} \vdash n_{ab} \\ l(\Lambda_{ab}) \leq M_{ab}}} \prod_a g(\cup_b s_{ab}^-; R_a) g(\cup_b s_{ba}^+; R_a) \\ &\quad \times \prod_{a,b} C(s_{ab}^+, s_{ab}^-, \Lambda_{ab}) g(\cup_{\alpha} [n_{ab;\alpha}]; \Lambda_{ab}) \end{aligned} \quad (2.19)$$

The new labels Λ_{ab} are precisely the $U(M_{ab})$ representations. (2.19) can be understood by noting that the number of states in the irrep Λ_{ab} , a Young diagram of $U(M_{ab})$ with n_{ab}

boxes, with specified charges $n_{ab;\alpha}$ under the diagonal $U(1)^{M_{ab}}$, is given by the Littlewood-Richardson multiplicity

$$g(\cup_\alpha [n_{ab;\alpha}]; \Lambda_{ab}) = \frac{1}{\prod_{a,b,\alpha} n_{ab;\alpha}!} \sum_{\sigma_{ab;\alpha} \in S_{n_{ab;\alpha}}} \chi_{\Lambda_{ab}}(\cup_\alpha \sigma_{ab;\alpha}) \quad (2.20)$$

Thus if we do not refine by $n_{ab;\alpha}$, but count all the states with fixed $\{n_{ab}\}$, we count the total number of states in the representation

$$\begin{aligned} \mathcal{N}(\{n_{ab}\}; \{N_a\}, \{M_{ab}\}) = & \sum_{\substack{R_a \vdash n_a \\ l(R_a) \leq N_a}} \sum_{\substack{s_{ab}^+ \vdash n_{ab} \\ s_{ab}^- \vdash n_{ab}}} \sum_{\substack{\Lambda_{ab} \vdash n_{ab} \\ l(\Lambda_{ab}) \leq M_{ab}}} \prod_a g(\cup_b s_{ab}^-; R_a) g(\cup_b s_{ba}^+; R_a) \\ & \times \prod_{a,b} C(s_{ab}^+, s_{ab}^-, \Lambda_{ab}) \text{Dim}(\Lambda_{ab}) \end{aligned} \quad (2.21)$$

where $\text{Dim}(\Lambda_{ab})$ is the size of $U(M_{ab})$ irrep Λ_{ab} . We can also, instead of counting individual states, count how many times a particular global symmetry representation $\otimes_{ab} \Lambda_{ab}$ appears

$$\mathcal{N}(\{\Lambda_{ab}\}; \{N_a\}, \{M_{ab}\}) = \sum_{\substack{R_a \vdash n_a \\ l(R_a) \leq N_a}} \sum_{\substack{s_{ab}^+ \vdash n_{ab} \\ s_{ab}^- \vdash n_{ab}}} \prod_a g(\cup_b s_{ab}^-; R_a) g(\cup_b s_{ba}^+; R_a) \prod_{a,b} C(s_{ab}^+, s_{ab}^-, \Lambda_{ab})$$

(2.22)

The following figures illustrate the structure of this formula to the case of $\mathbb{C}^3, \mathcal{C}$ and $\mathbb{C}^3/\mathbb{Z}_2$ quivers. The white nodes again represent LR multiplicities and the new black nodes represent Kronecker product multiplicities $C(s_{ab}^+, s_{ab}^-, \Lambda_{ab})$.

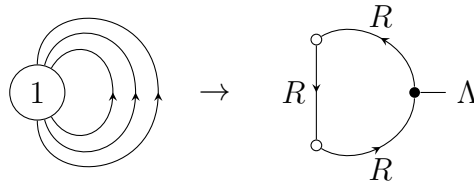


Figure 5: Covariant quiver for \mathbb{C}^3 .

The corresponding formula for \mathbb{C}^3 according to Figure 5

$$\mathcal{N}_{\mathbb{C}^3}(\Lambda; N) = \sum_{\substack{R \vdash n \\ l(R) \leq N}} C(R, R, \Lambda) \quad (2.23)$$

It was first obtained in [48] and the matching construction of orthogonal operators given in [20]. Since there is only single incoming and outgoing arrow from the white branching

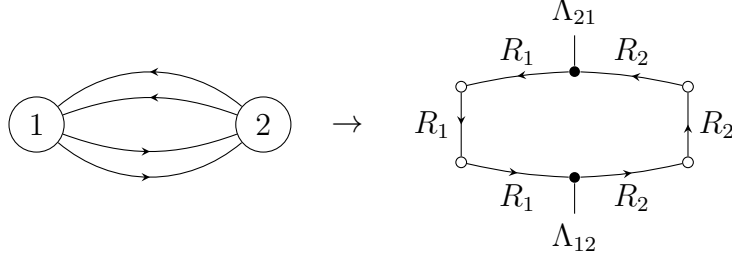


Figure 6: Covariant quiver for the conifold.

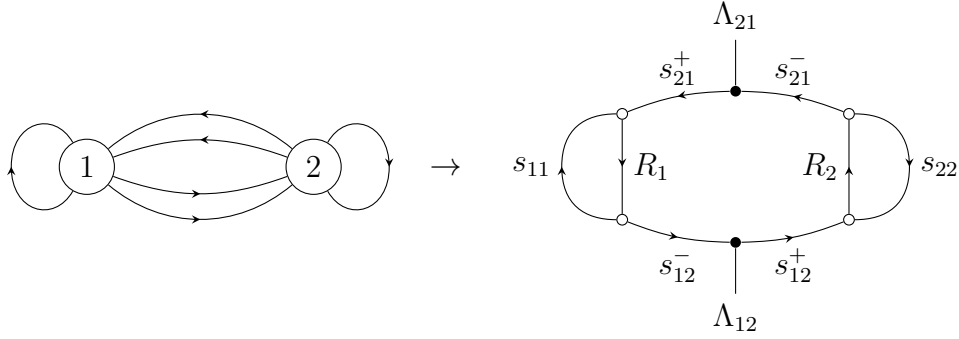


Figure 7: Covariant quiver for $\mathbb{C}^3/\mathbb{Z}_2$.

nodes in Figure 5, there is no actual branching, and the labels on both sides are R . That is, compared to general formula (2.22) we have $s^+ = s^- = R$.

For conifold we have Figure 6

$$\mathcal{N}_C(\Lambda_{12}, \Lambda_{21}; N) = \sum_{\substack{R_1 \vdash n \\ l(R_1) \leq N}} \sum_{\substack{R_2 \vdash n \\ l(R_2) \leq N}} C(R_1, R_2, \Lambda_{12}) C(R_2, R_1, \Lambda_{21}) \quad (2.24)$$

Again the white node multiplicities are trivial, setting s_{ab}^\pm to R_a .

For $\mathbb{C}^3/\mathbb{Z}_2$ we find non-trivial branching multiplicities, following the diagram Figure 7:

$$\begin{aligned} \mathcal{N}_{\mathbb{C}^3/\mathbb{Z}_2}(\Lambda_{12}, \Lambda_{21}, n_{11}, n_{22}; N) = & \sum_{\substack{R_1 \vdash n_1 \\ l(R_1) \leq N}} \sum_{\substack{R_2 \vdash n_2 \\ l(R_2) \leq N}} \sum_{s_{12}^- \vdash n_{12}} \sum_{s_{12}^+ \vdash n_{12}} \sum_{s_{21}^- \vdash n_{12}} \sum_{s_{21}^+ \vdash n_{12}} \sum_{s_{11} \vdash n_{11}} \sum_{s_{22} \vdash n_{22}} \\ & g(s_{11}, s_{12}^-; R_1) g(s_{11}, s_{12}^+; R_1) g(s_{22}, s_{21}^-; R_2) g(s_{22}, s_{21}^+; R_2) C(s_{12}^-, s_{12}^+, \Lambda_{12}) C(s_{21}^-, s_{21}^+, \Lambda_{21}) \end{aligned} \quad (2.25)$$

The only simplification compared to the generic formula (2.22) is that $s_{11}^+ = s_{11}^- \equiv s_{11}$ and $s_{22}^+ = s_{22}^- \equiv s_{22}$, since the original quiver has $M_{11} = M_{22} = 1$, the corresponding global symmetry factor is abelian, and so $\Lambda_{11} = [n_{11}]$, $\Lambda_{22} = [n_{22}]$ are trivial.

2.2 Infinite product generating functions

In this section we will use the covariant basis counting (2.21) to derive a simple infinite product formula valid when the numbers of fields are less than the ranks N_a . In this case counting gauge invariant operators is the same as counting closed loops in the quiver.

Counting the gauge invariant local operators for fixed ranks N_a , numbers M_{ab} of fields transforming in (N_a, \bar{N}_b) in the theory, and numbers n_{ab} for the total number of fields of type (N_a, \bar{N}_b) we have (2.21)

$$\begin{aligned} \mathcal{N}(\{n_{ab}\}; \{N_a\}, \{M_{ab}\}) = & \sum_{\substack{R_a \vdash n_a \\ l(R_a) \leq N_a}} \sum_{s_{ab}^+ \vdash n_{ab}} \sum_{s_{ab}^- \vdash n_{ab}} \sum_{\substack{\Lambda_{ab} \vdash n_{ab} \\ l(\Lambda_{ab}) \leq M_{ab}}} \prod_a g(\cup_b s_{ab}^-; R_a) g(\cup_b s_{ba}^+; R_a) \\ & \times \prod_{a,b} C(s_{ab}^+, s_{ab}^-, \Lambda_{ab}) \text{Dim}(\Lambda_{ab}) \end{aligned} \quad (2.26)$$

The finite N constraints are encoded in the requirement that the Young diagrams R_a have no more than N_a rows.

Let us convert it to a partition function with fugacities $\{t_{ab;\alpha}\}$ for numbers $\{n_{ab;\alpha}\}$. The contribution from a single irrep Λ_{ab} is

$$\chi_{\Lambda_{ab}}(\mathbb{T}_{ab}) \quad (2.27)$$

where \mathbb{T}_{ab} is a square matrix of size M_{ab} with entries $t_{ab;\alpha}$ along the diagonal. Thus we can replace $\text{Dim}(\Lambda_{ab})$ with $\chi_{\Lambda_{ab}}(\mathbb{T}_{ab})$ in (2.26) and sum over all representations without restriction on the number of boxes, to get the full partition function:

$$\begin{aligned} \mathcal{N}(\{t_{ab;\alpha}\}; \{N_a\}, \{M_{ab}\}) = & \sum_{\substack{R_a \\ l(R_a) \leq N_a}} \sum_{s_{ab}^+ \vdash n_{ab}} \sum_{s_{ab}^- \vdash n_{ab}} \sum_{\substack{\Lambda_{ab} \vdash n_{ab} \\ l(\Lambda_{ab}) \leq M_{ab}}} \prod_a g(\cup_b s_{ab}^+; R_a) g(\cup_b s_{ab}^-; R_a) \\ & \times \prod_{a,b} C(s_{ab}^+, s_{ab}^-, \Lambda_{ab}) \chi_{\Lambda_{ab}}(\mathbb{T}_{ab}) \end{aligned} \quad (2.28)$$

Note this is the same partition function as in the derivation in the previous section (2.11), but now using the covariant basis we can conveniently package $(t_{ab;\alpha})^{n_{ab;\alpha}}$ into $\chi_{\Lambda_{ab}}(\mathbb{T}_{ab})$.

The counting formula (2.28) can be used to derive an elegant infinite product formula for large N_a . If we assume $n_a \leq N_a$ so sums over R_a are unconstrained, we can do the

sums over $R_a, \Lambda_{ab}, s_{ab}^\pm$ to end up with a product of delta functions over the groups

$$\mathcal{N}(\{t_{ab;\alpha}\}; \{M_{ab}\}) = \sum_{\{\gamma_a\}} \sum_{\{\sigma_{ab}\}} \prod_a \delta_{S_{n_a}} \left(\left(\prod_b^\circ \sigma_{ba} \right) \gamma_a \left(\prod_b^\circ \sigma_{ab} \right) \gamma_a^{-1} \right) \prod_{a,b} \text{tr}_{n_{ab}}(\mathbb{T}_{ab} \sigma_{ab}) \quad (2.29)$$

where

$$\mathcal{N}(\{t_{ab;\alpha}\}; \{M_{ab}\}) \equiv \mathcal{N}(\{t_{ab;\alpha}\}; \{N_a = \infty\}, \{M_{ab}\}) \quad (2.30)$$

The limit $N_a = \infty$ holds as long as $n_a \leq N_a$.

The derivation is described in more detail in Appendix (D.1). The sum is over permutations $\gamma_1, \gamma_2, \dots, \gamma_G$, one for each node (or group), with $\gamma_a \in S_{n_a}$; as well as a sum over permutations σ_{ab} , one for every pair (a, b) of nodes of the quiver which have a non-zero number M_{ab} of arrows from a to b . The σ_{ab} are permutations in $S_{n_{ab}}$. Note that $\prod_b^\circ \sigma_{ba}$ is an outer product of permutations, e.g if there are 3 values of b for which n_{ba} is non-zero, say $b = 1, 2, 3$, then the product gives a permutation $\sigma_{11} \circ \sigma_{21} \circ \sigma_{31}$ which lives in the $S_{n_{1a}} \times S_{n_{2a}} \times S_{n_{3a}}$ subgroup of $S_{n_a} = S_{n_{1a}+n_{2a}+n_{3a}}$.

Consider cycles of length i . Let σ_{ab} have $p_{ab}^{(i)}$ cycles of this length. The delta functions associated with each node lead to the condition $\sum_b p_{ab}^{(i)} = \sum_b p_{ba}^{(i)}$. Given any γ_a, σ_{ab} which solve the delta function, we can generate the other solutions for the same σ_{ab} , by considering by multiplying γ_a on the right with permutations γ_a in the stabilizer of $(\prod_b^\circ \sigma_{ab})$. This generates a multiplicity of

$$\prod_i \prod_a \left(\sum_b p_{ab}^{(i)} \right)! i^{\sum_b p_{ab}^{(i)}} \quad (2.31)$$

We can see that the sums over γ_a in (2.29) only depends on the conjugacy class of σ_{ab} in $S_{n_{ab}}$, since conjugating σ_{ab} by elements of $S_{n_{ab}}$ can be absorbed in $\gamma_a \in S_{n_a}$ the summations by exploiting the invariance of these sums under left or right multiplication by elements of the $S_{n_{ab}}$ subgroups of S_{n_a} . This means that the sums over σ_{ab} can be converted into sums over $p_{ab}^{(i)}$. There is a multiplicity

$$\prod_i \prod_{a,b} \frac{n_{ab}!}{i^{p_{ab}^{(i)}} (p_{ab}^{(i)})!} \quad (2.32)$$

Combining these facts we arrive at

$$\mathcal{N}(\{t_{ab;\alpha}\}; \{M_{ab}\}) = \prod_{i=1}^{\infty} \left[\sum_{\{p_{ab}^{(i)}\}=0}^{\infty} \prod_a \delta \left(\sum_b p_{ba}^{(i)} - \sum_b p_{ab}^{(i)} \right) \left(\sum_b p_{ab}^{(i)} \right)! \prod_{a,b} \frac{(\sum_\alpha (t_{ab;\alpha})^i)^{p_{ab}^{(i)}}}{p_{ab}^{(i)}!} \right] \quad (2.33)$$

For each i we need to do a sum of the form

$$\mathcal{S}(\{t_{ab}\}) = \sum_{\{p_{ab}\}=0}^{\infty} \prod_a \delta \left(\sum_b p_{ba} - \sum_b p_{ab} \right) \left(\sum_b p_{ab} \right)! \prod_{a,b} \frac{(t_{ab})^{p_{ab}}}{p_{ab}!} \quad (2.34)$$

It is convenient to write the Kronecker delta as a contour integral, using

$$\delta(p) = \oint \frac{dz}{2\pi i z} z^p \quad (2.35)$$

which gives

$$\begin{aligned} \mathcal{S}(\{t_{ab}\}) &= \sum_{\{p_{ab}\}=0}^{\infty} \prod_a \left(\sum_b p_{ab} \right)! \oint \frac{dz_a}{2\pi i z_a} z_a^{\sum_b p_{ba} - \sum_b p_{ab}} \prod_{a,b} \frac{(t_{ab})^{p_{ab}}}{p_{ab}!} \\ &= \oint \left(\prod_a \frac{dz_a}{2\pi i z_a} \right) \sum_{\{p_{ab}\}=0}^{\infty} \prod_a \left(\sum_b p_{ab} \right)! \prod_{a,b} \frac{(z_a^{-1} z_b t_{ab})^{p_{ab}}}{p_{ab}!} \\ &= \oint \left(\prod_a \frac{dz_a}{2\pi i z_a} \right) \prod_a \frac{1}{1 - \sum_b z_a^{-1} z_b t_{ab}} \end{aligned} \quad (2.36)$$

We can obtain the desired sum by calculating residues.

We find that the result can be expressed in an elegant and intuitive form. Let \mathbf{V} be the set $\{1, 2, \dots, G\}$ of nodes in the quiver. We will let \mathbb{V} be any subset of \mathbf{V} , and define $\text{Sym}(\mathbb{V})$ to be the group of all permutations of the elements in \mathbb{V} . For each permutation σ we will define a monomial $T_\sigma(\{t_{ab}\})$ built from the set $\{t_{ab}\}$. Any permutation σ is a product of cycles $\sigma = \prod_j \sigma^{(j)}$. The monomial $T_\sigma(\{t_{ab}\})$ is a product over these cycles.

$$T_\sigma(\{t_{ab}\}) = \prod_j (-1)^{C_{\sigma^{(j)}}} T_{\sigma^{(j)}}(\{t_{ab}\}) \quad (2.37)$$

For a cycle, such as (a_1, a_2, \dots, a_k) with integers a_1, \dots, a_k chosen from $\{1, \dots, G\}$, the factor is

$$T_{(a_1, a_2, \dots, a_k)}(\{t_{ab}\}) = t_{a_1 a_2} t_{a_2 a_3} \cdots t_{a_{k-1} a_k} t_{a_k a_1} \quad (2.38)$$

We find that

$$\boxed{\mathcal{S}(\{t_{ab}\}) = \frac{1}{(1 - \sum_{\mathbb{V} \subset \mathbf{V}} \sum_{\sigma \in \text{Sym}(\mathbb{V})} T_\sigma(\{t_{ab}\}))}} \quad (2.39)$$

The sign of each term is $(-1)^{C_\sigma}$ where C_σ is the number of cycles in the corresponding permutation. Each cycle $\sigma^{(i)}$ corresponds to an elementary closed loop in the quiver, elementary in the sense that it does not involve visiting any node more than once. The

permutation σ corresponds to a product of disjoint elementary loops. For example, for a quiver with three nodes, this becomes

$$\begin{aligned} \mathcal{S}(t_{11}, t_{22}, t_{33}, t_{12}, t_{13}, t_{23}) \\ = (1 - t_{11} - t_{22} - t_{33} + t_{11}t_{22} - t_{12}t_{21} + t_{22}t_{33} - t_{23}t_{32} + t_{11}t_{33} - t_{13}t_{31} \\ - t_{11}t_{22}t_{33} + t_{12}t_{21}t_{33} + t_{13}t_{31}t_{22} + t_{11}t_{23}t_{32} - t_{12}t_{23}t_{31} - t_{13}t_{32}t_{21})^{-1} \end{aligned} \quad (2.40)$$

The first three terms after 1 come from the 3 1-element subsets of $\mathbf{V} = \{1, 2, 3\}$. The next three pairs come from the 3 two-element subsets of \mathbf{V} . The first of each pair comes from the identity permutation of the subset, the second from the swap. The last line comes from permutations of $\mathbb{V} = \mathbf{V}$.

The large N counting function can then be written as

$$\mathcal{N}(\{t_{ab;\alpha}\}; \{M_{ab}\}) = \prod_{i=1}^{\infty} \mathcal{S}(\{t_{ab} \rightarrow \sum_{\alpha=1}^{M_{ab}} (t_{ab;\alpha})^i\}) \quad (2.41)$$

In this equation, we have the counting for a quiver with G nodes and any number of arrows for any specified pair of start and end points. When there are no arrows between a specified start and end point, we set the corresponding t_{ab} variable to zero.

Let us now explain how to specialize the above formula for some specific cases. Take the half-BPS sector of $\mathcal{N} = 4$ SYM. This is described by one node and one arrow starting and ending at that node. The set \mathbf{V} has one element $\{1\}$ and there is one t_{11} parameter. There are two subsets, $\mathbb{V} = \emptyset$ or $\mathbb{V} = \mathbf{V}$. In calculating $\mathcal{S}(t_{11})$, the monomial coming from the emptyset is 1. The monomial from $\mathbb{V} = \mathbf{V}$ is $-t_{11}$. So

$$\mathcal{N}_{\mathbb{C}}(t_{11}) = \prod_{i=1}^{\infty} \frac{1}{1 - t_{11}^i} \quad (2.42)$$

For the one-node quiver with three lines starting and ending at the node, $\mathbf{V} = \{1\}$. The set of t -variables (“fugacities”) is $\{t_{11;1}, t_{11;2}, t_{11;3}\}$.

$$\mathcal{S}_{\mathbb{C}^3}(t_{11}) = (1 - t_{11})^{-1} \quad (2.43)$$

The counting function is

$$\mathcal{N}_{\mathbb{C}^3}(\{t_{11;\alpha}\}) = \prod_{i=1}^{\infty} \frac{1}{1 - t_{11;1}^i - t_{11;2}^i - t_{11;3}^i} \quad (2.44)$$

This formula was written down in [19].

Beyond these examples, the analogous formulae have not been previously written down. For the conifold, we have $\mathbf{V} = \{1, 2\}$. The \mathcal{S} function is

$$\mathcal{S}_{\mathcal{C}}(t_{12}, t_{21}) = (1 - t_{12}t_{21})^{-1} \quad (2.45)$$

The variables t_{11}, t_{22} are set to zero, since there are no arrows joining any node to itself. The 1 comes as usual from the empty set, the second term from the permutation (12) in $\text{Sym}(\mathbb{V})$ for $\mathbb{V} = \mathbf{V}$. All other terms are zero due to the vanishing of t_{11}, t_{22} . Since there is a multiplicity 2 for the arrows going from 1 to 2 and conversely from 2 to 1, we have variables $t_{12;1}, t_{12;2}, t_{21;1}, t_{21;2}$ and the counting function

$$\begin{aligned} \mathcal{N}_{\mathcal{C}}(\{t_{12;\alpha}, t_{21;\alpha}\}) &= \prod_{i=1}^{\infty} \frac{1}{1 - (t_{12;1}^i + t_{12;2}^i)(t_{21;1}^i + t_{21;2}^i)} \\ &= \prod_{i=1}^{\infty} \frac{1}{1 - t_{12;1}^i t_{21;1}^i - t_{12;2}^i t_{21;2}^i - t_{12;1}^i t_{21;2}^i - t_{12;2}^i t_{21;1}^i} \end{aligned} \quad (2.46)$$

For the example of \mathbb{C}^3/Z_2 , the \mathcal{S} function depends on $t_{11}, t_{22}, t_{12}, t_{21}$, The \mathcal{N} function depends on $t_{11}, t_{22}, t_{12;1}, t_{12;2}, t_{21;1}, t_{21;2}$.

$$\mathcal{S}_{\mathbb{C}^3/Z_2}(t_{11}, t_{22}, t_{12}, t_{21}) = (1 - t_{11} - t_{22} - t_{12}t_{21} + t_{11}t_{22})^{-1} \quad (2.47)$$

Here $\mathbf{V} = \{1, 2\}$. The monomials t_{11}, t_{22} come from choices $\mathbb{V} = \{1\}$ and $\mathbb{V} = \{2\}$. The term $t_{12}t_{21}$ comes from permutation (12) in $\text{Sym}(\mathbb{V})$ for $\mathbb{V} = \{1, 2\}$. The term $t_{11}t_{22}$ comes from permutation (1)(2) in $\text{Sym}(\mathbb{V})$ for $\mathbb{V} = \{1, 2\}$. The counting function is

$$\mathcal{N}_{\mathbb{C}^3/Z_2}(\{t_{11}, t_{22}, t_{12;\alpha}, t_{21;\alpha}\}) = \prod_{i=1}^{\infty} \frac{1}{1 - t_{11}^i - t_{22}^i - (t_{12;1}^i + t_{12;2}^i)(t_{21;1}^i + t_{21;2}^i) + t_{11}^i t_{22}^i} \quad (2.48)$$

3 Construction of free orthogonal basis

Motivated by the counting formulae (2.12), (2.22) we proceed in this section with the construction of an explicit operator basis. The prescriptions for counting in Figures 2,3,4,5,6,7 will be developed to produce an orthogonal basis of operators (in the free field inner product) to match the counting.

3.1 Review of \mathbb{C}^3

Let us first review $\mathcal{N} = 4$ $U(N)$ SYM, for which the orthogonal basis of free chiral operators has been constructed before [20, 23]. We can view $\mathcal{N} = 4$ as a special case of $\mathcal{N} = 1$

quiver gauge theory with the quiver shown in Figure 8. Theory contains three $\mathcal{N} = 1$

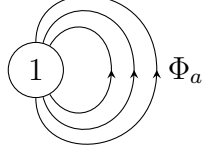


Figure 8: Quiver for \mathbb{C}^3 , arrows correspond to three chiral multiplets Φ_1, Φ_2, Φ_3 .

chiral multiplets Φ_a transforming in the adjoint of $U(N)$. There is a global $U(3)$ flavor symmetry. The chiral gauge invariant operators are built from the chiral adjoint scalars Φ_a , so we have single traces

$$\text{tr}(\Phi_{a_1} \Phi_{a_2} \dots \Phi_{a_n}) \quad (3.1)$$

and products of such traces. We will be interested in cases where N is finite and the operators involve more than N fields. In that case we need to take care of relationships between products of traces, arising from the fact that Φ_a are N -by- N matrices.

Consider all possible multitrace operators with $U(1)^3 \subset U(3)$ charges $\mathbf{n} = (n_1, n_2, n_3)$ and bare dimension $n = n_1 + n_2 + n_3$. A natural way to label the operators is by using a permutation $\sigma \in S_n$:

$$\mathcal{O}(\mathbf{n}, \sigma) = \prod_{k=1}^{n_1} (\Phi_1)_{i_{\sigma(k)}}^{i_k} \prod_{k=n_1+1}^{n_1+n_2} (\Phi_2)_{i_{\sigma(k)}}^{i_k} \prod_{k=n_1+n_2+1}^{n_1+n_2+n_3} (\Phi_3)_{i_{\sigma(k)}}^{i_k} \quad (3.2)$$

That is, the operator involves a product of fields $(\Phi_1)^{n_1} (\Phi_2)^{n_2} (\Phi_3)^{n_3}$ and the permutation σ indicates that k 'th upper index is contracted with $\sigma(k)$ 'th lower index. Each cycle in σ corresponds to a single trace.

At this point let us introduce some convenient notation. $(\Phi_a)_j^i$ is a matrix, which can be thought of as linear operator acting on N -dimensional vector space V_N . Then the object:

$$(\Phi_1^{\otimes n_1} \otimes \Phi_2^{\otimes n_2} \otimes \Phi_3^{\otimes n_3})_{j_1 \dots j_n}^{i_1 \dots i_n} \equiv \prod_{k=1}^{n_1} (\Phi_1)_{j_k}^{i_k} \prod_{k=n_1+1}^{n_1+n_2} (\Phi_2)_{j_k}^{i_k} \prod_{k=n_1+n_2+1}^{n_1+n_2+n_3} (\Phi_3)_{j_k}^{i_k} \quad (3.3)$$

is a linear operator acting on the N^n -dimensional vector space $V_N^{\otimes n}$. Permutations σ are also linear operators in $V_N^{\otimes n}$ which acts by permuting the V_N factors of the tensor product :

$$(\sigma)_{j_1 j_2 \dots j_n}^{i_1 i_2 \dots i_n} \equiv \delta_{j_{\sigma(1)}}^{i_1} \delta_{j_{\sigma(2)}}^{i_2} \dots \delta_{j_{\sigma(n)}}^{i_n} \quad (3.4)$$

Then (3.2) can be expressed as

$$\mathcal{O}(\mathbf{n}, \sigma) = \text{tr}_{V_N^{\otimes n}} (\sigma \Phi_1^{\otimes n_1} \otimes \Phi_2^{\otimes n_2} \otimes \Phi_3^{\otimes n_3}) \quad (3.5)$$

where the product of operators and the trace is over $V_N^{\otimes n}$, which means contracted indices of (3.3) and (3.3).

Let us also introduce diagrammatic notation for matrix multiplication and traces.

$$A_j^i = \begin{array}{c} \downarrow i \\ \boxed{A} \\ \downarrow j \end{array} \quad (AB)_j^i = \begin{array}{c} \downarrow i \\ \boxed{AB} \\ \downarrow j \end{array} = A_k^i B_j^k = \begin{array}{c} \downarrow i \\ \boxed{A} \\ \downarrow \\ \boxed{B} \\ \downarrow j \end{array} \quad \text{tr}(A) = \begin{array}{c} \top \\ \boxed{A} \\ \perp \end{array} \quad (3.6)$$

Incoming and outgoing arrows represent upper and lower indices respectively. Since in matrix multiplication conventionally lower index is contracted with upper, then in the diagram matrices are multiplied in the direction following arrows. When matrices are laid out vertically, the multiplication conventionally flows from top to bottom, and we can omit the arrows. The indices can, of course, belong to the vector space $V_N^{\otimes n}$, in which case lines represent the whole set $\{i_1 \dots i_n\}$ of contracted indices. Using this, we get a nice expression for the operator (3.5)

$$\mathcal{O}(\mathbf{n}, \sigma) = \begin{array}{c} \top \\ \boxed{\sigma} \\ \downarrow \\ \boxed{\Phi_1^{\otimes n_1} \otimes \Phi_2^{\otimes n_2} \otimes \Phi_3^{\otimes n_3}} \\ \perp \end{array} \quad (3.7)$$

Note an operator is not labelled by a unique σ . $\mathcal{O}(\mathbf{n}, \sigma)$ does not change if we conjugate σ by the subgroup:

$$\mathcal{O}(\mathbf{n}, \gamma \sigma \gamma^{-1}) = \mathcal{O}(\mathbf{n}, \sigma), \quad \gamma \in S_{n_1} \times S_{n_2} \times S_{n_3} \quad (3.8)$$

This can be seen from (3.2), where the conjugation can be brought from σ to act on $\Phi_1^{\otimes n_1} \otimes \Phi_2^{\otimes n_2} \otimes \Phi_3^{\otimes n_3}$, which is invariant. Furthermore, we still have the problem of finite N relationships.

One complete basis for the gauge invariant operators at finite N was constructed in [23], and is called ‘‘Restricted Schur’’ basis:

$$\mathcal{O}(\mathbf{L}) = \frac{1}{n_1! n_2! n_3!} \sum_{\sigma \in S_n} \chi_{R \rightarrow \mathbf{r}}^{\nu^-, \nu^+}(\sigma) \mathcal{O}(\mathbf{n}, \sigma) \quad (3.9)$$

The operators are uniquely specified by the set of group theoretic labels

$$\mathbf{L} = \{R, r_1, r_2, r_3, \nu^-, \nu^+\} \quad (3.10)$$

R, r_1, r_2, r_3 are Young diagrams

$$R \vdash n, \quad r_1 \vdash n_1, \quad r_2 \vdash n_2, \quad r_3 \vdash n_3 \quad (3.11)$$

R labels the representation of S_n and $\mathbf{r} = (r_1, r_2, r_3)$ labels the representation of the subgroup $S_{n_1} \times S_{n_2} \times S_{n_3} \subset S_n$ which appears in the decomposition of R in terms of subgroup irreps

$$R \rightarrow (r_1, r_2, r_3) \quad (3.12)$$

In case \mathbf{r} appears in the decomposition more than once, the two numbers ν^\pm each label runs over the multiplicity given by Littlewood-Richardson coefficient $1 \leq \nu^\pm \leq g(r_1, r_2, r_3; R)$. For a summary of the facts about subgroup decomposition and branching coefficients see Appendix A.2. The finite N constraint appears simply as a cutoff on the number of rows in R :

$$l(R) \leq N \quad (3.13)$$

and there are no further relationships between the operators.

The key ingredient in (3.9) is the coefficient $\chi_{R \rightarrow \mathbf{r}}^{\nu^-, \nu^+}(\sigma)$ called “restricted character”. It is a generalization of the usual character $\chi_R(\sigma) = \text{tr}(D^R(\sigma))$ and defined as

$$\chi_{R \rightarrow \mathbf{r}}^{\nu^-, \nu^+}(\sigma) = \text{tr} \left(P_{R \rightarrow \mathbf{r}}^{\nu^-, \nu^+} D^R(\sigma) \right) \quad (3.14)$$

$P_{R \rightarrow \mathbf{r}}^{\nu^-, \nu^+}$ is a projector-like operator ¹

$$P_{R \rightarrow \mathbf{r}}^{\nu^-, \nu^+} = \sum_{l_1, l_2, l_3=1}^{d_r} |R; \mathbf{r}, \nu^-, \mathbf{l}\rangle \langle R; \mathbf{r}, \nu^+, \mathbf{l}| \quad (3.15)$$

or in terms of Branching coefficients (see (A.13))

$$(P_{R \rightarrow \mathbf{r}}^{\nu^-, \nu^+})_{ij} = \sum_{\mathbf{l}} B_{i \rightarrow \mathbf{l}}^{R \rightarrow \mathbf{r}, \nu^-} B_{j \rightarrow \mathbf{l}}^{R \rightarrow \mathbf{r}, \nu^+} \quad (3.16)$$

Using diagrammatic notation (A.15) we can represent the restricted character

$$\chi_{R \rightarrow \mathbf{r}}^{\nu^-, \nu^+}(\sigma) = \begin{array}{c} \nu^+ \\ \circ \\ \curvearrowleft R \curvearrowright \\ \circ \\ \nu^- \end{array} \begin{array}{c} r_1 \\ \circ \\ \curvearrowleft r_2 \curvearrowright \\ \circ \\ r_3 \end{array} \quad (3.17)$$

¹ If $\nu^- = \nu^+ \equiv \nu$, then $P_{R \rightarrow \mathbf{r}}^{\nu, \nu}$ is precisely the projector to (\mathbf{r}, ν) in R . But the “off-diagonal” ones with $\nu^- \neq \nu^+$ are not strictly projectors, they are intertwining operators mapping between different copies of the same irrep \mathbf{r} in R

The edges now correspond to contracted indices in irreducible representations R, r_1, r_2, r_3 , as labelled.

The basis (3.9) is not only complete, it is, in fact, orthogonal in the free field Zamolodchikov metric obtained from the two point function

$$\langle (\Phi_a)_j^i (\Phi_b^\dagger)_l^k \rangle = \delta_{ab} \delta_l^i \delta_j^k \quad (3.18)$$

Then

$$\langle O(R, \mathbf{r}, \nu^-, \nu^+) O(\tilde{R}, \tilde{\mathbf{r}}, \tilde{\nu}^-, \tilde{\nu}^+) \rangle = \frac{h(R) f_N(R)}{h(r_1) h(r_2) h(r_3)} \delta_{R\tilde{R}} \delta_{r_1 \tilde{r}_1} \delta_{r_2 \tilde{r}_2} \delta_{r_3 \tilde{r}_3} \delta_{\nu^+ \tilde{\nu}^+} \delta_{\nu^- \tilde{\nu}^-} \quad (3.19)$$

$h(R)$ is the product of hooks of the Young diagram, and $f_N(R)$ is the weight of the diagram in $U(N)$. That is the only place that N dependence comes in, and it nicely captures the cutoff, because if the height of R exceeds N , then $f_N(R) = 0$, which means the operator is 0.

There is another complete orthogonal basis found in [20], where operators are organized into irreducible representation of the global symmetry $U(3)$. We will refer to it as “covariant basis”, since operators transform covariantly with the global symmetry group. The operators are

$$\mathcal{O}(\mathbf{K}) = \frac{1}{n!} \sum_{\sigma \in S_n} B_m^{\Lambda \rightarrow [\mathbf{n}], \beta} S_{ij, m}^{RR, \Lambda \tau} D_{ij}^R(\sigma) \mathcal{O}(\mathbf{n}, \sigma) \quad (3.20)$$

The group theory labels in this case are

$$\mathbf{K} = \{R, \Lambda, \tau, \mathbf{n}, \beta\} \quad (3.21)$$

where $R, \Lambda \vdash n$ are Young diagrams with $n = n_1 + n_2 + n_3$ boxes. R is the same as before, with a cutoff of at most N rows, and Λ is an irrep of $U(3)$ with at most 3 rows. τ is the multiplicity label for the Kronecker product of S_n irreps

$$R \otimes R \rightarrow \Lambda \quad (3.22)$$

and $S_{ij, m}^{RR, \Lambda \tau}$ is the associated Clebsch-Gordan coefficient. For the review of the facts about Kronecker product and Clebsch-Gordan coefficients see Appendix A.3. $\mathbf{n} = (n_1, n_2, n_3)$ specifies how many fields of each flavor there are (note in \mathbf{L} this information was contained in \mathbf{r}). $B_m^{\Lambda \rightarrow [\mathbf{n}], \beta}$ is the branching coefficient for the reduction from S_n irrep Λ to the trivial one-dimensional irrep $[n_1, n_2, n_3]$ of $S_{n_1} \times S_{n_2} \times S_{n_3}$, and β is the multiplicity label. In other words, β labels the invariants of Λ under $S_{n_1} \times S_{n_2} \times S_{n_3}$, and $B_m^{\Lambda \rightarrow [\mathbf{n}], \beta}$ are the

invariant vectors. Note, compared with the usual branching coefficient notation $B_{m \rightarrow i}^{\Lambda \rightarrow [\mathbf{n}], \beta}$, we suppress the index i since $[\mathbf{n}]$ is one-dimensional.

Again it will be useful to have a diagrammatic notation for the basis. Define

$$\chi(\mathbf{K}, \sigma) = B_m^{\Lambda \rightarrow [\mathbf{n}], \beta} S_{ij, m}^{RR, \Lambda \tau} D_{ij}^R(\sigma) \quad (3.23)$$

so that

$$\mathcal{O}(\mathbf{K}) = \frac{1}{n!} \sum_{\sigma \in S_n} \chi(\mathbf{K}, \sigma) \mathcal{O}(\mathbf{n}, \sigma) \quad (3.24)$$

The coefficient $\chi(\mathbf{K}, \sigma)$ can be expressed, using the diagrammatic notation (A.27) for the Clebsch-Gordan coefficient, as

$$\chi(\mathbf{K}, \sigma) = \boxed{\sigma} \begin{array}{c} \xrightarrow{R} \\ \xleftarrow{R} \end{array} \begin{array}{c} \tau \\ \Lambda \end{array} \begin{array}{c} \xrightarrow{\beta} \\ \xleftarrow{\beta} \end{array} \begin{array}{c} \circ \\ \circ \end{array} \begin{array}{c} \text{---} \\ \text{---} \end{array} [\mathbf{n}] \quad (3.25)$$

The open line, which normally has an associated state label, corresponds to the unique $i = 1$ basis state of $[\mathbf{n}]$ in the branching $B_{m \rightarrow i}^{\Lambda \rightarrow [\mathbf{n}], \beta}$.

The two-point function between the operators is

$$\langle \mathcal{O}(\mathbf{K}) \mathcal{O}(\tilde{\mathbf{K}})^\dagger \rangle = \frac{n_1! n_2! n_3! \text{Dim}_N(R)}{d_R^2} \delta_{R\tilde{R}} \delta_{\Lambda\tilde{\Lambda}} \delta_{\tau\tilde{\tau}} \delta_{\mathbf{n}\tilde{\mathbf{n}}} \delta_{\beta\tilde{\beta}} \quad (3.26)$$

3.2 Generalized restricted Schur basis

Let us assume we have a general quiver Q . We will often use $\mathbb{C}^3/\mathbb{Z}_2$ as an example, see Figure 1. The goal in this section is to derive a free orthogonal basis $\mathcal{O}_Q(\mathbf{L})$ for arbitrary quiver, analogous to the restricted Schur basis (3.9) in \mathbb{C}^3 . We extend this to covariant basis $\mathcal{O}_Q(\mathbf{K})$ in the next section.

In order to build a gauge-invariant operator² we contract the incoming and outgoing fields at each group node. In a more complicated quiver such as $\mathbb{C}^3/\mathbb{Z}_2$ there are different “paths” that an operator can take. We can build, for example:

$$\text{tr}(\Phi_{11}\Phi_{11}), \text{tr}(\Phi_{12;1}\Phi_{21;2}), \text{tr}(\Phi_{11}\Phi_{12;1}\Phi_{22}\Phi_{21;1}), \dots \quad (3.27)$$

It is possible to capture all the different possibilities by fixing the number of times $n_{ab;\alpha}$ each field appears, and then contracting the indices corresponding to each group according to a permutation σ_a . This defines an operator which, in correspondence with (3.7),

²We restrict to the mesonic sector, or, in other words, $\prod_a U(N_a)$ gauge group, not $\prod_a SU(N_a)$.

diagrammatically looks like:

$$\mathcal{O}_{\mathbb{C}^3/\mathbb{Z}_2}(\mathbf{n}, \boldsymbol{\sigma}) =$$
(3.28)

The lines represent indices in $V_N^{\otimes n_{ab;\alpha}}$. Note that if $n_{11} \neq n_{22}$, permutations σ_1, σ_2 are elements of symmetric groups of different size

$$\begin{aligned} \sigma_1 &\in S_{n_1}, & n_1 &\equiv n_{11} + n_{12;1} + n_{12;2} \\ \sigma_2 &\in S_{n_2}, & n_2 &\equiv n_{22} + n_{21;1} + n_{21;2} \end{aligned} \quad (3.29)$$

acting as operators in $V_{N_1}^{\otimes n_1}$ and $V_{N_2}^{\otimes n_2}$. If we rearrange the above diagram we get just the quiver itself with a permutation σ_a at each group node and an operator $(\Phi_{ab;\alpha})^{\otimes n_{ab;\alpha}}$ on each field line

$$\mathcal{O}_{\mathbb{C}^3/\mathbb{Z}_2}(\mathbf{n}, \boldsymbol{\sigma}) =$$
(3.30)

It is clear that we can define $\mathcal{O}_Q(\mathbf{n}, \boldsymbol{\sigma})$ in such a way for any quiver Q : it is a generalization of (3.5), but instead of contractions performed sequentially in a single trace, now the operators σ_a and $(\Phi_{ab;\alpha})^{\otimes n_{ab;\alpha}}$ are contracted along Q . With the diagrammatic representation of linear operators using boxes and lines, we are inserting the boxes for $(\Phi_{ab;\alpha})^{\otimes n_{ab;\alpha}}$ along the edge of the split-node quiver labelled α going from a to b , and we are inserting σ_a in the a 'th line joining the a 'th plus and minus nodes. Explicitly we can write:

$$\mathcal{O}_Q(\mathbf{n}, \boldsymbol{\sigma}) = \prod_{a,b} \prod_{\alpha=1}^{M_{ab}} \left(\Phi_{ab;\alpha}^{\otimes n_{ab;\alpha}} \right)_{J_{ab;\alpha}}^{I_{ab;\alpha}} \prod_a (\sigma_a)_{\bigcup_{b,\alpha} I_{ab;\alpha}}^{\bigcup_{b,\alpha} J_{ba;\alpha}} \quad (3.31)$$

The indices a, b run over all group nodes, and it is understood that we skip the terms where $M_{ab} = 0$. $\mathbf{I}_{ab;\alpha}$ and $\mathbf{J}_{ab;\alpha}$ are indices in the vector space $V_{N_a}^{\otimes n_{ab;\alpha}}$ and $\check{V}_{N_b}^{\otimes n_{ab;\alpha}}$, i.e. $\mathbf{I}_{ab;\alpha} = \{i_1, \dots, i_{n_{ab;\alpha}}\}$ and $\mathbf{J}_{ab;\alpha} = \{j_1, \dots, j_{n_{ab;\alpha}}\}$ with the i_1, i_2, \dots each living in V_{N_a} and j_1, j_2, \dots each in V_{N_b} . $(\Phi_{ab;\alpha})^{\otimes n_{ab;\alpha}}$ are linear maps $V_{N_a}^{\otimes n_{ab;\alpha}} \rightarrow V_{N_b}^{\otimes n_{ab;\alpha}}$, and σ_a are linear operators on $V_{N_a}^{\otimes n_a}$ where

$$n_a = \sum_{b,\alpha} n_{ab;\alpha} = \sum_{b,\alpha} n_{ba;\alpha} \quad (3.32)$$

The indices of σ_a are unions $\bigcup_{b,\alpha} \mathbf{J}_{ba;\alpha}$ and $\bigcup_{b,\alpha} \mathbf{I}_{ab;\alpha}$, meaning that upper indices of σ_a are contracted with lower indices of all fields $\Phi_{ba;\alpha}$ that enter node a , and lower indices of σ_a are contracted with upper indices of all fields $\Phi_{ab;\alpha}$ that leave node a .

As a basic example consider an operator in $\mathbb{C}^3/\mathbb{Z}_2$ with

$$\mathbf{n} = \{n_{11}, n_{22}, n_{12;1}, n_{12;2}, n_{21;1}, n_{21;2}\} = \{1, 1, 1, 0, 1, 0\} \quad (3.33)$$

that is, build from fields $(\Phi_{11}, \Phi_{22}, \Phi_{12;1}, \Phi_{21;1})$. We have

$$\mathcal{O}_{\mathbb{C}^3/\mathbb{Z}_2}(\mathbf{n}, \sigma_1, \sigma_2) = (\Phi_{11})_{j_1}^{i_1} (\Phi_{22})_{j_2}^{i_2} (\Phi_{12;1})_{j_3}^{i_3} (\Phi_{21;1})_{j_4}^{i_4} (\sigma_1)_{i_1 i_3}^{j_1 j_4} (\sigma_2)_{i_2 i_4}^{j_2 j_3} \quad (3.34)$$

with $\sigma_1, \sigma_2 \in S_2$. For different combinations of σ_a we get

$$\begin{aligned} \mathcal{O}(\mathbb{I}, \mathbb{I}) &= \text{tr}(\Phi_{11}) \text{tr}(\Phi_{22}) \text{tr}(\Phi_{12;1} \Phi_{21;1}) \\ \mathcal{O}((12), \mathbb{I}) &= \text{tr}(\Phi_{11} \Phi_{12;1} \Phi_{21;1}) \text{tr}(\Phi_{22}) \\ \mathcal{O}(\mathbb{I}, (12)) &= \text{tr}(\Phi_{11}) \text{tr}(\Phi_{22} \Phi_{21;1} \Phi_{12;1}) \\ \mathcal{O}((12), (12)) &= \text{tr}(\Phi_{11} \Phi_{12;1} \Phi_{22} \Phi_{21;1}) \end{aligned} \quad (3.35)$$

As in the previous section for the case of \mathbb{C}^3 , the operators $\mathcal{O}_Q(\mathbf{n}, \boldsymbol{\sigma})$ are not uniquely labelled by $\boldsymbol{\sigma}$, that is, the basis is overcomplete and different $\boldsymbol{\sigma}$ can correspond to the same operator. Specifically, we have an identification

$$\mathcal{O}_Q(\mathbf{n}, \boldsymbol{\sigma}) = \mathcal{O}_Q(\mathbf{n}, \text{Adj}_\gamma(\boldsymbol{\sigma})) \quad (3.36)$$

where

$$\gamma = \{\gamma_{ab;\alpha}\} \in \bigotimes_{a,b,\alpha} S_{n_{ab;\alpha}} \quad (3.37)$$

and the adjoint action is defined as

$$\text{Adj}_\gamma(\boldsymbol{\sigma}) = \{(\otimes_{b,\alpha} \gamma_{ba;\alpha}) \sigma_a (\otimes_{b,\alpha} \gamma_{ab;\alpha}^{-1})\} \quad (3.38)$$

This is easily seen from the definition (3.31) and the fact that each $n_{ab;\alpha}$ block of identical fields is invariant under permutations

$$\left(\Phi_{ab;\alpha}^{\otimes n_{ab;\alpha}}\right) = \gamma^{-1} \left(\Phi_{ab;\alpha}^{\otimes n_{ab;\alpha}}\right) \gamma \quad (3.39)$$

These permutations can then be moved to act on σ .

It is shown in [20,21] that for \mathbb{C}^3 the complete orthogonal bases (3.9) and (3.20) can be derived by essentially “solving” the invariance (3.8). We will use the same method here to find generalized bases $\mathcal{O}_Q(\mathbf{L})$ and $\mathcal{O}_Q(\mathbf{K})$ for any quiver Q . As an illustration let us take the simplest example of half-BPS operators [9]. The idea is that the invariance

$$\mathcal{O}_{\mathbb{C}}(\sigma) = \frac{1}{n!} \sum_{\gamma \in S_n} \mathcal{O}_{\mathbb{C}}(\gamma^{-1} \sigma \gamma) \quad (3.40)$$

can be rewritten as

$$\mathcal{O}_{\mathbb{C}}(\sigma) = \sum_{\tau} \left(\frac{1}{n!} \sum_{\gamma} \delta(\gamma \sigma \gamma^{-1} \tau^{-1}) \right) \mathcal{O}_{\mathbb{C}}(\tau) = \sum_{\tau} \left(\frac{1}{n!} \sum_{R \vdash n} \chi_R(\sigma) \chi_R(\tau) \right) \mathcal{O}_{\mathbb{C}}(\tau) \quad (3.41)$$

which looks like a projector to a lower-dimensional space labelled by Young diagram R . This motivates the Schur polynomial basis

$$\mathcal{O}_{\mathbb{C}}(R) = \frac{1}{n!} \sum_{\sigma} \chi_R(\sigma) \mathcal{O}_{\mathbb{C}}(\sigma) \quad (3.42)$$

which indeed turns out to be complete and orthogonal. For \mathbb{C}^3 we have similarly (3.8) leading to

$$\mathcal{O}_{\mathbb{C}^3}(\mathbf{n}, \sigma) \sim \sum_{\tau} \left(\sum_{R, \mathbf{r}, \nu^-, \nu^+} \chi_{R \rightarrow \mathbf{r}}^{\nu^-, \nu^+}(\sigma) \chi_{R \rightarrow \mathbf{r}}^{\nu^-, \nu^+}(\tau) \right) \mathcal{O}_{\mathbb{C}^3}(\mathbf{n}, \tau) \quad (3.43)$$

which suggests the basis (3.9). In order to generalize this to arbitrary quiver, we define “quiver characters” $\chi_Q(\mathbf{L}, \sigma)$ obeying, schematically

$$\sum_{\mathbf{L}} \chi_Q(\mathbf{L}, \sigma) \chi_Q(\mathbf{L}, \tau) \sim \sum_{\gamma} \delta(\sigma, \text{Adj}_{\gamma}(\tau)) \quad (3.44)$$

where \mathbf{L} is a generalized set of group theory labels. With a help of quiver characters we can analogously express invariance (3.36) as

$$\mathcal{O}_Q(\mathbf{n}, \sigma) \sim \sum_{\tau} \left(\sum_{\mathbf{L}} \chi_Q(\mathbf{L}, \sigma) \chi_Q(\mathbf{L}, \tau) \right) \mathcal{O}_Q(\mathbf{n}, \tau) \quad (3.45)$$

leading to define a basis

$$\mathcal{O}_Q(\mathbf{L}) \sim \sum_{\sigma} \chi_Q(\mathbf{L}, \sigma) \mathcal{O}_Q(\mathbf{n}, \sigma) \quad (3.46)$$

The details of the derivation can be found in Appendix C, the result is that we can define restricted quiver characters as

$$\boxed{\begin{aligned} \chi_Q(\mathbf{L}, \sigma) &= \prod_a D_{i_a j_a}^{R_a}(\sigma_a) B_{j_a \rightarrow \bigcup_{b,\alpha} l_{ab;\alpha}}^{R_a \rightarrow \bigcup_{b,\alpha} r_{ab;\alpha}, \nu_a^-} B_{i_a \rightarrow \bigcup_{b,\alpha} l_{ba;\alpha}}^{R_a \rightarrow \bigcup_{b,\alpha} r_{ba;\alpha}, \nu_a^+} \\ \mathbf{L} &\equiv \{R_a, r_{ab;\alpha}, \nu_a^-, \nu_a^+\} \end{aligned}} \quad (3.47)$$

They obey the required invariance and orthogonality properties, listed in Appendix B.2, which are analogous to those of symmetric group characters. The complete basis of operators with a convenient normalization can then be defined as:

$$\boxed{\mathcal{O}_Q(\mathbf{L}) = \frac{1}{\prod n_a!} \sqrt{\frac{\prod d(R_a)}{\prod d(r_{ab;\alpha})}} \sum_{\sigma} \chi_Q(\mathbf{L}, \sigma) \mathcal{O}_Q(\mathbf{n}, \sigma)} \quad (3.48)$$

The group theory labels \mathbf{L} are:

- $r_{ab;\alpha}$: a Young diagram with $n_{ab;\alpha}$ boxes for each set of fields $\Phi_{ab;\alpha}$.
- R_a : a Young diagram for each group factor, labelling representation of S_{n_a} , where $n_a = \sum_{b,\alpha} n_{ba;\alpha} = \sum_{b,\alpha} n_{ab;\alpha}$ is the number of incoming and outgoing fields.
- ν_a^- : multiplicity index for outgoing field reduction $R_a \rightarrow \bigcup_{b,\alpha} r_{ab;\alpha}$.
- ν_a^+ : multiplicity index for incoming field reduction $R_a \rightarrow \bigcup_{b,\alpha} r_{ba;\alpha}$.

The structure can most easily be seen with a diagram, which is the split-node quiver with permutations σ_a inserted

$$\chi_{\mathbb{C}^3/\mathbb{Z}_2}(\mathbf{L}, \sigma) = \begin{array}{c} \begin{array}{ccc} \nu_1^+ & \xleftarrow{r_{21;2}} & \nu_2^- \\ & \xleftarrow{r_{21;1}} & \\ \downarrow R_1 & & \uparrow R_2 \\ \boxed{\sigma_1} & & \boxed{\sigma_2} \\ \downarrow & & \uparrow \\ \nu_1^- & \xrightarrow{r_{12;1}} & \nu_2^+ \\ & \xrightarrow{r_{12;2}} & \end{array} \end{array} \quad (3.49)$$

Each group node carries a permutation in representation R_a (denoted by a box), which is then contracted via branching coefficients (denoted by white nodes) to representations $r_{ab;\alpha}$

associated with fields. There are multiplicities ν_a^\pm associated to each branching coefficient node. The lines denote contracted matrix indices $i_a, j_a, l_{ab;\alpha}$. Note that $\chi_Q(\mathbf{L}, \boldsymbol{\sigma})$ reduces precisely to (3.17) for the \mathbb{C}^3 quiver! Also, for the trivial quiver \mathbb{C} consisting of one node and one field Φ_{11} , corresponding to the half-BPS sector, we get $R_1 = r_{11}$, all the branching coefficients are unit matrices, and the quiver character *is* the usual symmetric group character.

Using the orthogonality properties of quiver characters we can write the inverse of the basis change (3.48):

$$\mathcal{O}_Q(\mathbf{n}, \boldsymbol{\sigma}) = \sum_{\mathbf{L}} \sqrt{\frac{\prod d(R_a)}{\prod d(r_{ab;\alpha})}} \chi_Q(\mathbf{L}, \boldsymbol{\sigma}) \mathcal{O}_Q(\mathbf{L}) \quad (3.50)$$

3.3 Two-point function

We will show here that the general basis (3.48) is orthogonal in free field metric for any quiver Q

$$\left\langle \mathcal{O}_Q(\mathbf{L}) \mathcal{O}_Q(\tilde{\mathbf{L}})^\dagger \right\rangle = \delta_{\mathbf{L}\tilde{\mathbf{L}}} \frac{\prod n_{ab;\alpha}!}{\prod n_a!} \prod_a f_{N_a}(R_a) \quad (3.51)$$

$f_{N_a}(R_a)$ is the product of weights of a $U(N_a)$ diagram R_a . We can see it is a straightforward generalization of the result (3.19) for \mathbb{C}^3 , except with a different normalization, due to different normalization of the operators (3.48), compared to (3.9). It is important to note, that again N -dependence is in the factors $f_{N_a}(R_a)$ which vanish if the height of R_a exceeds N_a . So at finite N the Hilbert space consists of operators $\mathcal{O}_Q(\mathbf{L})$ where the height of all R_a does not exceed N_a

$$\mathcal{H} = \{\mathcal{O}_Q(\mathbf{L}) \mid \forall_a l(R_a) \leq N_a\} \quad (3.52)$$

The derivation of (3.51) is similar to that of (3.19) in [23], but now using analogous properties of quiver characters $\chi_Q(\mathbf{L}, \boldsymbol{\sigma})$ from Appendix B.2. We have the free field metric

$$\left\langle (\Phi_{ab;\alpha})_j^i (\Phi_{cd;\beta})_l^k \right\rangle = \delta_{ac} \delta_{bd} \delta_{\alpha\beta} \delta_l^i \delta_j^k \quad (3.53)$$

Then the two point function of $\mathcal{O}_Q(\mathbf{n}, \boldsymbol{\sigma})$ operators is

$$\left\langle \mathcal{O}_Q(\mathbf{n}, \boldsymbol{\sigma}) \mathcal{O}_Q(\mathbf{n}, \tilde{\boldsymbol{\sigma}})^\dagger \right\rangle = \sum_{\boldsymbol{\gamma}} \prod_a \text{tr}_{V_{N_a}} n(\text{Adj}_{\boldsymbol{\gamma}}(\sigma_a) \tilde{\sigma}_a^{-1}) \quad (3.54)$$

The sum is over $\boldsymbol{\gamma} \equiv \{\gamma_{ab;\alpha} \in S_{n_{ab;\alpha}}\}$ – Wick contractions arising from each set of fields. For the derivation of (3.54) see Appendix D.3. Next, we apply (3.54) to the definition of

$\mathcal{O}_Q(\mathbf{L})$ (3.48):

$$\left\langle \mathcal{O}_Q(\mathbf{L}) \mathcal{O}_Q(\tilde{\mathbf{L}})^\dagger \right\rangle = c_L c_{\tilde{\mathbf{L}}} \sum_{\boldsymbol{\sigma}, \tilde{\boldsymbol{\sigma}}, \boldsymbol{\gamma}} \chi_Q(\mathbf{L}, \boldsymbol{\sigma}) \chi_Q(\tilde{\mathbf{L}}, \tilde{\boldsymbol{\sigma}}) \prod_a \text{tr}_{V_{N_a}}^{n_a} (\text{Adj}_{\boldsymbol{\gamma}}(\sigma_a) \tilde{\sigma}_a^{-1}) \quad (3.55)$$

where $c_L = \frac{1}{\prod n_a!} \sqrt{\frac{\prod d(R_a)}{\prod d(r_{ab;\alpha})}}$ is the normalization coefficient appearing in front of the sum in (3.48). Note that $\chi_Q(\mathbf{L}, \boldsymbol{\sigma})$ is a real number, so we drop complex conjugation. Now redefining $\sigma_a \rightarrow \text{Adj}_{\boldsymbol{\gamma}}(\sigma_a)$ and using invariance property (B.10) the dependence on $\boldsymbol{\gamma}$ drops out

$$\left\langle \mathcal{O}_Q(\mathbf{L}) \mathcal{O}_Q(\tilde{\mathbf{L}})^\dagger \right\rangle = \left(c_L c_{\tilde{\mathbf{L}}} \prod n_{ab;\alpha}! \right) \sum_{\boldsymbol{\sigma}, \tilde{\boldsymbol{\sigma}}} \chi_Q(\mathbf{L}, \boldsymbol{\sigma}) \chi_Q(\tilde{\mathbf{L}}, \tilde{\boldsymbol{\sigma}}) \prod_a \text{tr}_{V_{N_a}}^{n_a} (\sigma_a \tilde{\sigma}_a^{-1}) \quad (3.56)$$

Next, applying (B.13)

$$\begin{aligned} \left\langle \mathcal{O}_Q(\mathbf{L}) \mathcal{O}_Q(\tilde{\mathbf{L}})^\dagger \right\rangle &= \delta_{\mathbf{R}\tilde{\mathbf{R}}} \delta_{\mathbf{r}\tilde{\mathbf{r}}} \delta_{\nu^-\tilde{\nu}^-} \left(c_L^2 \prod n_{ab;\alpha}! \right) \\ &\times \sum_{\boldsymbol{\sigma}} \prod_a \frac{n_a!}{d(R_a)} \text{tr} \left(D^{R_a}(\sigma_a) P_{R_a \rightarrow \bigcup_{b,\alpha} r_{ab;\alpha}}^{\nu_a^+ \tilde{\nu}_a^+} \right) \text{tr}_{V_{N_a}}^{n_a} (\sigma_a) \end{aligned} \quad (3.57)$$

Finally (A.10) gives

$$\begin{aligned} \left\langle \mathcal{O}_Q(\mathbf{L}) \mathcal{O}_Q(\tilde{\mathbf{L}})^\dagger \right\rangle &= \delta_{\mathbf{L}\tilde{\mathbf{L}}} c_L^2 \frac{\prod n_{ab;\alpha}! \prod n_a! \prod d(r_{ab;\alpha})}{\prod d(R_a)} \prod_a f_{N_a}(R_a) \\ &= \delta_{\mathbf{L}\tilde{\mathbf{L}}} \frac{\prod n_{ab;\alpha}!}{\prod n_a!} \prod_a f_{N_a}(R_a) \end{aligned} \quad (3.58)$$

proving (3.51) .

3.4 Covariant basis

We can define another complete, free orthogonal basis, which is a generalization of (3.20)

$$\boxed{\mathcal{O}_Q(\mathbf{K}) = \frac{\sqrt{\prod d(R_a)}}{\prod n_a!} \sum_{\boldsymbol{\sigma}} \chi_Q(\mathbf{K}, \boldsymbol{\sigma}) \mathcal{O}_Q(\mathbf{n}, \boldsymbol{\sigma})} \quad (3.59)$$

We refer to it as the *covariant basis*, because the labels \mathbf{K} include representations of the global symmetry group $\prod_{a,b} U(M_{ab})$. The basis arises from the possibility to “solve the invariance” as in (3.45) using *covariant* quiver characters:

$$\chi_Q(\mathbf{K}, \boldsymbol{\sigma}) = \left(\prod_a D_{i_a j_a}^{R_a}(\sigma_a) B_{j_a \rightarrow \bigcup_b l_{ab}^-}^{R_a \rightarrow \bigcup_b s_{ab}^-, \nu_a^-} B_{i_a \rightarrow \bigcup_b l_{ba}^+}^{R_a \rightarrow \bigcup_b s_{ba}^+, \nu_a^+} \right) \left(\prod_{a,b} B_{l_{ab}}^{\Lambda_{ab} \rightarrow [\mathbf{n}_{ab}], \beta_{ab}} S_{l_{ab}^+ \tilde{l}_{ab}^-, l_{ab}}^{s_{ab}^+ s_{ab}^-, \Lambda_{ab} \tau_{ab}} \right) \quad (3.60)$$

with a different set of labels

$$\mathbf{K} = \{R_a, s_{ab}^+, s_{ab}^-, \nu_a^+, \nu_a^-, \Lambda_{ab}, \tau_{ab}, n_{ab;\alpha}, \beta_{ab}\} \quad (3.61)$$

The covariant quiver characters $\chi_Q(\mathbf{K}, \boldsymbol{\sigma})$ also obey an analogous set of character orthogonality identities, listed in Appendix B.3. For the details of the derivation of the basis and how the two options $\chi_Q(\mathbf{L}, \boldsymbol{\sigma})$ and $\chi_Q(\mathbf{K}, \boldsymbol{\sigma})$ arise see Appendix C.

The covariant quiver characters are again most neatly expressed diagrammatically, as a modification of the original quiver. For $\mathbb{C}^3/\mathbb{Z}_2$ (3.60) becomes

$$\chi_{\mathbb{C}^3/\mathbb{Z}_2}(\mathbf{K}, \boldsymbol{\sigma}) = \Lambda_{11} = [n_{11}] \quad \Lambda_{22} = [n_{22}] \quad (3.62)$$

The labels involved are:

- $R_a \vdash n_a$ diagram associated to each group node factor is the same as before, with finite N cutoff $l(R_a) \leq N_a$.
- Each set of M_{ab} arrows between given pair of nodes is collapsed into one, and there is an associated diagram $\Lambda_{ab} \vdash n_{ab}$, where $n_{ab} = \sum_{\alpha} n_{ab;\alpha}$. It labels a representation of the global symmetry $U(M_{ab})$, and so $l(\Lambda_{ab}) \leq M_{ab}$. Since in $\mathbb{C}^3/\mathbb{Z}_2$ we have $M_{11} = M_{22} = 1$, the associated $\Lambda_{11}, \Lambda_{22}$ are fixed to be single-row diagrams, one-dimensional irreps.
- There are two additional diagrams $s_{ab}^{\pm} \vdash n_{ab}$ associated to each line. In case $M_{ab} = 1$ they are equal $s_{ab}^+ = s_{ab}^-$ and the same as r_{ab} in the restricted basis.
- As in the restricted basis, we have branching at the white nodes $R_a \rightarrow \cup_b s_{ba}^+$ and $R_a \rightarrow \cup_b s_{ba}^-$ and the associated Littlewood-Richardson multiplicity labels ν_a^{\pm} .
- There is a black node on each field line denoting Kronecker product $s_{ab}^+ \otimes s_{ab}^- \rightarrow \Lambda_{ab}$ and the associated Clebsch-Gordan multiplicity label τ_{ab} .

- The extra labels β_{ab} , together with charges $\mathbf{n}_{ab} \equiv \{n_{ab;\alpha}\}$, identify a state in $U(M_{ab})$ irrep Λ_{ab} . That is equivalent to specifying a branching multiplicity label for $\Lambda_{ab} \rightarrow \cup_{\alpha}[n_{ab;\alpha}]$ reduction (see e.g. [12] for this fact).

Let us also note, that in the case of the trivial $\Lambda_{11}, \Lambda_{22}$ the corresponding Clebsch-Gordan coefficient still has to be included in (3.60)

$$S_{i \ j \ , \ 1}^{s^+ s^-, \Lambda=[n]} = \delta_{s^+ s^-} \frac{\delta_{ij}}{\sqrt{d(s^+)}} \quad (3.63)$$

It forces $s^+ = s^-$, and is itself proportional to a delta function, but it includes the coefficient $\frac{1}{\sqrt{d(s)}}$. Diagrammatically

$$\begin{array}{c} \Lambda = [n] \\ | \\ \xrightarrow{s} \bullet \xrightarrow{s} \end{array} = \frac{1}{\sqrt{d(s)}} \xrightarrow{s} \quad (3.64)$$

The key property of this basis is that the transformations under global symmetry group $\prod_{a,b} U(M_{ab})$ are made explicit

- $\{\Lambda_{ab}\}$ labels pick the representation of $\prod_{a,b} U(M_{ab})$
- $\{R_a, s_{ab}^+, s_{ab}^-, \nu_a^+, \nu_a^-, \tau_{ab}\}$ then distinguish different multiplets transforming under $\{\Lambda_{ab}\}$
- $\{\mathbf{n}_{ab}, \beta_{ab}\}$ label a state in $\{\Lambda_{ab}\}$.

The free two-point function in the covariant basis can be calculated in analogous way as in the previous section, now using the properties of covariant characters in Appendix B.3. With our normalization the result is exactly the same as (3.51):

$$\langle \mathcal{O}_Q(\mathbf{K}) \mathcal{O}_Q(\tilde{\mathbf{K}})^\dagger \rangle = \delta_{\mathbf{K}\tilde{\mathbf{K}}} \frac{\prod n_{ab;\alpha}!}{\prod n_a!} \prod_a f_{N_a}(R_a) \quad (3.65)$$

Finally, the inverse basis transformation is:

$$\mathcal{O}_Q(\mathbf{n}, \boldsymbol{\sigma}) = \sum_{\mathbf{K}} \sqrt{\prod d(R_a)} \chi_Q(\mathbf{K}, \boldsymbol{\sigma}) \mathcal{O}_Q(\mathbf{K}) \quad (3.66)$$

3.5 Examples

Let us go over a few specific examples of quivers, to illustrate our general methods.

3.5.1 Conifold

The quiver for the conifold theory is shown in Figure 9. The gauge group is $U(N_1) \times U(N_2)$ and we have bifundamental fields

$$A_1, A_2, B_1, B_2 \quad (3.67)$$

transforming in a global $U(2) \times U(2)$ flavor symmetry. Note according to the labelling in the previous section the fields correspond to $A_1 = \Phi_{12;1}$, $A_2 = \Phi_{12;2}$, $B_1 = \Phi_{21;1}$, $B_2 = \Phi_{21;2}$.

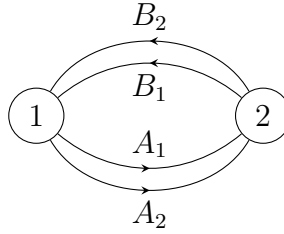


Figure 9: Quiver for the conifold theory.

The gauge invariant mesonic operators are traces of alternating products $\text{tr}(A_{i_1} B_{j_1} A_{i_2} B_{j_2} \dots)$. According to the general prescription (3.31), a general gauge invariant operator can be specified by charges and two permutations

$$\mathcal{O}_C(\mathbf{n}, \{\sigma_1, \sigma_2\}) = \text{tr}_{V_N^{\otimes n}} (\sigma_1(A_1^{\otimes n_1} \otimes A_2^{\otimes n_2}) \sigma_2(B_1^{\otimes m_1} \otimes B_2^{\otimes m_2})) \quad (3.68)$$

or diagrammatically

$$\mathcal{O}_C(\mathbf{n}, \{\sigma_1, \sigma_2\}) = \begin{array}{c} \begin{array}{c} \text{---} \downarrow \text{---} \\ \sigma_1 \\ \downarrow \quad \downarrow \\ A_1^{\otimes n_1} \quad A_2^{\otimes n_2} \\ \downarrow \quad \downarrow \\ \sigma_2 \\ \downarrow \quad \downarrow \\ B_1^{\otimes m_1} \quad B_2^{\otimes m_2} \\ \downarrow \text{---} \end{array} \end{array} \quad (3.69)$$

Here we denote $n = n_1 + n_2 = m_1 + m_2$ the total number of A 's or B 's, which has to be equal.

The counting is given by the split-node quiver, which was shown in Figure 3 and (2.14). Now the restricted quiver characters obtained by inserting (σ_1, σ_2) in the the same split-node quiver are

$$\chi_{\mathcal{C}}(\mathbf{L}, \{\sigma_1, \sigma_2\}) = \begin{array}{ccc} & \nu_1^+ & \nu_2^- \\ & \circ & \circ \\ R_1 \downarrow & \xleftrightarrow{r_{B_2}} & \xleftarrow{r_{B_1}} \\ \boxed{\sigma_1} & & \boxed{\sigma_2} \\ \downarrow & \xleftrightarrow{r_{A_1}} & \uparrow \\ \circ & \xleftarrow{r_{A_2}} & \circ \\ \nu_1^- & & \nu_2^+ \end{array} \quad (3.70)$$

leading to the restricted Schur basis operators (3.48):

$$\mathcal{O}_{\mathcal{C}}(\mathbf{L}) = \frac{1}{(n!)^2} \sqrt{\frac{d(R_1)d(R_2)}{d(r_{A_1})d(r_{A_2})d(r_{B_1})d(r_{B_2})}} \sum_{\sigma_1, \sigma_2} \chi_{\mathcal{C}}(\mathbf{L}, \{\sigma_1, \sigma_2\}) \mathcal{O}_{\mathcal{C}}(\mathbf{n}, \{\sigma_1, \sigma_2\}) \quad (3.71)$$

The labels are

$$\mathbf{L} = \{R_1, R_2, r_{A_1}, r_{A_2}, r_{B_1}, r_{B_2}, \nu_1^{\pm}, \nu_2^{\pm}\} \quad (3.72)$$

where $R_1, R_2 \vdash n$ are Young diagrams associated with each of the group factors, limited to at most N_1, N_2 rows, $r_{A_1}, r_{A_2}, r_{B_1}, r_{B_2}$ are Young diagrams associated with each field type. They are constrained such that R_1, R_2 appear in the Littlewood-Richardson products

$$\begin{aligned} r_{A_1} \otimes r_{A_2} &\rightarrow R_1 \\ r_{A_1} \otimes r_{A_2} &\rightarrow R_2 \\ r_{B_1} \otimes r_{B_2} &\rightarrow R_1 \\ r_{B_1} \otimes r_{B_2} &\rightarrow R_2 \end{aligned} \quad (3.73)$$

and ν_1^{\pm}, ν_2^{\pm} are the associated multiplicity labels, when R_1, R_2 appears more than once in the product.

In this case, as in (3.14) for \mathbb{C}^3 , we can write the restricted quiver character $\chi_{\mathcal{C}}(\mathbf{L}, \boldsymbol{\sigma})$ as a sort of restricted trace. Define a projector

$$(P_{R \rightarrow \mathbf{r} \leftarrow S}^{\nu_1^-, \nu_2^+})_{ij} = \sum_l B_{i \rightarrow l}^{R \rightarrow \mathbf{r}} B_{j \rightarrow l}^{S \rightarrow \mathbf{r}} \quad (3.74)$$

which projects from two different representations R, S of S_n into the same irrep $\mathbf{r} = (r_1, r_2)$ of the subgroup $S_{n_1} \times S_{n_2}$. Then we can write the quiver character as

$$\chi_{\mathcal{C}}(\mathbf{L}, \{\sigma_1, \sigma_2\}) = \text{tr} \left(D^{R_1}(\sigma_1) P_{R_1 \rightarrow \mathbf{r}_A \leftarrow R_2}^{\nu_1^-, \nu_2^+} D^{R_2}(\sigma_2) P_{R_2 \rightarrow \mathbf{r}_B \leftarrow R_2}^{\nu_2^-, \nu_1^+} \right) \quad (3.75)$$

The Restricted Schur basis operators are, explicitly:

$$\mathcal{O}_{\mathcal{C}}(\mathbf{L}) = c_{\mathbf{L}} \sum_{\sigma_1, \sigma_2} \text{tr} \left(D^{R_1}(\sigma_1) P_{R_1 \rightarrow \mathbf{r}_A \leftarrow R_2}^{\nu_1^-, \nu_2^+} D^{R_2}(\sigma_2) P_{R_2 \rightarrow \mathbf{r}_B \leftarrow R_2}^{\nu_2^-, \nu_1^+} \right) \mathcal{O}_{\mathcal{C}}(\mathbf{n}, \{\sigma_1, \sigma_2\}) \quad (3.76)$$

Let us demonstrate the simplest example, with the charges $\mathbf{n} = \{1, 1, 1, 1\}$, that is, each field occurs once. The only choice for r diagrams is

$$r_{A_1} = r_{A_2} = r_{B_1} = r_{B_2} = \square \quad (3.77)$$

Littlewood-Richardson product is

$$\square \otimes \square \rightarrow \square \square \oplus \begin{array}{|c|} \hline \square \\ \hline \square \\ \hline \end{array} \quad (3.78)$$

each diagram appearing once, so there is no multiplicity. We can choose each R_1, R_2 independently to be either of the diagrams, giving 4 operators

$$\begin{aligned} & \mathcal{O}(\square \square, \square \square) \\ &= \frac{1}{4} (\text{tr}(A_1 B_1) \text{tr}(A_2 B_2) + \text{tr}(A_1 B_2) \text{tr}(A_2 B_1) + \text{tr}(A_1 B_1 A_2 B_2) + \text{tr}(A_1 B_2 A_2 B_1)) \\ & \mathcal{O}(\begin{array}{|c|} \hline \square \\ \hline \square \\ \hline \end{array}, \begin{array}{|c|} \hline \square \\ \hline \square \\ \hline \end{array}) \\ &= \frac{1}{4} (\text{tr}(A_1 B_1) \text{tr}(A_2 B_2) + \text{tr}(A_1 B_2) \text{tr}(A_2 B_1) - \text{tr}(A_1 B_1 A_2 B_2) - \text{tr}(A_1 B_2 A_2 B_1)) \\ & \mathcal{O}(\square \square, \begin{array}{|c|} \hline \square \\ \hline \square \\ \hline \end{array}) \\ &= \frac{1}{4} (\text{tr}(A_1 B_1) \text{tr}(A_2 B_2) - \text{tr}(A_1 B_2) \text{tr}(A_2 B_1) + \text{tr}(A_1 B_1 A_2 B_2) - \text{tr}(A_1 B_2 A_2 B_1)) \\ & \mathcal{O}(\begin{array}{|c|} \hline \square \\ \hline \square \\ \hline \end{array}, \square \square) \\ &= \frac{1}{4} (\text{tr}(A_1 B_1) \text{tr}(A_2 B_2) - \text{tr}(A_1 B_2) \text{tr}(A_2 B_1) - \text{tr}(A_1 B_1 A_2 B_2) + \text{tr}(A_1 B_2 A_2 B_1)) \end{aligned} \quad (3.79)$$

It can be checked that they are orthogonal in the free field metric. These operators are particularly easy to evaluate, since all the representations are one-dimensional, and so all branching coefficients are equal to 1. The only dependence comes from $D^{R_1}(\sigma_1)$, $D^{R_2}(\sigma_2)$. Note also the way this basis captures finite- N cutoff: if $N = 1$ the height of R_1, R_2 is limited to 1, so the only operator that survives is $\mathcal{O}(\square \square, \square \square)$. It is easy to see that the others are 0 if the fields are replaced by scalar values.

Covariant basis operators (3.59) for conifold are

$$\mathcal{O}_c(\mathbf{K}) = \frac{\sqrt{d(R_1)d(R_2)}}{(n!)^2} \sum_{\sigma_1, \sigma_2} \chi_c(\mathbf{K}, \{\sigma_1, \sigma_2\}) \mathcal{O}_c(\mathbf{n}, \{\sigma_1, \sigma_2\}) \quad (3.80)$$

$$\chi_c(\mathbf{K}, \{\sigma_1, \sigma_2\}) = \begin{array}{c} \begin{array}{c} \beta_B \text{ } [m_1, m_2] \\ | \\ \circ \\ | \\ \Lambda_B \end{array} \\ \begin{array}{c} \xrightarrow{R_1} \tau_B \xrightarrow{R_2} \\ \xleftarrow{R_1} \tau_A \xleftarrow{R_2} \end{array} \\ \begin{array}{c} \beta_A \text{ } [n_1, n_2] \\ | \\ \circ \\ | \\ \Lambda_A \end{array} \end{array} \quad (3.81)$$

with the labels

$$\mathbf{K} = \{R_1, R_2, \Lambda_A, \Lambda_B, \tau_A, \tau_B, \mathbf{n}, \beta_A, \beta_B\} \quad (3.82)$$

The $R_1, R_2 \vdash n$ are Young diagrams associated to the group nodes like before. But now, instead of r_{A_i}, r_{B_i} we have global symmetry representation labels $\Lambda_A, \Lambda_B \vdash n$. They are constrained to appear in the irrep decomposition of the S_n Kronecker product

$$\begin{aligned} R_1 \otimes R_2 &\rightarrow \Lambda_A \\ R_1 \otimes R_2 &\rightarrow \Lambda_B \end{aligned} \quad (3.83)$$

If Λ_A, Λ_B appear multiple times in the decomposition, τ_A, τ_B is the multiplicity label. The remaining labels $\{n_A, n_B, \beta_A, \beta_B\}$ then label a specific state in the $U(M) \times U(M)$ irrep (Λ_A, Λ_B) . Note, compared to the general case (3.61), we do not need additional labels $s_A^\pm, s_B^\pm, \nu_1^\pm, \nu_2^\pm$. This is because there is no “branching” in the quiver – all arrows outgoing from node 1 go to node 2 and vice-versa, which enforces $R_1 = s_A^- = s_B^+$ and $R_2 = s_A^+ = s_B^-$.

Let us again work out the example with $n = 2$, that is 2 A fields and 2 B fields. Like with Restricted Schur basis, we have 4 choices for R_1, R_2 . In this simple case Λ_A, Λ_B are uniquely determined by the choice of R_1, R_2 , since

$$\begin{array}{l} \begin{array}{c} \square \square \otimes \square \square \rightarrow \square \square \\ \square \square \otimes \begin{array}{c} \square \\ \square \end{array} \rightarrow \begin{array}{c} \square \\ \square \end{array} \\ \begin{array}{c} \square \\ \square \end{array} \otimes \begin{array}{c} \square \\ \square \end{array} \rightarrow \square \square \end{array} \end{array} \quad (3.84)$$

that is, only one irrep appears in the product, so $\Lambda_A = \Lambda_B = R_1 \otimes R_2$. For each choice of

$R_1, R_2, \Lambda_A, \Lambda_B$ we list the highest-weight state in (Λ_A, Λ_B) :

$$\begin{aligned}
\mathcal{O}^{\text{hw}}(R_1 = \begin{array}{|c|c|} \hline & \\ \hline \end{array}, R_2 = \begin{array}{|c|c|} \hline & \\ \hline \end{array}, \Lambda_A = \Lambda_B = \begin{array}{|c|c|} \hline & \\ \hline \end{array}) &= \frac{1}{2} \text{tr}(A_1 B_1) \text{tr}(A_1 B_1) + \frac{1}{2} \text{tr}(A_1 B_1 A_1 B_1) \\
\mathcal{O}^{\text{hw}}(R_1 = \begin{array}{|c|} \hline & \\ \hline \end{array}, R_2 = \begin{array}{|c|} \hline & \\ \hline \end{array}, \Lambda_A = \Lambda_B = \begin{array}{|c|c|} \hline & \\ \hline \end{array}) &= \frac{1}{2} \text{tr}(A_1 B_1) \text{tr}(A_1 B_1) - \frac{1}{2} \text{tr}(A_1 B_1 A_1 B_1) \\
\mathcal{O}^{\text{hw}}(R_1 = \begin{array}{|c|c|} \hline & \\ \hline \end{array}, R_2 = \begin{array}{|c|} \hline & \\ \hline \end{array}, \Lambda_A = \Lambda_B = \begin{array}{|c|} \hline & \\ \hline \end{array}) &= \frac{1}{4} (\text{tr}(A_1 B_1) \text{tr}(A_2 B_2) - \text{tr}(A_1 B_2) \text{tr}(A_2 B_1) + \text{tr}(A_1 B_1 A_2 B_2) - \text{tr}(A_1 B_2 A_2 B_1)) \\
\mathcal{O}^{\text{hw}}(R_1 = \begin{array}{|c|} \hline & \\ \hline \end{array}, R_2 = \begin{array}{|c|c|} \hline & \\ \hline \end{array}, \Lambda_A = \Lambda_B = \begin{array}{|c|} \hline & \\ \hline \end{array}) &= \frac{1}{4} (\text{tr}(A_1 B_1) \text{tr}(A_2 B_2) - \text{tr}(A_1 B_2) \text{tr}(A_2 B_1) - \text{tr}(A_1 B_1 A_2 B_2) + \text{tr}(A_1 B_2 A_2 B_1))
\end{aligned} \tag{3.85}$$

3.5.2 $\mathbb{C}^3/\mathbb{Z}_2$

We have used the theory of $D3$ branes on a $\mathbb{C}^3/\mathbb{Z}_2$ singularity throughout, so here we just collect the references.

The quiver and the split-node quiver is displayed in Figure 4. The gauge symmetry is $U(N_1) \times U(N_2)$ and the global symmetry in the free limit is $U(2) \times U(2)$. The split-node quiver leads to counting (2.15). The restricted characters $\chi_{\mathbb{C}^3/\mathbb{Z}_2}(\mathbf{L}, \boldsymbol{\sigma})$ that give an explicit implementation of the counting are shown in (3.49). Combining with the operators $\mathcal{O}_{\mathbb{C}^3/\mathbb{Z}_2}(\mathbf{n}, \boldsymbol{\sigma})$ shown in (3.30) we get the basis $\mathcal{O}_{\mathbb{C}^3/\mathbb{Z}_2}(\mathbf{L})$ (3.48). The labels are

$$\mathbf{L} = \{R_1, R_2, r_{11}, r_{22}, r_{12;1}, r_{12;2}, r_{21;1}, r_{21;2}, \nu_1^\pm, \nu_2^\pm\} \tag{3.86}$$

The covariant basis $\mathcal{O}_{\mathbb{C}^3/\mathbb{Z}_2}(\mathbf{K})$ is built with covariant characters shown in (3.62).

3.5.3 dP_0

The theory of $D3$ branes on $\mathbb{C}^3/\mathbb{Z}^3$ singularity [49], also known as dP_0 , has a quiver shown in Figure 10. The gauge group is $U(N_1) \times U(N_2) \times U(N_3)$, and we have a total of 9 bifundamental chiral multiplets

$$\{\Phi_{12;\alpha}, \Phi_{23;\alpha}, \Phi_{31;\alpha}\}, \quad \alpha \in \{1, 2, 3\} \tag{3.87}$$

There is a global flavor symmetry group $U(3) \times U(3) \times U(3)$. The counting of finite- N gauge invariant operators following (2.12) is given by the labelled split-node quiver, also

in Figure 10:

$$\begin{aligned}
\mathcal{N}_{dP_0}(\{n_{ab;\alpha}\}; N_1, N_2, N_3) = & \sum_{\substack{R_1 \vdash n \\ l(R_1) \leq N_1}} \sum_{\substack{R_2 \vdash n \\ l(R_2) \leq N_1}} \sum_{\substack{R_3 \vdash n \\ l(R_3) \leq N_1}} \sum_{\{r_{12;\alpha}\}} \sum_{\{r_{23;\alpha}\}} \sum_{\{r_{31;\alpha}\}} \\
& g(\{r_{31;\alpha}\}; R_1) g(\{r_{12;\alpha}\}; R_1) g(\{r_{12;\alpha}\}; R_2) g(\{r_{23;\alpha}\}; R_2) g(\{r_{23;\alpha}\}; R_3) g(\{r_{31;\alpha}\}; R_3)
\end{aligned} \tag{3.88}$$

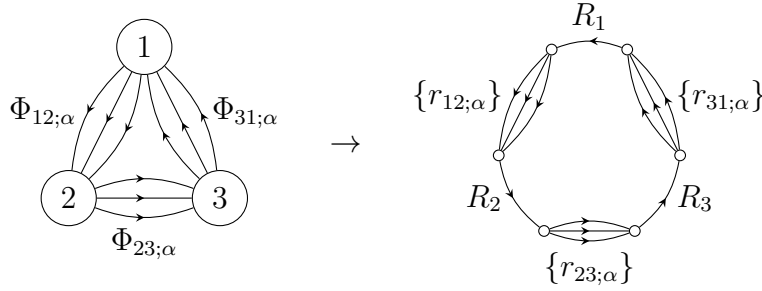


Figure 10: Quiver for dP_0 theory, and the split-node quiver for operator counting.

The gauge invariant mesonic operators are traces of products going around the quiver $\text{tr}(\Phi_{12;\alpha_1} \Phi_{23;\alpha_2} \Phi_{31;\alpha_3} \Phi_{12;\alpha_4} \dots)$. According to the general prescription (3.31), a general gauge invariant operator can be specified by charges and three permutations

$$\mathcal{O}_{dP_0}(\mathbf{n}, \{\sigma_1, \sigma_2, \sigma_3\}) = \text{tr}_{V_N^{\otimes n}} (\sigma_1 (\Phi_{12;\alpha})^{\otimes \{n_{12;\alpha}\}} \sigma_2 (\Phi_{23;\alpha})^{\otimes \{n_{23;\alpha}\}} \sigma_3 (\Phi_{31;\alpha})^{\otimes \{n_{31;\alpha}\}}) \tag{3.89}$$

Here $n = \sum_{\alpha} n_{12;\alpha} = \sum_{\alpha} n_{23;\alpha} = \sum_{\alpha} n_{31;\alpha}$ is the total number of $\Phi_{12;\alpha}$'s or $\Phi_{23;\alpha}$'s or $\Phi_{31;\alpha}$'s. Since the dP_0 quiver is “linear”, without any branchings like in $\mathbb{C}^3/\mathbb{Z}_2$, we can think of the operators $\mathcal{O}_{dP_0}(\mathbf{n}, \boldsymbol{\sigma})$ as traces in $V_N^{\otimes n}$.

Restricted Schur basis operators (3.48) are:

$$\mathcal{O}_{dP_0}(\mathbf{L}) = c_{\mathbf{L}} \sum_{\sigma_1, \sigma_2, \sigma_3} \chi_{dP_0}(\mathbf{L}, \{\sigma_1, \sigma_2, \sigma_3\}) \mathcal{O}_{dP_0}(\mathbf{n}, \{\sigma_1, \sigma_2, \sigma_3\}) \tag{3.90}$$

with the restricted quiver character as a further decorated split-node quiver:

$$\chi_{dP_0}(\mathbf{L}, \{\sigma_1, \sigma_2, \sigma_3\}) = \text{Diagram} \quad (3.91)$$

The labels are

$$\mathbf{L} = \{R_1, R_2, R_3, r_{12;\alpha}, r_{23;\alpha}, r_{31;\alpha}, \nu_1^\pm, \nu_2^\pm, \nu_3^\pm\} \quad (3.92)$$

Covariant basis operators (3.59) for dP_0 are

$$\mathcal{O}_{dP_0}(\mathbf{K}) = \frac{\sqrt{d(R_1)d(R_2)d(R_3)}}{(n!)^3} \sum_{\sigma_1, \sigma_2, \sigma_3} \chi_{dP_0}(\mathbf{K}, \{\sigma_1, \sigma_2, \sigma_3\}) \mathcal{O}_{dP_0}(\mathbf{n}, \{\sigma_1, \sigma_2, \sigma_3\}) \quad (3.93)$$

$$\chi_{dP_0}(\mathbf{K}, \{\sigma_1, \sigma_2, \sigma_3\}) = \text{Diagram} \quad (3.94)$$

with the labels

$$\mathbf{K} = \{R_1, R_2, R_3, \Lambda_{12}, \Lambda_{23}, \Lambda_{31}, \tau_{ab}, n_{ab;\alpha}, \beta_{ab}\} \quad (3.95)$$

That is, an operator $U(M)^3$ multiplet is defined by the global symmetry irrep $(\Lambda_{12}, \Lambda_{23}, \Lambda_{31})$, the diagrams $R_1, R_2, R_3 \vdash n$ for each gauge group factor and 3 multiplicity labels τ_{ab} for Clebsch-Gordan decompositions

$$\begin{aligned} R_1 \otimes R_2 &\rightarrow \Lambda_{12} \\ R_2 \otimes R_3 &\rightarrow \Lambda_{23} \\ R_3 \otimes R_1 &\rightarrow \Lambda_{31} \end{aligned} \quad (3.96)$$

3.5.4 $\mathbb{C}^2/\mathbb{Z}_n \times \mathbb{C}$

As a final example let us take the quiver of the $\mathbb{C}^2/\mathbb{Z}_n \times \mathbb{C}$ theory [4], Figure 11. In $\mathcal{N} = 1$ language it is a circular quiver with n nodes and fields $\Phi_{a,a+1}, \Phi_{a,a-1}, \Phi_{a,a}$.

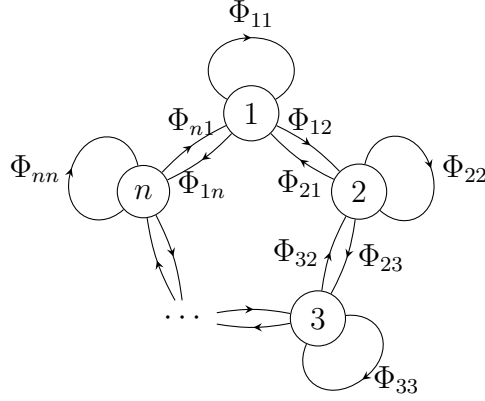


Figure 11: $\mathbb{C}^2/\mathbb{Z}_n \times \mathbb{C}$ quiver

The corresponding split-node quiver is shown in Figure 12. This leads to finite- N

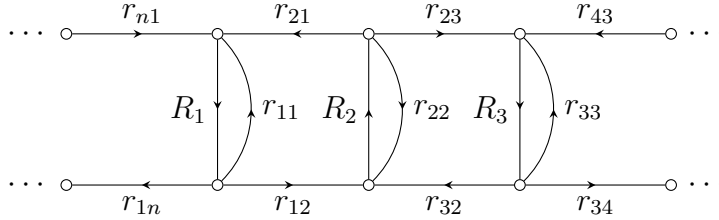


Figure 12: Split-node quiver for $\mathbb{C}^2/\mathbb{Z}_n \times \mathbb{C}$

counting of operators

$$\begin{aligned} \mathcal{N}_{\mathbb{C}^2/\mathbb{Z}_n \times \mathbb{C}}(\{n_{ab}\}, \{N_a\}) &= \sum_{\substack{\{R_a \vdash n_a\} \\ l(R_a) \leq N_a}} \sum_{\{r_{a,a+1}\}} \sum_{\{r_{a,a-1}\}} \sum_{\{r_{a,a}\}} \\ &\prod_a g(r_{a,a}, r_{a,a-1}, r_{a,a+1}; R_a) g(r_{a,a}, r_{a-1,a}, r_{a+1,a}; R_a) \end{aligned} \quad (3.97)$$

The restricted Schur basis $\mathcal{O}_Q(\mathbf{L})$ can be constructed by writing down quiver characters according to the split-node quiver, with the multiplicity labels ν_a^\pm .

4 Chiral ring structure constants

In this section we obtain general expressions for the chiral ring structure constants. In Section 4.1 we work out the result for the restricted Schur basis

$$\mathcal{O}_Q(\mathbf{L}^{(1)})\mathcal{O}_Q(\mathbf{L}^{(2)}) \equiv \sum_{\mathbf{L}^{(3)}} G(\mathbf{L}^{(1)}, \mathbf{L}^{(2)}; \mathbf{L}^{(3)}) \mathcal{O}_Q(\mathbf{L}^{(3)}) \quad (4.1)$$

and in Section 4.2 we deal with the covariant basis

$$\mathcal{O}_Q(\mathbf{K}^{(1)})\mathcal{O}_Q(\mathbf{K}^{(2)}) \equiv \sum_{\mathbf{K}^{(3)}} G(\mathbf{K}^{(1)}, \mathbf{K}^{(2)}; \mathbf{K}^{(3)}) \mathcal{O}_Q(\mathbf{K}^{(3)}) \quad (4.2)$$

We find that $G(\mathbf{L}^{(1)}, \mathbf{L}^{(2)}; \mathbf{L}^{(3)})$ and $G(\mathbf{K}^{(1)}, \mathbf{K}^{(2)}; \mathbf{K}^{(3)})$ can be written diagrammatically. They involve two types of vertices — solid vertices for inner products; and white vertices for outer products.

The main result is that all Young diagram labels combine according to the Littlewood-Richardson rule. For the restricted Schur basis the resulting diagram (4.9) involves the branching coefficients for $R_a^{(3)} \rightarrow (R_a^{(1)}, R_a^{(2)})$ and $r_{ab;\alpha}^{(3)} \rightarrow (r_{ab;\alpha}^{(1)}, r_{ab;\alpha}^{(2)})$

$$G(\mathbf{L}^{(1)}, \mathbf{L}^{(2)}; \mathbf{L}^{(3)}) \sim \prod_a \begin{array}{c} \downarrow R_a^{(3)} \\ \circ \\ \swarrow R_a^{(1)} \quad \searrow R_a^{(2)} \end{array} \prod_{a,b,\alpha} \begin{array}{c} \downarrow r_{ab;\alpha}^{(3)} \\ \circ \\ \swarrow r_{ab;\alpha}^{(1)} \quad \searrow r_{ab;\alpha}^{(2)} \end{array} \quad (4.3)$$

and so the chiral ring structure constant vanishes unless the Littlewood-Richardson coefficients $g(R_a^{(1)}, R_a^{(2)}; R_a^{(3)})$ and $g(r_{ab;\alpha}^{(1)}, r_{ab;\alpha}^{(2)}; r_{ab;\alpha}^{(3)})$ are all non-zero.

Analogously, the covariant basis structure constants (4.25) involve the branching coefficients for $R_a^{(3)} \rightarrow (R_a^{(1)}, R_a^{(2)})$, $\Lambda_{ab}^{(3)} \rightarrow (\Lambda_{ab}^{(1)}, \Lambda_{ab}^{(2)})$ and $s_{ab}^{(3)\pm} \rightarrow (s_{ab}^{(1)\pm}, s_{ab}^{(2)\pm})$

$$G(\mathbf{K}^{(1)}, \mathbf{K}^{(2)}; \mathbf{K}^{(3)}) \sim \prod_a \begin{array}{c} \downarrow R_a^{(3)} \\ \circ \\ \swarrow R_a^{(1)} \quad \searrow R_a^{(2)} \end{array} \prod_{a,b} \begin{array}{c} \downarrow \Lambda_{ab}^{(3)} \\ \circ \\ \swarrow \Lambda_{ab}^{(1)} \quad \searrow \Lambda_{ab}^{(2)} \end{array} \begin{array}{c} \downarrow s_{ab}^{(3)+} \\ \circ \\ \swarrow s_{ab}^{(1)+} \quad \searrow s_{ab}^{(2)+} \end{array} \begin{array}{c} \downarrow s_{ab}^{(3)-} \\ \circ \\ \swarrow s_{ab}^{(1)-} \quad \searrow s_{ab}^{(2)-} \end{array} \quad (4.4)$$

and thus vanish unless $g(R_a^{(1)}, R_a^{(2)}; R_a^{(3)})$, $g(\Lambda_{ab}^{(1)}, \Lambda_{ab}^{(2)}; \Lambda_{ab}^{(3)})$, $g(s_{ab}^{(1)\pm}, s_{ab}^{(2)\pm}; s_{ab}^{(3)\pm})$ are all non-zero.

Note that, if we consider correlators of n holomorphic operators and one anti-holomorphic, the coefficient would involve the appropriate Littlewood-Richardson coefficient for the branching $R_a^{(n+1)} \rightarrow (R_a^{(1)}, R_a^{(2)}, \dots, R_a^{(n)})$ and so on for other labels. We leave it as an exercise for the reader to write out the explicit formulae for that case, following the analogous expressions we present for $n = 2$, i.e two holomorphic operators fusing into one.

4.1 Restricted Schur basis

Consider the product of operators (3.48)

$$\begin{aligned}
& \mathcal{O}_Q(\mathbf{L}^{(1)})\mathcal{O}_Q(\mathbf{L}^{(2)}) \\
&= \frac{1}{\prod n_a^{(1)}!} \frac{1}{\prod n_a^{(2)}!} \sum_{\boldsymbol{\sigma}^{(1)}} \sum_{\boldsymbol{\sigma}^{(2)}} \hat{\chi}_Q(\mathbf{L}^{(1)}, \boldsymbol{\sigma}^{(1)}) \hat{\chi}_Q(\mathbf{L}^{(2)}, \boldsymbol{\sigma}^{(2)}) \mathcal{O}_Q(\boldsymbol{\sigma}^{(1)}) \mathcal{O}_Q(\boldsymbol{\sigma}^{(2)}) \\
&= \frac{1}{\prod n_a^{(1)}!} \frac{1}{\prod n_a^{(2)}!} \sum_{\boldsymbol{\sigma}^{(1)}} \sum_{\boldsymbol{\sigma}^{(2)}} \hat{\chi}_Q(\mathbf{L}^{(1)}, \boldsymbol{\sigma}^{(1)}) \hat{\chi}_Q(\mathbf{L}^{(2)}, \boldsymbol{\sigma}^{(2)}) \mathcal{O}_Q(\boldsymbol{\sigma}^{(1)} \circ \boldsymbol{\sigma}^{(2)})
\end{aligned} \tag{4.5}$$

Here we use a conveniently normalized quiver character

$$\hat{\chi}_Q(\mathbf{L}, \boldsymbol{\sigma}) \equiv \sqrt{\frac{\prod d(R_a)}{\prod d(r_{ab;\alpha})}} \chi_Q(\mathbf{L}, \boldsymbol{\sigma}) \tag{4.6}$$

The outer product $\boldsymbol{\sigma}^{(1)} \circ \boldsymbol{\sigma}^{(2)}$ consists of pairs of permutations $\sigma_a^{(1)} \circ \sigma_a^{(2)}$ in $S_{n_a^{(1)}} \times S_{n_a^{(2)}} \subset S_{n_a^{(1)}+n_a^{(2)}}$. We can expand the permutation-basis operators as a sum of Fourier basis operators using (3.50) to get

$$\begin{aligned}
& \mathcal{O}_Q(\mathbf{L}^{(1)})\mathcal{O}_Q(\mathbf{L}^{(2)}) \\
&= \frac{1}{\prod n_a^{(1)}!} \frac{1}{\prod n_a^{(2)}!} \sum_{\boldsymbol{\sigma}^{(1)}} \sum_{\boldsymbol{\sigma}^{(2)}} \sum_{\mathbf{L}^{(3)}} \hat{\chi}_Q(\mathbf{L}^{(1)}, \boldsymbol{\sigma}^{(1)}) \hat{\chi}_Q(\mathbf{L}^{(2)}, \boldsymbol{\sigma}^{(2)}) \hat{\chi}_Q(\mathbf{L}^{(3)}, \boldsymbol{\sigma}^{(1)} \circ \boldsymbol{\sigma}^{(2)}) \mathcal{O}_Q(\mathbf{L}^{(3)}) \\
&\equiv \sum_{\mathbf{L}^{(3)}} G(\mathbf{L}^{(1)}, \mathbf{L}^{(1)}; \mathbf{L}^{(3)}) \mathcal{O}_Q(\mathbf{L}^{(3)})
\end{aligned} \tag{4.7}$$

The sum $\mathbf{L}^{(3)}$ runs over labels with $\mathbf{n}^{(3)} = \mathbf{n}^{(1)} + \mathbf{n}^{(2)}$. This leads to the expression for the chiral ring structure constants

$$G(\mathbf{L}^{(1)}, \mathbf{L}^{(1)}; \mathbf{L}^{(3)}) = \frac{1}{\prod n_a^{(1)}!} \frac{1}{\prod n_a^{(2)}!} \sum_{\boldsymbol{\sigma}^{(1)}} \sum_{\boldsymbol{\sigma}^{(2)}} \hat{\chi}_Q(\mathbf{L}^{(1)}, \boldsymbol{\sigma}^{(1)}) \hat{\chi}_Q(\mathbf{L}^{(2)}, \boldsymbol{\sigma}^{(2)}) \hat{\chi}_Q(\mathbf{L}^{(3)}, \boldsymbol{\sigma}^{(1)} \circ \boldsymbol{\sigma}^{(2)}) \tag{4.8}$$

which can be evaluating by doing the sums over $\boldsymbol{\sigma}^{(1)}, \boldsymbol{\sigma}^{(2)}$.

Let us first describe the answer and then sketch the steps in the derivation. The final

result is, diagrammatically:

$$G(\mathbf{L}^{(1)}, \mathbf{L}^{(2)}; \mathbf{L}^{(3)}) = f_{\mathbf{L}^{(1)}\mathbf{L}^{(2)}}^{\mathbf{L}^{(3)}} \sum_{\{\mu_a\}} \sum_{\{\mu_{ab;\alpha}\}} \prod_a \left(\begin{array}{c} \text{Diagram 1} \quad \text{Diagram 2} \end{array} \right) \quad (4.9)$$

with the constant prefactor

$$f_{\mathbf{L}^{(1)}\mathbf{L}^{(2)}}^{\mathbf{L}^{(3)}} = \sqrt{\frac{\prod_a d(R_a^{(1)})d(R_a^{(2)})d(R_a^{(3)})}{\prod_{a,b,\alpha} d(r_{ab;\alpha}^{(1)})d(r_{ab;\alpha}^{(2)})d(r_{ab;\alpha}^{(3)})}} \frac{1}{\prod_a d(R_a^{(1)})d(R_a^{(2)})} \frac{1}{\prod_{a,b,\alpha} d(r_{ab;\alpha}^{(1)})d(r_{ab;\alpha}^{(2)})} \quad (4.10)$$

For illustration purposes in (4.9) we draw three outgoing arrows $r_{ab;\alpha}$ from each branching node ν_a^- and three incoming arrows $r_{ba;\alpha}$ to each branching node ν_a^+ . The precise structure depends on the quiver (on the other hand, the lines and nodes labelled by $^{(1),(2),(3)}$ are always three, associated with the three operators).

The explicit expression corresponding to (4.9) is

$$G(\mathbf{L}^{(1)}, \mathbf{L}^{(2)}; \mathbf{L}^{(3)}) = f_{\mathbf{L}^{(1)}\mathbf{L}^{(2)}}^{\mathbf{L}^{(3)}} \sum_{\{\mu_a\}} \sum_{\{\mu_{ab;\alpha}\}} \prod_a \mathcal{F} \left(\cup_I R_a^{(I)}, \{\cup_{I,b,\alpha} r_{ab;\alpha}^{(I)}\}, \cup_I \nu_a^{(I)-}; \mu_a, \{\cup_{b,\alpha} \mu_{ab;\alpha}\} \right) \times \mathcal{F} \left(\cup_I R_a^{(I)}, \{\cup_{I,b,\alpha} r_{ba;\alpha}^{(I)}\}, \cup_I \nu_a^{(I)+}; \mu_a, \{\cup_{b,\alpha} \mu_{ba;\alpha}\} \right) \quad (4.11)$$

with the object \mathcal{F} equal to the single connected piece in (4.9):

$$\mathcal{F} \left(\cup_I R^{(I)}, \{\cup_{I,\alpha} r_{\alpha}^{(I)}\}, \cup_I \nu^{(I)}; \mu, \{\cup_{\alpha} \mu_{\alpha}\} \right) = B_{i^{(1)} \rightarrow \cup_{\alpha} l_{\alpha}^{(1)}}^{R^{(1)} \rightarrow \cup_{\alpha} r_{\alpha}^{(1)}; \nu^{(1)+}} B_{i^{(2)} \rightarrow \cup_{\alpha} l_{\alpha}^{(2)}}^{R^{(2)} \rightarrow \cup_{\alpha} r_{\alpha}^{(2)}; \nu^{(2)+}} B_{i^{(3)} \rightarrow \cup_{\alpha} l_{\alpha}^{(3)}}^{R^{(3)} \rightarrow \cup_{\alpha} r_{\alpha}^{(3)}; \nu^{(3)+}} B_{i^{(3)} \rightarrow i^{(1)}, i^{(2)}}^{R^{(3)} \rightarrow R^{(1)}, R^{(2)}; \mu} \prod_{\alpha} B_{l_{\alpha}^{(3)} \rightarrow l_{\alpha}^{(1)}, l_{\alpha}^{(2)}}^{r_{\alpha}^{(3)} \rightarrow r_{\alpha}^{(1)}, r_{\alpha}^{(2)}; \mu_{\alpha}} \quad (4.12)$$

The two pieces $\mathcal{F}(\cup_I R_a^{(I)}, \{\cup_{I,b,\alpha} r_{ab;\alpha}^{(I)}\}, \cup_I \nu_a^{(I)-}; \mu_a, \{\cup_{b,\alpha} \mu_{ab;\alpha}\})$ and $\mathcal{F}(\cup_I R_a^{(I)}, \{\cup_{I,b,\alpha} r_{ba;\alpha}^{(I)}\}, \cup_I \nu_a^{(I)+}; \mu_a, \{\cup_{b,\alpha} \mu_{ba;\alpha}\})$ originally appear with reversed arrows, but have the same expression (4.12) due to reality of branching coefficients.

The key feature of (4.9) is that sums μ_a are over multiplicity $g(R_a^{(1)}, R_a^{(2)}; R_a^{(3)})$ and $\mu_{ab;\alpha}$ are over $g(r_{ab;\alpha}^{(1)}, r_{ab;\alpha}^{(2)}; r_{ab;\alpha}^{(3)})$, and so the structure constant vanishes, unless all diagrams of $\mathbf{L}^{(3)}$ appear in the respective Littlewood-Richardson products

$$\boxed{\begin{array}{l} R_a^{(1)} \otimes R_a^{(2)} \rightarrow R_a^{(3)} \\ r_{ab;\alpha}^{(1)} \otimes r_{ab;\alpha}^{(2)} \rightarrow r_{ab;\alpha}^{(3)} \end{array}} \quad (4.13)$$

The branching coefficients in (4.9) are contracted in the natural way, given these selection rules. For each group node a there are two terms – one for ν^+ and one for ν^- . Within each term, the branching coefficients arising from each operator $B^{R_a^{(I)} \rightarrow \cup_{b,\alpha} r_{ab;\alpha}^{(I)}; \nu_a^{(I)\pm}}$ are coupled via extra branching coefficients: $B^{R_a^{(3)} \rightarrow R_a^{(1)}, R_a^{(2)}; \mu_a}$ for R_a 's, and $B^{r_{ab;\alpha}^{(3)} \rightarrow r_{ab;\alpha}^{(1)}, r_{ab;\alpha}^{(2)}; \mu_{ab;\alpha}}$ for $r_{ab;\alpha}$'s.

Let us take as an example the structure constants of \mathbb{C}^3 , which were discussed in the restricted Schur basis in [50]. The operators are defined via quiver characters (3.17), and for a single-node quiver (4.9) reduces to:

$$G_{\mathbb{C}^3}(\mathbf{L}^{(1)}, \mathbf{L}^{(2)}; \mathbf{L}^{(3)}) = f_{\mathbf{L}^{(1)}\mathbf{L}^{(2)}}^{\mathbf{L}^{(3)}} \sum_{\substack{\mu, \\ \mu_1, \mu_2, \mu_3}} \nu^{(1)+} \nu^{(2)+} \nu^{(3)+} \nu^{(1)-} \nu^{(2)-} \nu^{(3)-} \quad (4.14)$$

Let us now go over the steps in the derivation of (4.9). For clarity we mostly use diagrammatic notation. The starting point is the sum (4.8), which we write out as a trace of a product of group factors

$$G(\mathbf{L}^{(1)}, \mathbf{L}^{(2)}; \mathbf{L}^{(3)}) = \tilde{f}_{\mathbf{L}^{(1)}\mathbf{L}^{(2)}}^{\mathbf{L}^{(3)}} \text{tr} \prod_a \left(\frac{1}{n_a^{(1)}! n_a^{(2)}!} \sum_{\sigma_a^{(1)}, \sigma_a^{(2)}} \begin{array}{c} \bigcup_{b,\alpha} r_{ba;\alpha}^{(1)} \\ \downarrow \\ \nu_a^{(1)+} \\ \downarrow \\ \boxed{\sigma_a^{(1)}} \\ \downarrow \\ R_a^{(1)} \\ \downarrow \\ \nu_a^{(1)-} \\ \downarrow \\ \bigcup_{b,\alpha} r_{ab;\alpha}^{(1)} \end{array} \begin{array}{c} \bigcup_{b,\alpha} r_{ba;\alpha}^{(2)} \\ \downarrow \\ \nu_a^{(2)+} \\ \downarrow \\ \boxed{\sigma_a^{(2)}} \\ \downarrow \\ R_a^{(2)} \\ \downarrow \\ \nu_a^{(2)-} \\ \downarrow \\ \bigcup_{b,\alpha} r_{ab;\alpha}^{(2)} \end{array} \begin{array}{c} \bigcup_{b,\alpha} r_{ba;\alpha}^{(3)} \\ \downarrow \\ \nu_a^{(3)+} \\ \downarrow \\ \boxed{(\sigma_a^{(1)} \circ \sigma_a^{(2)})^{-1}} \\ \downarrow \\ R_a^{(3)} \\ \downarrow \\ \nu_a^{(3)-} \\ \downarrow \\ \bigcup_{b,\alpha} r_{ab;\alpha}^{(3)} \end{array} \right) \quad (4.15)$$

with a prefactor

$$\tilde{f}_{\mathbf{L}^{(1)}\mathbf{L}^{(2)}}^{\mathbf{L}^{(3)}} = \sqrt{\frac{\prod_a d(R_a^{(1)})d(R_a^{(2)})d(R_a^{(3)})}{\prod_{a,b,\alpha} d(r_{ab;\alpha}^{(1)})d(r_{ab;\alpha}^{(2)})d(r_{ab;\alpha}^{(3)})}} \quad (4.16)$$

The trace \mathbf{tr} refers to the contraction of the indices associated with the $\cup_{a,b} r_{ba;\alpha}^{(I)}$ at the top of the diagram to those of $\cup_{a,b} r_{ab;\alpha}^{(I)}$ at the bottom. The identification occurs across different group factors, to make up the quivers for the three quiver characters. The diagram, with free upper and lower external legs, corresponds to an expression with indices $\{\cup_{I,a,b,\alpha} i_{ba;\alpha}^{(I)}\}$ for the upper legs and $\{\cup_{I,a,b,\alpha} j_{ab;\alpha}^{(I)}\}$ for the lower legs, each set living in $\otimes_{I,a,b,\alpha} r_{ab;\alpha}^{(I)}$. The trace operation multiplies with $\prod_{I,a,b,\alpha} \delta_{i_{ab;\alpha}^{(I)} j_{ab;\alpha}^{(I)}}$ and sums over the indices.

Applying (A.19) and (A.5) we have

$$\sum_{\gamma_1, \gamma_2} \begin{array}{c} \downarrow \\ \boxed{\gamma_1} \\ \downarrow R_1 \end{array} \begin{array}{c} \downarrow \\ \boxed{\gamma_2} \\ \downarrow R_2 \end{array} \begin{array}{c} \uparrow \\ \boxed{(\gamma_1 \circ \gamma_2)^{-1}} \\ \uparrow R_3 \end{array} = \frac{n_1! n_2!}{d(R_1) d(R_2)} \sum_{\mu} \begin{array}{c} \begin{array}{c} \nearrow R_1 \\ \downarrow R_2 \\ \searrow R_3 \end{array} \\ \mu \\ \begin{array}{c} \nwarrow R_1 \\ \downarrow R_2 \\ \nearrow R_3 \end{array} \end{array} \quad (4.17)$$

Using this to perform $\sigma_a^{(1)}, \sigma_a^{(2)}$ sums we get

$$G(\mathbf{L}^{(1)}, \mathbf{L}^{(2)}; \mathbf{L}^{(3)}) = \tilde{f}_{\mathbf{L}^{(1)}\mathbf{L}^{(2)}}^{\mathbf{L}^{(3)}} \mathbf{tr} \prod_a \left(\frac{1}{d(R_a^{(1)}) d(R_a^{(2)})} \sum_{\mu_a} \begin{array}{c} \begin{array}{ccc} \cup_{b,\alpha} r_{ba;\alpha}^{(1)} & \cup_{b,\alpha} r_{ba;\alpha}^{(2)} & \cup_{b,\alpha} r_{ba;\alpha}^{(3)} \\ \swarrow \nu_a^{(1)+} & \downarrow \nu_a^{(2)+} & \searrow \nu_a^{(3)+} \\ R_a^{(1)} & \mu_a & R_a^{(2)} \\ \swarrow R_a^{(1)} & \downarrow \mu_a & \searrow R_a^{(3)} \\ \nu_a^{(1)-} & \downarrow \nu_a^{(2)-} & \searrow \nu_a^{(3)-} \\ \cup_{b,\alpha} r_{ab;\alpha}^{(1)} & \cup_{b,\alpha} r_{ab;\alpha}^{(2)} & \cup_{b,\alpha} r_{ab;\alpha}^{(3)} \end{array} \end{array} \right) \quad (4.18)$$

At this point the diagram is still not factorized, because legs are contracted between different factors in \prod_a . Next, focus on the lower piece of the diagram, containing ν^- (equivalently we can pick the upper piece – they are symmetric). We can insert the following sum over

γ_1, γ_2

$$\begin{aligned}
& \frac{1}{n_{ab;\alpha}^{(1)}! n_{ab;\alpha}^{(2)}!} \sum_{\gamma_1, \gamma_2} \text{Diagram} \\
&= \frac{1}{d(r_{ab;\alpha}^{(1)}) d(r_{ab;\alpha}^{(2)})} \sum_{\mu_{ab;\alpha}} \text{Diagram} \quad (4.19)
\end{aligned}$$

On the left hand side γ_1 acts on one of the outgoing legs $r_{ab;\alpha}^{(1)}$ (for some choice of b, α), γ_2 acts on $r_{ab;\alpha}^{(2)}$, and $(\gamma_1 \circ \gamma_2)^{-1}$ acts on $r_{ab;\alpha}^{(3)}$. It is equal to the original ν^- factor in (4.19), because we can pull γ 's through the branching coefficients and cancel. Next we can sum over all $\gamma_1 \circ \gamma_2 \in S_{n_{ab;\alpha}^{(1)}} \times S_{n_{ab;\alpha}^{(2)}}$, which allows us to apply (4.17) again, resulting in the right hand side. Performing this for each b, α we completely “cap off” the outgoing $r_{ab;\alpha}^{(I)}$ legs, contracting each $r_{ab;\alpha}^{(1)} \otimes r_{ab;\alpha}^{(2)} \rightarrow r_{ab;\alpha}^{(3)}$ respectively, and introducing $\{\mu_{ab;\alpha}\}$ sums. The leftover branching coefficient with $\mu_{ab;\alpha}$ (at the bottom of the right hand side) contracts the incoming legs $r_{ba;\alpha}^{(I)}$ of the respective ν^+ diagram in (4.19). Consequently, the diagram completely factorizes, and we get (4.9), with prefactor arising from

$$f_{\mathbf{L}^{(1)}\mathbf{L}^{(2)}}^{\mathbf{L}^{(3)}} = \frac{\tilde{f}_{\mathbf{L}^{(1)}\mathbf{L}^{(2)}}^{\mathbf{L}^{(3)}}}{\prod_a d(R_a^{(1)}) d(R_a^{(2)}) \prod_{a,b,\alpha} d(r_{ab;\alpha}^{(1)}) d(r_{ab;\alpha}^{(2)})} \quad (4.20)$$

The equations corresponding to the diagrammatic manipulations above are given in Appendix D.4.

4.2 Covariant basis

Here we calculate the chiral ring structure constants for the covariant basis (3.59) operators $\mathcal{O}_Q(\mathbf{K})$. As in the previous section, the product is

$$\mathcal{O}_Q(\mathbf{K}^{(1)}) \mathcal{O}_Q(\mathbf{K}^{(2)}) = \sum_{\mathbf{K}^{(3)}} G(\mathbf{K}^{(1)}, \mathbf{K}^{(2)}; \mathbf{K}^{(3)}) \mathcal{O}_Q(\mathbf{K}^{(3)}) \quad (4.21)$$

with the structure constants

$$\begin{aligned}
& G(\mathbf{K}^{(1)}, \mathbf{K}^{(2)}; \mathbf{K}^{(3)}) \\
&= \frac{1}{\prod n_a^{(1)}!} \frac{1}{\prod n_a^{(2)}!} \sum_{\boldsymbol{\sigma}^{(1)}} \sum_{\boldsymbol{\sigma}^{(2)}} \hat{\chi}_Q(\mathbf{K}^{(1)}, \boldsymbol{\sigma}^{(1)}) \hat{\chi}_Q(\mathbf{K}^{(2)}, \boldsymbol{\sigma}^{(2)}) \hat{\chi}_Q(\mathbf{K}^{(3)}, \boldsymbol{\sigma}^{(1)} \circ \boldsymbol{\sigma}^{(2)})
\end{aligned} \tag{4.22}$$

Here we use conveniently normalized covariant quiver characters

$$\hat{\chi}_Q(\mathbf{K}) \equiv \sqrt{\prod d(R_a)} \chi_Q(\mathbf{K}). \tag{4.23}$$

Let us first present the answer and some examples, and sketch the derivation afterwards. Recall from the definition (3.60) of the covariant quiver characters, that the labels are $\mathbf{K} = \{R_a, s_{ab}^+, s_{ab}^-, \nu_a^+, \nu_a^-, \Lambda_{ab}, \tau_{ab}, n_{ab;\alpha}, \beta_{ab}\}$, as displayed in (3.62). The result of the sum (4.22) is, like in the previous section, that *all* of the Young diagram labels multiply according to the Littlewood-Richardson rule

$$\boxed{
\begin{aligned}
R_a^{(1)} \otimes R_a^{(2)} &\rightarrow R_a^{(3)} \\
\Lambda_{ab}^{(1)} \otimes \Lambda_{ab}^{(2)} &\rightarrow \Lambda_{ab}^{(3)} \\
s_{ab}^{(1)+} \otimes s_{ab}^{(2)+} &\rightarrow s_{ab}^{(3)+} \\
s_{ab}^{(1)-} \otimes s_{ab}^{(2)-} &\rightarrow s_{ab}^{(3)-}
\end{aligned}
} \tag{4.24}$$

That is, $G(\mathbf{K}^{(1)}, \mathbf{K}^{(2)}; \mathbf{K}^{(3)})$ vanishes unless the labels from $\mathbf{K}^{(3)}$ are contained in the Littlewood-Richardson tensor product (also called outer product) of the Young diagrams. The non-vanishing coefficients are given, similarly as in (4.9), by connecting up all coupled legs via branching coefficients, and summing over the multiplicities for the new branchings.

Specifically, we get:

$$G(\mathbf{K}^{(1)}, \mathbf{K}^{(2)}; \mathbf{K}^{(3)}) = f_{\mathbf{K}^{(1)}\mathbf{K}^{(2)}}^{\mathbf{K}^{(3)}} \sum_{\{\mu_a\}} \sum_{\{\mu_{ab}^+\}} \sum_{\{\mu_{ab}^-\}} \sum_{\{\mu_{ab}^\Lambda\}} \prod_a \left(\begin{array}{c} \text{Quiver 1} \end{array} \right) \prod_{a,b} \left(\begin{array}{c} \text{Quiver 2} \end{array} \right) \quad (4.25)$$

The first quiver (Quiver 1) has nodes μ_a at the top, $\nu_a^{(1)-}$, $\nu_a^{(2)-}$, $\nu_a^{(3)-}$ in the middle, and $\bigcup_b s_{ab}^{(1)-}$, $\bigcup_b s_{ab}^{(2)-}$, $\bigcup_b s_{ab}^{(3)-}$ at the bottom. Arrows are labeled $R_a^{(1)}$, $R_a^{(2)}$, $R_a^{(3)}$. The second quiver (Quiver 2) has nodes $\bigcup_b \mu_{ba}^+$ at the top, $\nu_a^{(1)+}$, $\nu_a^{(2)+}$, $\nu_a^{(3)+}$ in the middle, and $\bigcup_b s_{ba}^{(1)+}$, $\bigcup_b s_{ba}^{(2)+}$, $\bigcup_b s_{ba}^{(3)+}$ at the bottom. Arrows are labeled $R_a^{(1)}$, $R_a^{(2)}$, $R_a^{(3)}$. The third quiver (Quiver 3) has nodes μ_{ab}^- at the top, $\tau_{ab}^{(1)}$, $\tau_{ab}^{(2)}$, $\tau_{ab}^{(3)}$ in the middle, and $s_{ab}^{(1)-}$, $s_{ab}^{(2)-}$, $s_{ab}^{(3)-}$ at the bottom. Arrows are labeled $\Lambda_{ab}^{(1)}$, $\Lambda_{ab}^{(2)}$, $\Lambda_{ab}^{(3)}$. The fourth quiver (Quiver 4) has nodes μ_{ab}^Λ at the top, $\beta_{ab}^{(1)}$, $\beta_{ab}^{(2)}$, $\beta_{ab}^{(3)}$ in the middle, and $\mathbf{n}_{ab}^{(1)}$, $\mathbf{n}_{ab}^{(2)}$, $\mathbf{n}_{ab}^{(3)}$ at the bottom. Arrows are labeled $\Lambda_{ab}^{(1)}$, $\Lambda_{ab}^{(2)}$, $\Lambda_{ab}^{(3)}$.

with

$$f_{\mathbf{K}^{(1)}\mathbf{K}^{(2)}}^{\mathbf{K}^{(3)}} = \frac{\sqrt{\prod_a d(R_a^{(1)})d(R_a^{(2)})d(R_a^{(3)})}}{\prod_a d(R_a^{(1)})d(R_a^{(2)}) \prod_{a,b} d(s_{ab}^{(1)-})d(s_{ab}^{(2)-})d(s_{ab}^{(1)+})d(s_{ab}^{(2)+})d(\Lambda_{ab}^{(1)})d(\Lambda_{ab}^{(2)})} \quad (4.26)$$

As for the restricted Schur basis, we get two factors of \mathcal{F} defined in (4.12) for each group node, now s_{ab}^\pm playing the role of $r_{ab;\alpha}$. In addition to that, for each edge in the quiver we get a factor coupling $\Lambda_{ab}^{(1)} \otimes \Lambda_{ab}^{(2)} \rightarrow \Lambda_{ab}^{(3)}$. Again for illustration we use three outgoing arrows from each branching node ν_a^- and three incoming arrows to each ν_a^+ . The explicit

expression is:

$$\begin{aligned}
G(\mathbf{K}^{(1)}, \mathbf{K}^{(2)}; \mathbf{K}^{(3)}) &= f_{\mathbf{K}^{(1)}\mathbf{K}^{(2)}}^{\mathbf{K}^{(3)}} \sum_{\{\mu_a\}} \sum_{\{\mu_{ab}^+\}} \sum_{\{\mu_{ab}^-\}} \sum_{\{\mu_{ab}^\Lambda\}} \\
&\prod_a \mathcal{F} \left(\cup_I R_a^{(I)}, \{\cup_{I,b} s_{ab}^{(I)-}\}, \cup_I \nu_a^{(I)-}; \mu_a, \{\cup_b \mu_{ab}^-\} \right) \mathcal{F} \left(\cup_I R_a^{(I)}, \{\cup_{I,b} s_{ba}^{(I)+}\}, \cup_I \nu_a^{(I)+}; \mu_a, \{\cup_b \mu_{ba}^+\} \right) \\
&\prod_{a,b} \left(S_{l_{ab}^{(1)+} l_{ab}^{(1)-}, l_{ab}^{(1)}}^{s_{ab}^{(1)+} s_{ab}^{(1)-}, \Lambda_{ab}^{(1)} \tau_{ab}^{(1)}} S_{l_{ab}^{(2)+} l_{ab}^{(2)-}, l_{ab}^{(2)}}^{s_{ab}^{(2)+} s_{ab}^{(2)-}, \Lambda_{ab}^{(2)} \tau_{ab}^{(2)}} S_{l_{ab}^{(3)+} l_{ab}^{(3)-}, l_{ab}^{(3)}}^{s_{ab}^{(3)+} s_{ab}^{(3)-}, \Lambda_{ab}^{(3)} \tau_{ab}^{(3)}} \right. \\
&\quad \times B_{l_{ab}^{(3)-} \rightarrow l_{ab}^{(1)-}, l_{ab}^{(2)-}}^{s_{ab}^{(3)-} \rightarrow s_{ab}^{(1)-}, s_{ab}^{(2)-}; \mu_{ab}^-} B_{l_{ab}^{(3)+} \rightarrow l_{ab}^{(1)+}, l_{ab}^{(2)+}}^{s_{ab}^{(3)+} \rightarrow s_{ab}^{(1)+}, s_{ab}^{(2)+}; \mu_{ab}^+} B_{l_{ab}^{(3)} \rightarrow l_{ab}^{(1)}, l_{ab}^{(2)}}^{\Lambda_{ab}^{(3)} \rightarrow \Lambda_{ab}^{(1)}, \Lambda_{ab}^{(2)}; \mu_{ab}^\Lambda} \Big) \\
&\times \left(B_{k_{ab}^{(1)} \rightarrow [n_{ab}^{(1)}], \beta_{ab}^{(1)}}^{\Lambda_{ab}^{(1)} \rightarrow [n_{ab}^{(1)}], \beta_{ab}^{(1)}} B_{k_{ab}^{(2)} \rightarrow [n_{ab}^{(2)}], \beta_{ab}^{(2)}}^{\Lambda_{ab}^{(2)} \rightarrow [n_{ab}^{(2)}], \beta_{ab}^{(2)}} B_{k_{ab}^{(3)} \rightarrow [n_{ab}^{(3)}], \beta_{ab}^{(3)}}^{\Lambda_{ab}^{(3)} \rightarrow [n_{ab}^{(3)}], \beta_{ab}^{(3)}} B_{k_{ab}^{(3)} \rightarrow k_{ab}^{(1)}, k_{ab}^{(2)}}^{\Lambda_{ab}^{(3)} \rightarrow \Lambda_{ab}^{(1)}, \Lambda_{ab}^{(2)}; \mu_{ab}^\Lambda} \right)
\end{aligned} \tag{4.27}$$

In its most general form $G(\mathbf{K}^{(1)}, \mathbf{K}^{(2)}; \mathbf{K}^{(3)})$ looks more complicated than $G(\mathbf{L}^{(1)}, \mathbf{L}^{(2)}; \mathbf{L}^{(3)})$, because it has to deal with both s_{ab}^\pm and Λ_{ab} . However, for linear quivers like \mathbb{C}^3 (3.25), conifold (3.81), dP_0 (3.94) it simplifies significantly, because $s_{ba}^+ = R_a = s_{ab}^-$, so there are no s_{ab}^\pm or ν_a^\pm labels at all. In that case the \mathcal{F} factors reduce to

$$\mathcal{F}(R_a^{(I)}, R_a^{(I)}, \nu_a^{(I)-} = 1; \mu_a, \mu_{ab}^-) = R_a^{(1)} \begin{array}{c} \mu_a \\ \circ \\ \downarrow \\ \circ \\ \mu_{ab}^- \end{array} R_a^{(3)} = \delta_{\mu_a \mu_{ab}^-} d(R_a^{(1)}) d(R_a^{(2)}) \tag{4.28}$$

using (A.17). Thus, for example, we can write the chiral ring structure constants for \mathbb{C}^3 as just the term for the single edge in the quiver

$$\begin{aligned}
G_{\mathbb{C}^3}(\mathbf{K}^{(1)}, \mathbf{K}^{(2)}; \mathbf{K}^{(3)}) &= \frac{\sqrt{d(R^{(1)})d(R^{(2)})d(R^{(3)})}}{d(R^{(1)})d(R^{(2)})d(\Lambda^{(1)})d(\Lambda^{(2)})} \\
&\times \sum_{\mu} \sum_{\mu^\Lambda} \left(\begin{array}{c} \mu \\ \circ \\ \begin{array}{c} R^{(1)} \quad R^{(2)} \quad R^{(3)} \\ \diagup \quad \diagdown \quad \diagup \quad \diagdown \quad \diagup \quad \diagdown \\ \tau^{(1)} \quad \tau^{(2)} \quad \tau^{(3)} \\ \diagdown \quad \diagup \quad \diagdown \quad \diagup \quad \diagdown \quad \diagup \\ R^{(1)} \quad R^{(2)} \quad R^{(3)} \\ \circ \\ \mu \end{array} \\ \begin{array}{c} \Lambda^{(1)} \quad \Lambda^{(2)} \quad \Lambda^{(3)} \\ \diagup \quad \diagdown \quad \diagup \quad \diagdown \quad \diagup \quad \diagdown \\ \mu^\Lambda \end{array} \end{array} \right) \tag{4.29}
\end{aligned}$$

A diagrammatic form of the fusion coefficient for the \mathbb{C}^3 case, manifestly exhibiting the $R^{(1)} \otimes R^{(2)} \rightarrow R^{(3)}$ LR-selection rule was given in [20]. For the conifold we have a product of

two terms, one for each edge, using the labeling (3.82) $\mathbf{K} = \{R_1, R_2, \Lambda_A, \Lambda_B, \tau_A, \tau_B, \mathbf{n}, \beta_A, \beta_B\}$:

$$G_C(\mathbf{K}^{(1)}, \mathbf{K}^{(2)}; \mathbf{K}^{(3)}) = \frac{\sqrt{d(R_1^{(1)})d(R_1^{(2)})d(R_1^{(3)})d(R_2^{(1)})d(R_2^{(2)})d(R_2^{(3)})}}{d(R_1^{(1)})d(R_1^{(2)})d(R_2^{(1)})d(R_2^{(2)})d(\Lambda_A^{(1)})d(\Lambda_A^{(2)})d(\Lambda_B^{(1)})d(\Lambda_B^{(2)})} \\ \times \sum_{\mu_1 \mu_2} \sum_{\mu_A^\Lambda \mu_B^\Lambda} \left(\begin{array}{c} \text{Diagram 1: A network of nodes } \mu_1, \mu_2, \mu_A^\Lambda, \mu_B^\Lambda \text{ connected by edges } R_1^{(i)}, R_2^{(i)}, \Lambda_A^{(i)}, \Lambda_B^{(i)}, \tau_A^{(i)}, \tau_B^{(i)} \text{ for } i=1,2,3. \\ \text{Diagram 2: A tree-like structure with nodes } \beta_A^{(i)}, \beta_B^{(i)}, \mathbf{n}_A^{(i)}, \mathbf{n}_B^{(i)} \text{ and edges } \Lambda_A^{(i)}, \Lambda_B^{(i)} \text{ for } i=1,2,3. \end{array} \right) \quad (4.30)$$

The derivation of (4.25) parallels that of the last section, except in addition we have to deal with Clebsch-Gordan coefficient (black) nodes and Λ_{ab} . The sum over $\sigma^{(1)}, \sigma^{(2)}$ in (4.22) is performed the same way as in (4.15) and we get analogously to (4.18):

$$G(\mathbf{K}^{(1)}, \mathbf{K}^{(2)}; \mathbf{K}^{(3)}) = \frac{\tilde{f}_{\mathbf{K}^{(1)}\mathbf{K}^{(2)}}^{\mathbf{K}^{(3)}}}{\prod d(R_a^{(1)})d(R_a^{(2)})} \text{tr} \prod_a \sum_{\mu_a} \left(\begin{array}{c} \text{Diagram 1: Top part of the trace operation showing nodes } \nu_a^{(i)+}, \nu_a^{(i)-} \text{ and edges } R_a^{(i)}, s_{ba}^{(i)+}, s_{ab}^{(i)-}. \\ \text{Diagram 2: Bottom part of the trace operation showing nodes } \Lambda_{ab}^{(i)} \text{ and edges } s_{ab}^{(i)+}, s_{ab}^{(i)-}. \end{array} \right) \quad (4.31)$$

As before, the trace-operation identifies and sums the corresponding indices from $\cup_{a,b} s_{ba}^{(I)}$ at the top of the diagram to the indices from $\cup_{a,b} s_{ab}^{(I)}$. Now we have extra Clebsch-Gordan

nodes between $s_{ab}^{(I)-}$ and $s_{ab}^{(I)+}$. Note the outgoing lines next to $\Lambda_{ab}^{(I)}$ are a shorthand for the whole collection of labels $(\tau_{ab}^{(I)}, \Lambda_{ab}^{(I)}, \beta_{ab}^{(I)}, \mathbf{n}_{ab}^{(I)})$ like in (3.62), including the β_{ab} white branching coefficient node.

In order to factorize this diagram we apply (4.19) *twice*: both on $s_{ab}^{(I)-}$ legs below $\nu_a^{(I)-}$ nodes, and on $s_{ab}^{(I)+}$ legs above $\nu_a^{(I)+}$. This introduces two sums over new branching coefficients μ_{ab}^+, μ_{ab}^- (compared to just one in the last section) and splits the diagram into *three* parts:

$$\begin{aligned}
G(\mathbf{K}^{(1)}, \mathbf{K}^{(2)}; \mathbf{K}^{(3)}) &= \frac{\tilde{f}_{\mathbf{K}^{(1)}\mathbf{K}^{(2)}}^{\mathbf{K}^{(3)}}}{\prod_a d(R_a^{(1)})d(R_a^{(2)}) \prod_{a,b} d(s_{ab}^{(1)-})d(s_{ab}^{(2)-})d(s_{ab}^{(1)+})d(s_{ab}^{(2)+})} \\
&\times \sum_{\{\mu_a\}} \sum_{\{\mu_{ab}^+\}} \sum_{\{\mu_{ab}^-\}} \prod_a \left(\begin{array}{c} \text{Diagram 1} \quad \text{Diagram 2} \quad \text{Diagram 3} \end{array} \right) \quad (4.32)
\end{aligned}$$

The diagrams are as follows:

- Diagram 1 (Top Left):** A diamond-shaped graph with a central node μ_a at the top. It has two intermediate nodes $\nu_a^{(1)-}$ and $\nu_a^{(2)-}$ on the left and right respectively. The bottom node is $\bigcup_b \mu_{ab}^-$. Edges are labeled $R_a^{(1)}$, $R_a^{(2)}$, $R_a^{(3)}$, $\bigcup_b s_{ab}^{(1)-}$, $\bigcup_b s_{ab}^{(2)-}$, and $\bigcup_b s_{ab}^{(3)-}$.
- Diagram 2 (Top Right):** A diamond-shaped graph with a central node μ_a at the bottom. It has two intermediate nodes $\nu_a^{(1)+}$ and $\nu_a^{(2)+}$ on the left and right respectively. The top node is $\bigcup_b \mu_{ba}^+$. Edges are labeled $R_a^{(1)}$, $R_a^{(2)}$, $R_a^{(3)}$, $\bigcup_b s_{ba}^{(1)+}$, $\bigcup_b s_{ba}^{(2)+}$, and $\bigcup_b s_{ba}^{(3)+}$.
- Diagram 3 (Bottom):** A diamond-shaped graph with a central node $\Lambda_{ab}^{(2)}$ (black dot) at the center. It has two intermediate nodes $\Lambda_{ab}^{(1)}$ and $\Lambda_{ab}^{(3)}$ on the left and right respectively. The top node is $\bigcup_b \mu_{ab}^-$ and the bottom node is $\bigcup_b \mu_{ab}^+$. Edges are labeled $s_{ab}^{(1)-}$, $s_{ab}^{(1)+}$, $s_{ab}^{(3)-}$, and $s_{ab}^{(3)+}$.

The diagram involving $\Lambda_{ab}^{(I)}$ factorizes into a piece for each b , so we have (now including

β_{ab} nodes):

$$\prod_{a,b} \begin{array}{c} \mu_{ab}^- \\ \begin{array}{c} s_{ab}^{(1)-} \quad s_{ab}^{(2)-} \quad s_{ab}^{(3)-} \\ \nearrow \quad \downarrow \quad \nwarrow \\ \Lambda_{ab}^{(1)} \quad \Lambda_{ab}^{(2)} \quad \Lambda_{ab}^{(3)} \\ \circ \quad \circ \quad \circ \\ \beta_{ab}^{(1)} \quad \beta_{ab}^{(2)} \quad \beta_{ab}^{(3)} \\ \nwarrow \quad \downarrow \quad \nearrow \\ s_{ab}^{(1)+} \quad s_{ab}^{(2)+} \quad s_{ab}^{(3)+} \\ \mu_{ab}^+ \end{array} \\ \tau_{ab}^{(1)} \quad \tau_{ab}^{(2)} \quad \tau_{ab}^{(3)} \end{array} \begin{array}{c} n_{ab}^{(1)} \\ \circ \\ \beta_{ab}^{(1)} \end{array} \begin{array}{c} n_{ab}^{(3)} \\ \circ \\ \beta_{ab}^{(3)} \end{array} \quad (4.33)$$

Finally, we couple $\Lambda_{ab}^{(1)} \otimes \Lambda_{ab}^{(2)} \rightarrow \Lambda_{ab}^{(3)}$ by inserting the following sum

$$\frac{1}{n_{ab}^{(1)}! n_{ab}^{(2)}!} \sum_{\gamma_1, \gamma_2} \begin{array}{c} \mu_{ab}^- \\ \begin{array}{c} s_{ab}^{(1)-} \quad s_{ab}^{(2)-} \quad s_{ab}^{(3)-} \\ \nearrow \quad \downarrow \quad \nwarrow \\ \Lambda_{ab}^{(1)} \quad \Lambda_{ab}^{(2)} \\ \circ \quad \circ \\ \gamma_1 \quad \gamma_2 \\ \nwarrow \quad \downarrow \quad \nearrow \\ s_{ab}^{(1)+} \quad s_{ab}^{(2)+} \quad s_{ab}^{(3)+} \\ \mu_{ab}^+ \end{array} \end{array} \begin{array}{c} \Lambda_{ab}^{(3)} \\ \boxed{(\gamma_1 \circ \gamma_2)^{-1}} \end{array} \quad (4.34)$$

$$= \frac{1}{d(\Lambda_{ab}^{(1)})d(\Lambda_{ab}^{(2)})} \sum_{\mu_{ab}^\Lambda} \begin{array}{c} \mu_{ab}^- \\ \begin{array}{c} s_{ab}^{(1)-} \quad s_{ab}^{(2)-} \quad s_{ab}^{(3)-} \\ \nearrow \quad \downarrow \quad \nwarrow \\ \Lambda_{ab}^{(1)} \quad \Lambda_{ab}^{(2)} \quad \Lambda_{ab}^{(3)} \\ \circ \quad \circ \quad \circ \\ \tau_{ab}^{(1)} \quad \tau_{ab}^{(2)} \quad \tau_{ab}^{(3)} \\ \nwarrow \quad \downarrow \quad \nearrow \\ s_{ab}^{(1)+} \quad s_{ab}^{(2)+} \quad s_{ab}^{(3)+} \\ \mu_{ab}^+ \end{array} \end{array} \begin{array}{c} \mu_{ab}^\Lambda \\ \begin{array}{c} \Lambda_{ab}^{(1)} \quad \Lambda_{ab}^{(2)} \quad \Lambda_{ab}^{(3)} \\ \circ \quad \circ \quad \circ \\ \beta_{ab}^{(1)} \quad \beta_{ab}^{(2)} \quad \beta_{ab}^{(3)} \\ \nwarrow \quad \downarrow \quad \nearrow \\ n_{ab}^{(1)} \quad n_{ab}^{(2)} \quad n_{ab}^{(3)} \end{array} \end{array}$$

The diagram on the left hand side with inserted γ_1, γ_2 is equal to (4.33), due to the property of Clebsch-Gordan coefficients (A.28), which allows to pull γ 's through, and then cancel via μ_{ab}^- and μ_{ab}^+ branching coefficients using (A.16). Then applying (4.17) again we get the right hand side. Plugging this in (4.32) gives the final answer (4.25).

5 Quivers and topological field theories on Riemann surfaces

The formulae for counting, two-point functions and chiral ring fusion coefficients derived in the previous sections have all been given in terms of permutations. For getting an orthogonal basis of operators, it has been convenient to Fourier transform from permutations to Young diagrams, which allow easy coding of finite N relations. In this section we will primarily focus on the large N limit, where $n_a \leq N_a$. We will find that all the combinatoric data of counting and correlators we have considered so far can be expressed neatly in terms of topological field theory on a Riemann surface obtained by thickening the quiver. The topological field theory (TFT) will be a lattice topological field theory based on S_n . The choice of n will depend on the $\{n_{ab;\alpha}\}$ specifying the numbers of fields of type α corresponding to each of the arrows in the quiver starting from a and ending at b . A more elegant mathematical language might be to work with S_∞ defined through an inductive limit, but in this paper we will stick with a down to earth presentation based on S_n , bearing in mind that the n can be arbitrarily large, depending on the numbers of fields in the quiver gauge theory observables being considered. These lattice topological field theories have been discussed in connection with Chern Simons theory [51] and in connection with the large N limit of two-dimensional Yang Mills in [52]. We will give a brief review in the next subsection, and introduce some defect observables associated with subgroups of S_n . We will then show how the counting and correlators of large N quiver gauge theories can be expressed with these TFTs on Riemann surfaces obtained by thickening the quiver.

5.1 S_n topological lattice gauge theory and defect operators

The partition function on a surface is defined by starting with a triangulation on the surface, or a more generally a cell-decomposition where the 2-cells can be polygons. We associate S_n group variables with each edge, and a weight function for each cell (or plaquette). The weight is the $\delta(\sigma_P)$, where σ_P is the product of group elements around the plaquette. We will call this the plaquette weight Z_P

$$Z_P(\sigma_P) = \delta(\sigma_P) = \sum_{R \vdash n} \frac{d(R)}{n!} \chi_R(\sigma_P) \quad (5.1)$$

The sum is over all Young diagrams with n boxes, equivalently all irreps of S_n . The partition function of the manifold is defined as

$$Z = \frac{1}{(n!)^V} \sum_{\sigma_1, \dots, \sigma_E \in S_n} \prod_P Z_P(\sigma_P) \quad (5.2)$$

where V is the number of vertices in the triangulation. The topological property follows from an invariance under refinement, or conversely coarsening, of the cell decomposition. If we sum over an edge variable between two cells, as shown in Figure 13, thus eliminating the edge and fusing the two cells P_1 and P_2 into a single cell P , we have

$$\begin{aligned} \sum_{\sigma} Z_{P_1} Z_{P_2} &= \sum_{\gamma} \delta(\sigma_1 \gamma \sigma_5 \sigma_6) \delta(\sigma_2 \sigma_3 \sigma_4 \gamma^{-1}) \\ &= \delta(\sigma_1 \sigma_2 \sigma_3 \sigma_4 \sigma_5 \sigma_6) \\ &= Z_P \end{aligned} \quad (5.3)$$

We denote this topological invariance property TOP1.

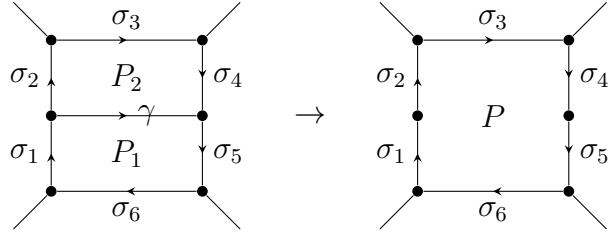


Figure 13: TOP1

In a configuration such as shown in Figure 14, where a bivalent vertex has holonomies σ_1, σ_2 on the two sides, the only combination appearing in the partition function is $\sigma_1 \sigma_2$. Hence we can rename $\sigma_1 \rightarrow \sigma_1 \sigma_2$, do the sum over σ_2 to get rid of a factor of $1/n!$, corresponding to the removal of the vertex. This leaves the partition function (5.2) invariant. We will call this topological invariance property TOP2.

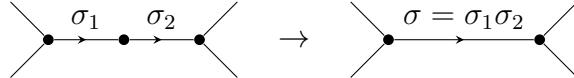


Figure 14: TOP2

Given a cell decomposition of a Riemann surface of genus G , we can use the topological invariance (TOP1 and TOP2) to coarsen it to a single cell with $2G$ edges, and a single

vertex. The partition function is thus

$$Z(\Sigma_G) = \frac{1}{n!} \sum_{s_1, t_1, \dots, s_G, t_G \in S_n} \delta(s_1 t_1 s_1^{-1} t_1^{-1} s_2 t_2 s_2^{-1} t_2^{-1} \cdots s_G t_G s_G^{-1} t_G^{-1}) \quad (5.4)$$

Manipulations which are familiar in the large N expansion of $U(N)$ 2dYM (see [32] or the review [53]) show that this can be expressed in terms of characters

$$Z(\Sigma_G) = \sum_{R \vdash n} \left(\frac{d(R)}{n!} \right)^{2-2G} \quad (5.5)$$

This formula for S_n topological field theory can also be arrived at by considering the Frobenius algebra of conjugacy classes of S_n (see e.g [54]) or by building up the Riemann surface from pants diagrams [55].) It has an interpretation in terms of covers of Σ_G summed with inverse automorphism factor.

The case with boundaries will be of particular interest. We will express the construction of the boundary observables in a way which allows some generalized defect observables which we will need. For a genus G surface with B boundaries, we will choose a base point on each boundary and associate permutations σ_i to that boundary. We require the cell-decomposition to include the boundary vertices (0-cells) among its vertices, and the boundary circles among its 1-cells. For the case of the three-holed sphere we can choose another base-point in the middle and extend edges to the boundary vertices. Cutting along these edges gives a contractible 2-cell. Denoting the permutations associated with the edges as $\gamma_1, \gamma_2, \gamma_3$ we get the partition function

$$\begin{aligned} Z(G=0, B=3) &= \frac{1}{n!} \sum_{\gamma_1, \gamma_2, \gamma_3 \in S_n} \delta(\gamma_1 \sigma_1 \gamma_1^{-1} \gamma_2 \sigma_2 \gamma_2^{-1} \gamma_3 \sigma_3 \gamma_3^{-1}) \\ &= \sum_{R \vdash n} \frac{\chi_R(\sigma_1) \chi_R(\sigma_2) \chi_R(\sigma_3)}{d_R} \end{aligned} \quad (5.6)$$

The factor of $1/n!$ is due to the interior vertex, no such factors are introduced for the vertices used in the definition of the boundary observables. We could also have chosen not to include an interior vertex, and just draw two lines joining the vertex from one boundary circle to the vertices on the other boundary circles. Then, the definition (5.2) leads us to write

$$Z(G=0, B=3) = \sum_{\gamma_1, \gamma_2 \in S_n} \delta(\gamma_1 \sigma_1 \gamma_1^{-1} \gamma_2 \sigma_2 \gamma_2^{-1} \sigma_3) \quad (5.7)$$

This is the same as the expression above (5.6), since the γ_3 can be absorbed into a re-definition of the summation variables γ_1, γ_2 . The expression in terms of characters is a

special case of the standard result

$$\begin{aligned}
Z(G, B, \sigma_1, \dots, \sigma_B) &= \frac{1}{n!} \sum_{\gamma_1, \dots, \gamma_B \in S_n} \sum_{s_i, t_i} \delta\left(\prod_{i=1}^G s_i t_i s_i^{-1} t_i^{-1} \cdot \prod_{i=1}^B \gamma_i \sigma_i \gamma_i^{-1}\right) \\
&= \sum_{R \vdash n} \left(\frac{d(R)}{n!}\right)^{2-2G-B} \prod_{i=1}^B \chi_R(\sigma_i)
\end{aligned} \tag{5.8}$$

in the normalization that appears naturally from the large N expansion of two dimensional Yang Mills theory [53] and which has a natural covering space interpretation.

We will now describe some more general observables in 2D S_n lattice gauge theory. A *closed H -defect* will be a closed non-self-intersecting loop on the surface, equipped with the choice of a point on the loop. The insertion of the defect in the partition function amounts to constraining the permutation sums in (5.2) to require that the permutation associated with the loop is in the subgroup $H \subset S_n$, and the sum over elements in H is weighted by $\frac{1}{|H|}$, the inverse order of the subgroup. In the presence of the defect, the cell decomposition used to calculate the partition function must include the loop among its 1-cells (possibly as a composite of smaller 1-cells), and the point on the loop should be among the vertices of the cell decomposition. As a simple example, consider the circle shown in Figure 15. The topological properties TOP1 and TOP2 of the partition function ensure that we can choose a very simple cell decomposition compatible with the insertion of the defect. This is shown in Figure 16. There is one 2-cell bounded by 1-cells carrying the permutations $\gamma\sigma\gamma^{-1}\sigma^{-1}$. This gives

$$Z(T^2; D_H) = \frac{1}{|H|} \sum_{\gamma \in H} \sum_{\sigma \in S_n} \delta(\gamma\sigma\gamma^{-1}\sigma^{-1}) \tag{5.9}$$

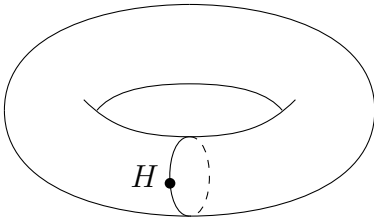


Figure 15: Torus with defect H

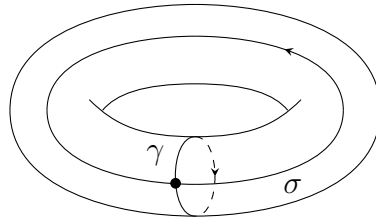


Figure 16: Cell decomposition : one 2-cell

Refinements of the cell decomposition will give the same answer. We will see shortly how this partition function comes up in counting BPS operators in $\mathcal{N} = 4$ SYM. If we have two of these closed H -defects, with subgroups H_1, H_2 , along parallel circles on a torus (Figure 17), we can compute the partition function by introducing one circle transverse

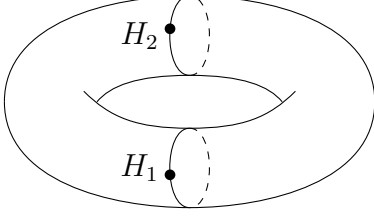


Figure 17: Torus with defects H_1, H_2

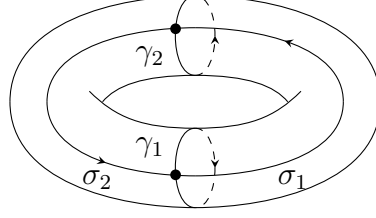


Figure 18: Cell decomposition: 2 2-cells

to the two defects (Figure 18). There are now two 2-cells in the cell decomposition. The partition function with these defect insertions is

$$Z(T^2; D_{H_1}, D_{H_2}) = \frac{1}{|H_1||H_2|} \sum_{\gamma_1 \in H_1} \sum_{\gamma_2 \in H_2} \sum_{\sigma_1, \sigma_2 \in S_n} \delta(\gamma_1 \sigma_1 \gamma_2^{-1} \sigma_1^{-1}) \delta(\gamma_2 \sigma_2 \gamma_1^{-1} \sigma_2^{-1}) \quad (5.10)$$

We will shortly see applications of this formula to the counting of chiral operators for the conifold.

These closed H -defects can also be inserted at the boundaries of Riemann surfaces. If we insert an H_1 -defect at one end of a cylinder ($S^1 \times I$) and an H_2 defect at the other end, the partition function is

$$Z(S^1 \times I; D_{H_1}, D_{H_2}) = \frac{1}{|H_1||H_2|} \sum_{\gamma_1 \in H_1} \sum_{\gamma_2 \in H_2} \sum_{\sigma \in S_n} \delta(\gamma_1 \sigma \gamma_2 \sigma^{-1}) \quad (5.11)$$

By choosing H_1 and H_2 to be appropriate wreath products, this partition function was shown to count Feynman graphs in [56]. This formula arose because Feynman graphs can be put in one-to-one correspondence with points in a double coset, which consists of permutations σ , subject to equivalences defined by left and right multiplication by permutations γ_1, γ_2 in H_1, H_2 respectively. The symmetry factor of a fixed Feynman diagram was computed by fixing the permutation σ along a line joining the two ends of the cylinder.

This introduces us to the second type of defect we will need here. It is a line joining two distinct points, with the associated permutation fixed. We will call this a *open Wilson line* defect. In the applications to chiral operator counting for quiver theories, we will often use open-line defects, where the permutation is fixed to be the identity, which we can call *unit open Wilson line* defects. In particular we will consider a 3-holed sphere, with the permutation associated with line, shown on the left, constrained to be the identity (Figure 19). If we have permutations $\gamma_1, \gamma_2, \gamma_3$ at the boundaries, all measured according to the orientation induced on the boundaries by the orientation of the surface and we introduce the unit open Wilson lines shown (left Figure in 19), then the partition function

(equation 5.2) is non-vanishing provided

$$\gamma_1 \gamma_2 \gamma_3 = 1 \quad (5.12)$$

so that $\gamma_3^{-1} = (\gamma_1 \gamma_2)$. This is to be contrasted with the 3-holed sphere partition function without these defect insertions (5.6) where γ_3 can be any permutation that appears when taking the product of a permutation in the conjugacy class of γ_2 and a permutation in the conjugacy class of γ_1 . An obvious generalization is to consider a $k + 1$ holed sphere with unit open Wilson lines joining a point on the $k + 1$ 'th boundary to points on the k boundaries. Then we will have

$$\gamma_{k+1}^{-1} = \left(\prod_{i=1}^k \gamma_i \right) \quad (5.13)$$

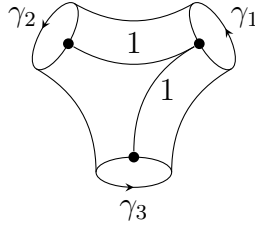


Figure 19: 3-holed sphere with defect, imposing $\gamma_3^{-1} = \gamma_1 \gamma_2$

This type of 3-holed vertex shows up in G -equivariant TFT for $G = S_n$ [57, 58]. We will comment more on this in Section 5.3.

5.2 Counting, correlators and defects in S_n TFT

Consider the number of chiral operators for \mathbb{C}^3 . We specify (n_1, n_2, n_3) as the number of X, Y, Z . We will work in the region $n = n_1 + n_2 + n_3 \leq N$. The operators are parameterized by the permutation σ which relates the upper and lower indices of these chiral fields, transforming in the fundamental and anti-fundamental of $U(N)$. Two permutations $\sigma, \sigma' \in S_n$ give the same operator if there is some $\gamma \in S_{n_1} \times S_{n_2} \times S_{n_3}$ relating them as $\sigma' = \gamma \sigma \gamma^{-1}$. In the region $n \leq N$, there are no additional finite N relations. The finite N relations were considered in Section 3 and solved using a representation theoretic basis involving Young diagrams and branching coefficients. Here we focus on the large N limit and associated geometry. An easy way to count the permutation σ subject to the specified equivalence is to use the Burnside Lemma for group actions (see e.g. [59]). This gives the number of

orbits as the average number of fixed points of the group action. Applied to the case at hand, we have

$$\mathcal{N}_{\mathbb{C}^3}(n_1, n_2, n_3) = \frac{1}{n_1!n_2!n_3!} \sum_{\gamma \in S_{n_1} \times S_{n_2} \times S_{n_3}} \sum_{\sigma \in S_n} \delta(\gamma \sigma \gamma^{-1} \sigma^{-1}) \quad (5.14)$$

This is of the form (5.9) with $H = S_{n_1} \times S_{n_2} \times S_{n_3}$ and $n = n_1 + n_2 + n_3$

$$\mathcal{N}_{\mathbb{C}^3}(n_1, n_2, n_3) = Z(T^2; D_H) \quad H = S_{n_1} \times S_{n_2} \times S_{n_3} \quad (5.15)$$

There is a simple relation between the quiver of \mathbb{C}^3 and the T^2 Riemann surface, with defect, that we have ended up with. Take the three edges of the quiver and collapse them to a single one. In general, we will use the operation of collapsing all the edges having the same start and end-points to a single one. Take a cylinder corresponding to the node and a cylinder corresponding to the edge of the quiver. Insert an H -defect around the cylinder corresponding to the edge. Glue the cylinders together. This is illustrated in Figure 20.

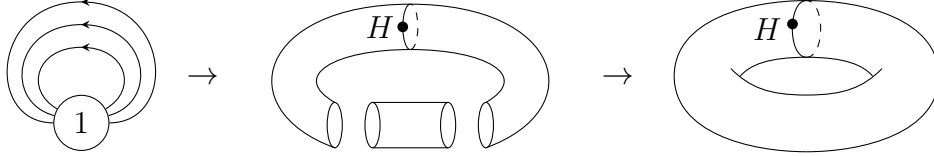


Figure 20: Transforming \mathbb{C}^3 quiver into a Riemann surface

Using (3.54) (alternatively see [20]) The two-point function for the \mathbb{C}^3 case is

$$\langle \mathcal{O}_\sigma \mathcal{O}_{\tilde{\sigma}}^\dagger \rangle = \sum_{\tau \in S_n} \sum_{\gamma \in H} \delta(\gamma \sigma \gamma^{-1} \tilde{\sigma}^{-1} \tau) N^{C_\tau} \quad (5.16)$$

We can modify the surface in Figure 16 to arrive at the surface, where the S_n TFT computes the correlator. Replace the loop labelled σ by a pair of loops related to the original loop by deforming slightly away in opposite directions. Cut out the region between them. Label these $\sigma, \tilde{\sigma}$. Cut out another hole based at the same point and insert the sum $\sum_{\tau \in S_n} N^{C_\tau} \tau$ at the boundary of the hole. This is shown in Figure 21. Traversing round the 2-cell gives the contractible path associated with $\gamma \sigma \gamma^{-1} \tilde{\sigma} \tau$. Hence the two-point function is the S_n -TFT partition functions associated with the surface shown in Figure 21. The cut-out regions are shaded and there is an observable $\sum_{\tau} N^{C_\tau} \tau$ inserted at the loop labelled τ .

The three-point function for the \mathbb{C}^3 case (see equation 4.5) is

$$\langle \mathcal{O}_{\sigma^{(1)}} \mathcal{O}_{\sigma^{(2)}} (\mathcal{O}_{\tilde{\sigma}})^\dagger \rangle = \sum_{\tau \in S_n} \sum_{\gamma \in H} \delta(\gamma(\sigma^{(1)} \circ \sigma^{(2)}) \gamma^{-1} \tilde{\sigma}^{-1} \tau) N^{C_\tau} \quad (5.17)$$

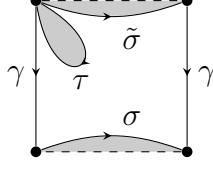


Figure 21: \mathbb{C}^3 torus with holes

Here $\sigma_1 \in S_{n^{(1)}}$, $\sigma_2 \in S_{n^{(2)}}$, $\tilde{\sigma} \in S_{n^{(1)}+n^{(2)}}$ and we defined $n = n^{(1)} + n^{(2)}$. This is computed by S_n TFT on the same surface shown in Figure 21, but with the boundary permutation σ replaced by $\sigma^{(1)} \circ \sigma^{(2)}$.

For the case of the conifold, we fix the numbers $n_{12}^{(1)}, n_{12}^{(2)}$ of operators in the (N, \bar{N}) representation, and $n_{21}^{(1)}, n_{21}^{(2)}$ in the representation (\bar{N}, N) . We have $n = n_{12}^{(1)} + n_{12}^{(2)} = n_{21}^{(1)} + n_{21}^{(2)}$. We define $H_{12} = S_{n_{12}^{(1)}} \times S_{n_{12}^{(2)}}$ and $H_{21} = S_{n_{21}^{(1)}} \times S_{n_{21}^{(2)}}$. The operators are described by two permutations (σ_1, σ_2) each in S_n , which relate fundamental and anti-fundamental indices for the two gauge groups. There are equivalences

$$(\sigma_1, \sigma_2) \sim (\gamma_{21}\sigma_1\gamma_{12}^{-1}, \gamma_{12}\sigma_2\gamma_{21}^{-1}) \quad (5.18)$$

Restricting to $n \leq N$, where there are no further finite N constraints, and using the Burnside Lemma

$$\mathcal{N}_{\mathcal{C}}(n_{12}^{(1)}, n_{12}^{(2)}, n_{21}^{(1)}, n_{21}^{(2)}) = \frac{1}{|H_1||H_2|} \sum_{\gamma_{12} \in H_{12}} \sum_{\gamma_{21} \in H_{21}} \delta(\gamma_{21}\sigma_1\gamma_{12}^{-1}\sigma_1^{-1})\delta(\gamma_{12}\sigma_2\gamma_{21}^{-1}\sigma_2^{-1}) \quad (5.19)$$

Comparing to (5.10) we see that

$$\mathcal{N}_{\mathcal{C}}(n_{12}^{(1)}, n_{12}^{(2)}, n_{21}^{(1)}, n_{21}^{(2)}) = Z(T^2; D_{H_{12}}, D_{H_{21}}) \quad (5.20)$$

The procedure for going from the quiver to the TFT data is the same as in the case of \mathbb{C}^3 . Collapse multiple edges with the same start and end-points to a single edge. Take a cylinder for each gauge group and a cylinder for each edge. This is essentially the operation of thickening the quiver diagram into a surface. Equivalently, we can describe this as forming a split-node version of the quiver where multiple edges have been replaced with single edges, and then thickening all the edges of this quiver. The cylinders for the matter edges are equipped with closed H -defects. Glue the cylinders together. This is illustrated in Figure 22. The TFT partition function can be computed using a simple cell decomposition with two 2-cells, summing over additional permutations σ_1, σ_2 extending along lines located along the thickened tubes for each gauge group as in Figure 18.

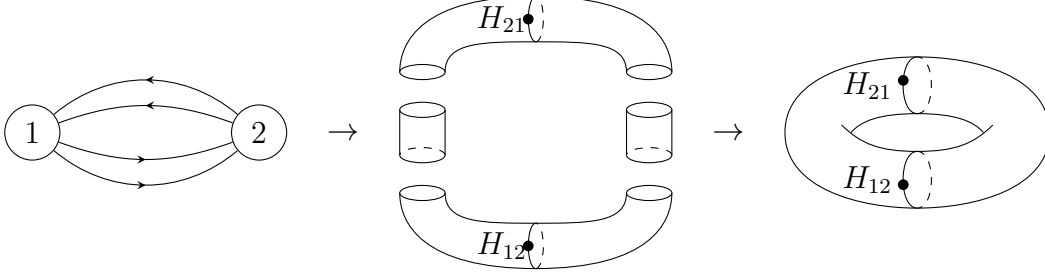


Figure 22: Transforming conifold quiver into a Riemann surface

The two-point functions for the conifold, in the permutation basis for the operators, are

$$\langle \mathcal{O}_{\sigma_1, \sigma_2} (\mathcal{O}_{\tilde{\sigma}_1, \tilde{\sigma}_2})^\dagger \rangle = \sum_{\gamma_{12} \in H_{12}} \sum_{\gamma_{21} \in H_{21}} \sum_{\tau_1 \in S_n} \sum_{\tau_2 \in S_n} N^{C_{\tau_1}} N^{C_{\tau_2}} \delta(\gamma_{21} \sigma_1 \gamma_{12}^{-1} \tilde{\sigma}_1^{-1} \tau_1) \delta(\gamma_{12} \sigma_2 \gamma_{21}^{-1} \tilde{\sigma}_2^{-1} \tau_2) \quad (5.21)$$

To obtain this as a partition function in TFT, we use Figure 23. The lines associated with σ_1 and σ_2 , extending along the lines for each gauge group, have been cut to separate σ_1, σ_2 from $\tilde{\sigma}_1, \tilde{\sigma}_2$. And we have inserted on the 2-cells previously associated to each gauge group additional boundaries carrying permutations $\sum_{\tau_1} N^{C_{\tau_1}} \tau_1$ and $\sum_{\tau_2} N^{C_{\tau_2}} \tau_2$. The two contractible 2-cells, associated to one gauge group each, give following (5.2), the correct delta functions in (5.21).

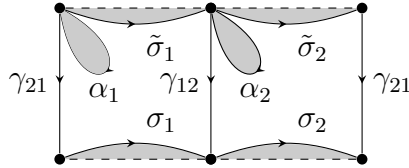


Figure 23: Conifold torus with holes

The three point functions $\langle \mathcal{O}_{\sigma_1^{(1)}, \sigma_2^{(1)}} \mathcal{O}_{\sigma_1^{(2)}, \sigma_2^{(2)}} (\mathcal{O}_{\tilde{\sigma}_1, \tilde{\sigma}_2})^\dagger \rangle$ are obtained by the replacement $\sigma_a \rightarrow \sigma_a^{(1)} \circ \sigma_a^{(2)}$ in (5.21), which is a simple replacement in the TFT defect operators of Figure 23.

For $\mathbb{C}^3/\mathbb{Z}_2$, with specified numbers $n_{11}, n_{12}^{(1)}, n_{12}^{(2)}, n_{21}^{(1)}, n_{21}^{(2)}, n_{22}$, we have the counting

$$\begin{aligned} & \mathcal{N}_{\mathbb{C}^3/\mathbb{Z}_2}(n_{11}, n_{12}^{(1)}, n_{12}^{(2)}, n_{21}^{(1)}, n_{21}^{(2)}, n_{22}) \\ &= \frac{1}{|H_{12}| |H_{21}| |H_{11}| |H_{22}|} \sum_{\gamma_{11} \in S_{n_{11}}} \sum_{\gamma_{22} \in S_{n_{22}}} \sum_{\gamma_{12} \in H_{12}} \sum_{\gamma_{21} \in H_{21}} \sum_{\sigma_1 \in S_{n_1}} \sum_{\sigma_2 \in S_{n_2}} \quad (5.22) \\ & \delta((\gamma_{11} \circ \gamma_{21}) \sigma_1 (\gamma_{11}^{-1} \circ \gamma_{12}^{-1}) \sigma_1^{-1}) \delta((\gamma_{22} \circ \gamma_{12}) \sigma_2 (\gamma_{22}^{-1} \circ \gamma_{21}^{-1}) \sigma_2^{-1}) \end{aligned}$$

with $H_{12} = S_{n_{12}^{(1)}} \times S_{n_{12}^{(2)}}$, $H_{21} = S_{n_{21}^{(1)}} \times S_{n_{21}^{(2)}}$ and

$$\begin{aligned} n_1 &= n_{21}^{(1)} + n_{21}^{(2)} + n_{11} = n_{11} + n_{12}^{(1)} + n_{12}^{(2)} \\ n_2 &= n_{12}^{(1)} + n_{12}^{(2)} + n_{22} = n_{12}^{(1)} + n_{12}^{(2)} + n_{22} \end{aligned} \quad (5.23)$$

Note that $n_{21}^{(1)} + n_{21}^{(2)} = n_{12}^{(1)} + n_{12}^{(2)}$. The total number of distinct indices being permuted is $n_{11} + n_{22} + n_{12}^{(1)} + n_{12}^{(2)}$, so this will be related to S_n TFT with $n = n_{11} + n_{22} + n_{12}^{(1)} + n_{12}^{(2)}$. The relations between S_n and its different subgroups is best expressed with the diagram in 3.28. The counting is reproduced as a TFT partition function on a genus two surface. To describe this surface, and the associated defects, we first replace multiple edges with same start and end points by single edges, then we form the split-node version of this quiver. This has edges for the gauge group and for the matter fields. Build the surface by taking a tube for each edge. The vertices become three-holed spheres. Insert closed H -defects on the matter tubes, so that the permutations around these loops are constrained as $\gamma_{ab} \in S_{n_{ab}} \subset S_n$. We introduce unit open Wilson lines connecting the H -defects on the 3-holed spheres, as in Figure 19. The construction of the genus two Riemann surface is shown in Figure 24. This ensures that the holonomies are $\gamma_{11} \circ \gamma_{21}$ and $\gamma_{22}^{-1} \circ \gamma_{21}^{-1}$ at the left and right upper ends of the gauge group cylinders ; they are $\gamma_{11}^{-1} \circ \gamma_{12}^{-1}$ and $\gamma_{22} \circ \gamma_{12}$ at the left and right lower circles of the two cylinders. There are line defects with holonomies σ_1 constrained to be in $S_{n_1} \in S_n$, and $\sigma_2 \in S_{n_2} \in S_n$. The TFT partition function in the presence of these defects leads to the delta functions in (5.22), coming from the two 2-cells of the gauge-group cylinders. So we can state that

$$\mathcal{N}_{\mathbb{C}^3/Z_2}(n_{11}, n_{12}^{(1)}, n_{12}^{(2)}, n_{21}^{(1)}, n_{21}^{(2)}, n_{22}) = Z(\Sigma_{G=2}; D_{H_{11}}, D_{H_{21}}, D_{H_{12}}, D_{H_{21}}; W) \quad (5.24)$$

H_{ab} are the groups $S_{n_{ab}}$. W stands for the set of unit open Wilson lines on the three-holed spheres and the constraints requiring the σ_1, σ_2 to live in in the subgroups S_{n_1}, S_{n_2} .

Again, going from counting to 2-point functions, is a simple step in the S_n TFT, as shown in Figure 25. The σ_1 -edge on the first cylinder is split into two edges joined to form a circle surrounding a hole in the surface, now carrying fixed permutations $\sigma_1, \tilde{\sigma}_1$ from the two chosen operators. Likewise the σ_2 edge is split into a pair of edges carrying $\sigma_2, \tilde{\sigma}_2$ permutations. An additional hole in each gauge group cylinder carries $\sum_{\tau_a \in S_{n_a}} N^{C_{\tau_a}} \tau_a$.

$$\begin{aligned} &\langle \mathcal{O}_{\sigma_1, \sigma_2} (\mathcal{O}_{\tilde{\sigma}_1, \tilde{\sigma}_2})^\dagger \rangle \\ &= \sum_{\gamma_{11} \in S_{n_{11}}} \sum_{\gamma_{22} \in S_{n_{22}}} \sum_{\gamma_{12} \in H_{12}} \sum_{\gamma_{21} \in H_{21}} \sum_{\tau_1 \in S_{n_1}} \sum_{\tau_2 \in S_{n_2}} \\ &N^{C_{\tau_1} + C_{\tau_2}} \delta((\gamma_{11} \circ \gamma_{21}) \sigma_1 (\gamma_{11}^{-1} \circ \gamma_{12}^{-1}) \tilde{\sigma}_1^{-1} \tau_1) \delta((\gamma_{22} \circ \gamma_{12}) \sigma_2 (\gamma_{22}^{-1} \circ \gamma_{21}^{-1}) \tilde{\sigma}_2^{-1} \tau_2) \end{aligned} \quad (5.25)$$

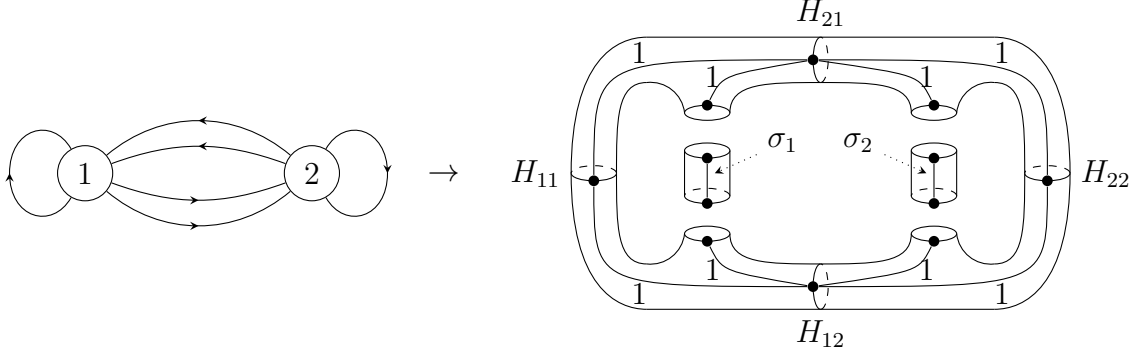


Figure 24: Transforming $\mathbb{C}^3/\mathbb{Z}_2$ quiver into a Riemann surface

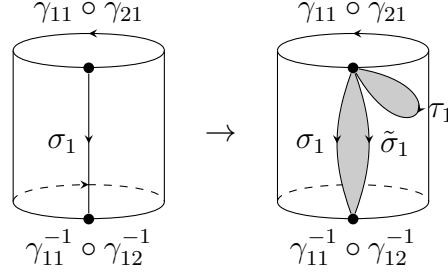


Figure 25: Splitting σ_a in gauge group cylinder to go from counting to 2-point function.

We have the equality

$$\langle \mathcal{O}_{\sigma_1, \sigma_2} (\mathcal{O}_{\tilde{\sigma}_1, \tilde{\sigma}_2})^\dagger \rangle = Z(\Sigma_{G=2, B=2}; \sigma_1, \sigma_2, \tilde{\sigma}_1, \tilde{\sigma}_2; D_{H_{11}}, D_{H_{11}}, D_{H_{12}}, D_{H_{21}}; W, S) \quad (5.26)$$

Again the quiver correlator to S_n TFT correspondence generalizes simply from two to three-point functions

$$\begin{aligned} & \langle \mathcal{O}_{\sigma_1^{(1)}, \sigma_2^{(1)}} \mathcal{O}_{\sigma_1^{(2)}, \sigma_2^{(2)}} (\mathcal{O}_{\tilde{\sigma}_1, \tilde{\sigma}_2})^\dagger \rangle \\ &= Z(\Sigma_{G=2, B=2}; \sigma_1^{(1)} \circ \sigma_1^{(2)}, \sigma_2^{(1)} \circ \sigma_2^{(2)}, \tilde{\sigma}_1, \tilde{\sigma}_2; D_{H_{11}}, D_{H_{22}}, D_{H_{12}}, D_{H_{21}}; W) \end{aligned} \quad (5.27)$$

In this case, $n = \tilde{n}_{11} + \tilde{n}_{22} + \tilde{n}_{12}^{(1)} + \tilde{n}_{12}^{(2)}$. And we have selection rules $n_{ab}^{(1)} + n_{ab}^{(2)} = \tilde{n}_{ab}$.

The generalization of the above constructions to an arbitrary quiver should be clear from the above examples. Having chosen n_{ab}^α and $n_{ab} = \sum_\alpha n_{ab}^\alpha$, the counting will be given in terms of gauge theory with an S_n group which contains all the $S_{n_{ab}}$ and S_{n_a} . The way these are embedded in S_n can be drawn with a diagram such as Figure (3.28). There are constraints

$$n_a = \sum_b n_{ba} = \sum_b n_{ab} \quad (5.28)$$

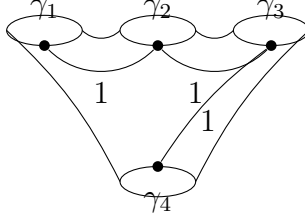


Figure 26: 4-holed sphere with defects, imposing $\gamma_4^{-1} = \gamma_1\gamma_2\gamma_3$

and groups $H_{ab} = \times_{\alpha} S_{n_{ab}^{\alpha}}$. There are subsets $\mathcal{S}(n_{ab})$ of the integers $\{1, \dots, n\}$ corresponding to strands in the diagram of the type (3.28). There are subsets $\mathcal{S}(n_a)$ related to $\mathcal{S}(n_{ab})$ by equations reflecting (5.28) but in terms of subset embeddings :

$$\mathcal{S}(n_a) = \bigcup_b \mathcal{S}(n_{ba}) = \bigcup_b \mathcal{S}(n_{ab}) \quad (5.29)$$

The integer n is given by

$$n = \sum_a n_{aa} + \sum_{a < b} n_{ab} \quad (5.30)$$

Correspondingly the set $\mathcal{S}(n) = \{1, \dots, n\}$ is a union reflecting (5.30)

$$\mathcal{S}(n) = \bigcup_a \mathcal{S}(n_{aa}) \bigcup_{a < b} \mathcal{S}(n_{ba}) \quad (5.31)$$

To express the counting in terms of TFT, we use S_n -TFT with n given above. To get the surface, we collapse all the directed edges from a fixed a to b into a single directed edge. We form the split node quiver, thicken it by introducing cylinders for the matter edges and the gauge groups, multi-holed spheres at the incoming and outgoing nodes. We insert closed- $S_{n_{ab}}$ defects on the $a \rightarrow b$ cylinders. The multi-holed spheres have appropriate unit-Wilson lines as in Figure 26. The cylinder for gauge group a has a Wilson line constrained to have holonomy σ_a in $S_{n_a} \subset S_n$. To go from counting of operators to 2-point and 3-point correlators involves the same steps as above, applied separately to each cylinder.

5.3 Fundamental groups, covering spaces and worldsheets

We have emphasized the interpretation of the quiver counting and correlators in terms of 2D S_n lattice TFT on Riemann surfaces Σ_G equipped with defects, since the latter is a concrete computable physical model. There are other fascinating geometry constructions that should link to quiver free field observables via the S_n -TFT. These will be interesting

research avenues for the future. The simplest constructions in lattice S_n TFT on a Riemann surface can be interpreted in terms of covering spaces of the Riemann surface, of degree n . This is indeed crucial to the string interpretation of the large N expansion of two dimensional Yang Mills theory [32, 52, 53]. The S_n holonomies of S_n gauge theory on Σ_G are interpreted in terms of permutations of the covering sheets induced by lifting paths in Σ_G to covers of Σ_G . The presence of closed H -defects, where H takes the form of product subgroups such as $S_{n_{11}} \times S_{n_{21}} \times \dots$, can be interpreted in terms of covers involving multiple types of sheets. Variations on the standard covering space mathematics occur in the context of the large N expansion of two dimensional Yang Mills [32, 60, 61], particularly when Wilson loops (possibly intersecting ones) are introduced. Another setting for permutation defects is in 2D conformal field theory [62]. From an AdS/CFT perspective, the appearance of covering spaces of a two dimensional space for a large class of quiver gauge theories suggests the interpretation of the covering spaces as string worldsheets, and the two dimensional base-space of the TFT as a part of the dual spacetime. Can this interpretation be developed in terms of the Sasaki-Einstein duals of the gauge theory at non-zero coupling [37] ?

A systematic account of the relation between cutting and gluing of Riemann surfaces and constructions of 2D TFT connects with the description of TFT as a functor between a category of 1-dimensional objects and two dimensional cobordisms on the one hand and a category of Frobenius algebras on the other. These constructions [54, 63] have been generalized [57, 58, 64, 65] to the equivariant case, which should be relevant here. The paper [57] includes lattice constructions similar to what we have used in describing the H -defects. To get the counting and correlators of quiver theories, we need to specialize the general G -equivariant discussion to S_n , but allow n to be arbitrary as part of an inductive S_∞ construction. This type of S_∞ TFT (in the non-equivariant setting) has already been discussed [66].

Many developments in 2D TFT treat the base space of the TFT as string worldsheet. Here, as emphasized through the analogies to large N 2dYM, the base space of the TFT should be considered as the target space of strings. The covering spaces are string worldsheets. This is also a feature of Matrix strings where S_n orbifold CFTs (which are related to S_n TFTs) are treated as spacetime CFTs [67]. There should also be a TFT on the worldsheets, with $1/N$ playing the role of string coupling, with different regions of the worldsheets mapping to different spacetime regions (cut-out by the defects in the spacetime TFT) being characterized by distinct worldsheet phases. It will be very interesting to infer the systematics of this worldsheet TFT, by using the link to the spacetime S_n TFT provided by covering space theory.

5.4 Young diagram basis and TFT constructions

We have not so far expressed our construction of orthogonal bases at finite N in terms of 2D TFT. We expect this should be possible by Fourier transforming from the permutation basis to representation bases. An encouraging hint is that the basic quantities entering the counting, namely the Littlewood-Richardson coefficients $g(R_1, R_2, R_3)$ as well as the Kronecker product coefficients $C(R_1, R_2, R_3)$ can be constructed in S_n TFT using the kind of defects we have considered. Consider the partition function $Z(\sigma_1, \sigma_2, \sigma_3)$ of the 3-holed sphere shown in Figure 19

$$Z(\Sigma_{G=0, B=3}; \sigma_1, \sigma_2, \sigma_3) = \delta(\sigma_1 \sigma_2 \sigma_3) \quad (5.32)$$

Sum over $\sigma_1 \in S_{n_1} \subset S_{n=n_1+n_2}$ and $\sigma_2 \in S_{n_2} \subset S_{n=n_1+n_2}$ with the normalization $\frac{1}{n_1!n_2!}$. Multiply by $\chi_{R_1}(\sigma_1)\chi_{R_2}(\sigma_2)\chi_{R_3}(\sigma_3)$ and sum over $R_1 \vdash n_1, R_2 \vdash n_2, R_3 \vdash n$ to get

$$\begin{aligned} & Z(\Sigma_{G=0, B=3}; R_1, R_2, R_3) \\ &= \frac{1}{n_1!n_2!} \sum_{\sigma_1 \in S_{n_1}} \sum_{\sigma_2 \in S_{n_2}} \chi_{R_1}(\sigma_1)\chi_{R_2}(\sigma_2)\chi_{R_3}(\sigma_3) Z(\Sigma_{G=0, B=3}; \sigma_1, \sigma_2, \sigma_3) \\ &= \frac{1}{n_1!n_2!} \sum_{\sigma_1, \sigma_2} \chi_{R_1}(\sigma_1)\chi_{R_2}(\sigma_2)\chi_{R_3}(\sigma_1 \circ \sigma_2) \\ &= g(R_1, R_2, R_3) \end{aligned} \quad (5.33)$$

To get $C(R_1, R_2, R_3)$ take a cylinder, with boundary permutations σ_1, σ_3 and insert a closed defect in the middle with permutation σ_2 (see Figure 27). All three are in S_n . The partition function is

$$Z(S^1 \times I; \sigma_1, \sigma_2, \sigma_3) = \sum_{\gamma_1, \gamma_2 \in S_n} \delta(\sigma_1 \gamma_1 \sigma_2^{-1} \gamma_1^{-1}) \delta(\sigma_2 \gamma_2 \sigma_1^{-1} \gamma_2^{-1}) \quad (5.34)$$

Sum over permutations, weighted by characters to get a representation basis partition functions

$$\begin{aligned} & Z(S^1 \times I; R_1, R_2, R_3) \\ &= \frac{1}{(n!)^3} \sum_{R_1, R_2, R_3 \vdash n} \chi_{R_1}(\sigma_1)\chi_{R_2}(\sigma_2)\chi_{R_3}(\sigma_3) Z(S^1 \times I; \sigma_1, \sigma_2, \sigma_3) \\ &= \frac{1}{n!} \sum_{\sigma_1 \in S_n} \chi_{R_1}(\sigma_1)\chi_{R_2}(\sigma_1)\chi_{R_3}(\sigma_1) \\ &= C(R_1, R_2, R_3) \end{aligned} \quad (5.35)$$

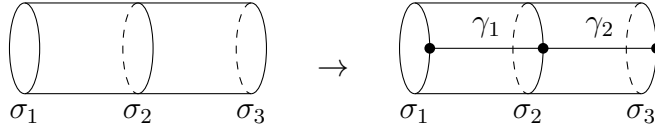


Figure 27: Cylinder with $\sigma_1, \sigma_2, \sigma_3$ insertions

6 Interacting chiral ring

So far we have constructed the finite- N chiral ring of the *free* quiver theories, that is, with zero superpotential. In the context of AdS/CFT theories without superpotential arise at special points of a moduli space of CFTs, generically with non-zero superpotential. For the generic CFTs, the free chiral ring gets modified by identifying F-terms with zero.

In general, there are physical arguments that the mesonic chiral ring of the gauge theory on $D3$ branes at a Calabi-Yau singularity Y^6 is the coordinate ring of the symmetric product space $\text{Sym}^N(Y^6)$. In other words, the partition function of the chiral ring is counting the states of N identical bosons on Y^6 . In some cases this can be argued by using the geometric invariant theory [68].

Such arguments, however, work at the level of counting, and do not provide an explicit construction of the operators, which could be identified with dual BPS states in AdS. Here we make the first steps in the construction of the interacting chiral ring at finite N , using the free orthogonal basis derived in the previous sections.

6.1 Review of the chiral ring

As an example we take the theory on $D3$ branes at a conifold singularity. It has the quiver shown in Figure 9 that we have analyzed before, but at a generic fixed point there is a non-zero superpotential

$$W_{\mathcal{C}} = \text{tr}(A_1 B_1 A_2 B_2) - \text{tr}(A_1 B_2 A_2 B_1) \quad (6.1)$$

In general, such quiver-superpotential pairs (for \mathbb{C}^3 , $\mathbb{C}^3/\mathbb{Z}_2$, dP_0 and many others) can be constructed using the technology of brane tilings [69, 70].

When we have W , the chiral ring gets modified compared to the free theory: the operators have to be identified up to F-terms

$$F = \left\{ \frac{\partial W}{\partial \Phi_{ab;\alpha}} \right\} \quad (6.2)$$

For example, the conifold F-terms are

$$F_C = \{B_1 A_2 B_2 - B_2 A_2 B_1, \quad B_2 A_1 B_1 - B_1 A_1 B_2, \\ A_2 B_2 A_1 - A_1 B_2 A_2, \quad A_1 B_1 A_2 - A_2 B_1 A_1\} \quad (6.3)$$

In the interacting chiral ring they are identified with 0

$$F \sim 0 \quad (6.4)$$

For the conifold expressions (6.3) implies that within the chiral ring we can commute A 's through B 's and vice versa. The resulting mesonic chiral ring at large N is thus spanned by

$$S^{i_1 i_2 \dots i_n} S^{j_1 j_2 \dots j_n} \text{tr}(A_{i_1} B_{j_1} A_{i_2} B_{j_2} \dots A_{i_n} B_{j_n}) \quad (6.5)$$

where S is a symmetric tensor, and products of such symmetrized traces.

To get the interacting chiral ring at finite N we have to enforce both finite N constraints, and F-terms. Note that they might not be independent, for example, at $N = 1$ the F-terms F_C themselves vanish, so the free and interacting chiral rings are the same. In order to clarify the situation, let us define the construction more rigorously.

Let $V^{(\infty)}$ be the ring of chiral gauge invariant operators of the free theory at $N = \infty$, that is, treating operators as formal products of traces, without any finite N identifications. The basis can be labelled by \mathbf{L} or \mathbf{K} as constructed in the previous sections

$$V^{(\infty)} = \{\mathcal{O}(\mathbf{L})\} \quad (6.6)$$

At finite N some operators in $V^{(\infty)}$ vanish – they form an ideal³ $V_N \subset V^{(\infty)}$

$$V_N = \{\mathcal{O}(\mathbf{L}) \mid l(R_a) > N\} \quad (6.7)$$

The quotient is the free chiral ring at finite N

$$V^{(N)} = V^{(\infty)} / V_N \quad (6.8)$$

which is spanned by operators with $l(R_a) \leq N$. Now, let V_F be the space of all gauge invariant operators at $N = \infty$, which are identified with zero by F-terms. It is spanned by all operators containing an F-term anywhere within a trace

$$V_F = \{\text{tr}(f \Phi_{i_1 j_1; \alpha_1} \Phi_{i_2 j_2; \alpha_2} \dots) \mathcal{O}(\mathbf{L}) \mid f \in F\} \quad (6.9)$$

³ V_N is an ideal of $V^{(\infty)}$ because a product of vanishing operator and any other operator is also vanishing

V_F is also an ideal of $V^{(\infty)}$. The $N = \infty$ interacting chiral ring is then the quotient

$$V_{\text{int}}^{(\infty)} = V^{(\infty)} / V_F \quad (6.10)$$

It is spanned by products of symmetrized traces as in (6.5). Finally, the finite N interacting chiral ring is

$$V_{\text{int}}^{(N)} = V^{(\infty)} / (V_F \cup V_N) \quad (6.11)$$

that is, we identify operators in $V^{(\infty)}$ if they differ by V_F or V_N . This quotient can be implemented explicitly using computational algebraic geometry [71]. This is practical at small N but becomes computationally prohibitive at large N .

To illustrate the different spaces ($V^{(\infty)}$, $V^{(N)}$, $V_{\text{int}}^{(\infty)}$, $V_{\text{int}}^{(N)}$, V_F , V_N) we list the corresponding partition functions for the conifold theory. The operators in $V^{(\infty)}$ are counted by (2.46):

$$Z^{(\infty)} = \prod_{k=1}^{\infty} \frac{1}{(1 - a_1^k b_1^k - a_1^k b_2^k - a_2^k b_1^k - a_2^k b_2^k)} \quad (6.12)$$

The finite N free chiral ring $V^{(N)}$ counting is given explicitly by our construction (2.14)

$$\begin{aligned} Z^{(N)} = & \sum_{\substack{R_1, R_2 \\ l(R_a) \leq N}} \sum_{\substack{r_{A_1}, r_{A_2} \\ r_{B_1}, r_{B_2}}} a_1^{|r_{A_1}|} a_2^{|r_{A_2}|} b_1^{|r_{B_1}|} b_2^{|r_{B_2}|} \\ & \times g(r_{A_1}, r_{A_2}; R_1) g(r_{B_1}, r_{B_2}; R_1) g(r_{A_1}, r_{A_2}; R_2) g(r_{B_1}, r_{B_2}; R_2) \end{aligned} \quad (6.13)$$

The size of V_N is the difference

$$Z_N = Z^{(\infty)} - Z^{(N)} \quad (6.14)$$

The partition function of $V_{\text{int}}^{(\infty)}$ can be written from first principles, by counting products of symmetrized traces, containing equal number of A 's and B 's:

$$Z_{\text{int}}^{(\infty)} = \prod_{n=1}^{\infty} \prod_{n_1=0}^n \prod_{m_1=0}^n \frac{1}{(1 - a_1^{n_1} b_1^{m_1} a_2^{n-n_1} b_2^{n-m_1})} \quad (6.15)$$

which also gives us V_F via (6.10):

$$Z_F = Z^{(\infty)} - Z_{\text{int}}^{(\infty)} \quad (6.16)$$

Finally, according to the argument that $V_{\text{int}}^{(N)}$ is the coordinate ring of $\text{Sym}^N(\mathcal{C})$, the partition function for it, using the technology of plethystics [72], is

$$Z_{\text{int}}^{(N)} = \left[\prod_{n=0}^{\infty} \prod_{n_1=0}^n \prod_{m_1=0}^n \frac{1}{(1 - \nu a_1^{n_1} b_1^{m_1} a_2^{n-n_1} b_2^{n-m_1})} \right]_{\nu^N} \quad (6.17)$$

Here $[\dots]_{\nu^N}$ denotes taking the coefficient of ν^N term. This allows to calculate the size of the union $V_F \cup V_N$

$$Z_{F \cup N} = Z^{(\infty)} - Z_{\text{int}}^{(N)} \quad (6.18)$$

6.2 Chiral ring from operators

In this section we apply our technology to explicitly derive the size of the conifold finite N chiral ring $V_{\text{int}}^{(N)}$ for a simple choice of charges

$$n_1 = m_1 = 1, \quad n_2 = m_2 = N \quad (6.19)$$

That is, we look at operators of the form $(A_1 B_1)(A_2 B_2)^N$. This is restrictive but is valid for any N . Any direct computational method of tackling this runs into having to deal with N^2 variables, which is not viable at large N .

Specifically, the goal is to calculate $[Z_{\text{int}}^{(N)}]_{a_1 b_1 a_2^N b_2^N}$ *without* using the N -boson counting (6.17), but instead relying on the explicit description

$$V_{\text{int}}^{(N)} = V^{(\infty)} / (V_F \cup V_N) \quad (6.20)$$

We can write the corresponding partition function as

$$\begin{aligned} Z_{\text{int}}^{(N)} &= Z^{(\infty)} - (Z_N + Z_F - Z_{N \cap F}) \\ &= Z_{\text{int}}^{(\infty)} - (Z_N - Z_{N \cap F}) \end{aligned} \quad (6.21)$$

In other words, to get the finite N ring counting $Z_{\text{int}}^{(N)}$ we can take the ring spanned by symmetrized traces $Z_{\text{int}}^{(\infty)}$ and subtract the number of finite N constraints Z_N , but excluding $Z_{N \cap F}$ compensating for the fact that some V_N is already included in V_F . We know $Z_{\text{int}}^{(\infty)}$ (6.15) and Z_N (6.14), but the calculation of $Z_{N \cap F}$ is non-trivial. In fact, the choice of charges (6.19) is the first example where the intersection $V_F \cap V_N$ is non-empty.

First, let us calculate the expected result using the N -boson description. The combination

$$Z_{\text{int}}^{(\infty)} - Z_{\text{int}}^{(N)} = Z_N - Z_{N \cap F} \quad (6.22)$$

counts the number of boson states with more than N bosons. With our choice of charges there are just two such states, involving $N + 1$ bosons:

$$|(A_1 B_1), (A_2 B_2)^{\otimes N}\rangle \quad |(A_1 B_2), (A_2 B_1), (A_2 B_2)^{\otimes (N-1)}\rangle \quad (6.23)$$

Thus, we expect

$$Z_N - Z_{N \cap F} = 2 \quad (6.24)$$

We confirm this with the explicit description of operators forming V^∞, V_N, V_F in Appendix D.5.

6.3 Giant gravitons in the conifold

In this section we find dual operators to certain giant graviton states, following the identification of [73–76]. Related discussions in the context of the conifold or ABJM theory appear in [40, 77]. The main purpose here is to identify the operators previously considered in connection with giants among those spanning the complete orthogonal bases we have described.

In general, D3 branes wrapping non-contractible cycles in geometry are identified with baryonic operators. In the conifold theory we have $AdS_5 \times T^{1,1}$ geometry in the bulk, where $T^{1,1}$ is the base of the conifold cone. In homogeneous coordinates the conifold is given by an identification

$$\mathcal{C}: \quad (a_1, a_2, b_1, b_2) \sim (\lambda a_1, \lambda a_2, \lambda^{-1} b_1, \lambda^{-1} b_2), \quad \lambda \in \mathbb{C} \quad (6.25)$$

The $T^{1,1}$ base can be expressed as:

$$\begin{aligned} T^{1,1}: \quad & |a_1|^2 + |a_2|^2 = |b_1|^2 + |b_2|^2 = 1, \\ & (a_1, a_2, b_1, b_2) \sim (e^{i\alpha} a_1, e^{i\alpha} a_2, e^{-i\alpha} b_1, e^{-i\alpha} b_2), \quad \alpha \in \mathbb{R} \end{aligned} \quad (6.26)$$

Minimal non-contractible D3 branes in $T^{1,1}$, using Mikhailov's [78] construction, are given by

$$a_i = 0 \quad (B = 1), \quad b_i = 0 \quad (B = -1) \quad (6.27)$$

The baryon number ($B = \pm 1$) corresponds to the homology class of $T^{1,1}$. The dual operators in the chiral ring are determinants

$$a_i = 0 \leftrightarrow \mathcal{O} = \det(A_i), \quad b_i = 0 \leftrightarrow \mathcal{O} = \det(B_i) \quad (6.28)$$

In the basis constructed in this paper we deal only mesonic operators, that is, $B = 0$ sector. We can identify composite giant configurations with total $B = 0$, for example

$$a_1 b_1 = 0 \quad \Leftrightarrow \quad \mathcal{O}_{11} = \det(A_1) \det(B_1) \quad (6.29)$$

The dual operator is mesonic and, in fact, can be expressed nicely in our basis

$$\mathcal{O}_{11} = \det(A_1 B_1) = \mathcal{O} \left(\begin{array}{c} r_{B_1} = \begin{array}{|c|} \hline \square \\ \hline \square \\ \hline \square \\ \hline \end{array} \\ \begin{array}{ccc} \begin{array}{|c|} \hline \square \\ \hline \square \\ \hline \square \\ \hline \end{array} & \begin{array}{c} \begin{array}{c} \circ \quad \circ \\ \downarrow \quad \uparrow \\ \circ \quad \circ \end{array} \\ r_{B_2} = \emptyset \\ r_{A_2} = \emptyset \end{array} & \begin{array}{|c|} \hline \square \\ \hline \square \\ \hline \square \\ \hline \end{array} \\ \end{array} \right) \quad (6.30)$$

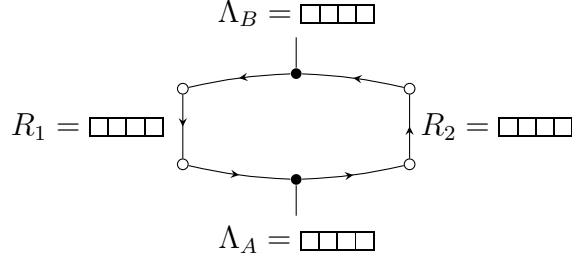


Figure 29: Representation containing AdS giants

and B_1, B_2 , so for an operator like $\det(A_1 B_1)$ there are no F-term identifications. In other words, the elements of the interacting chiral ring are equivalence classes up to F-terms, but an operator only involving A_1, B_1 is the unique operator in its equivalence class. Therefore, these operators are protected from mixing, in a similar way like half-BPS operators in \mathbb{C}^3 . We can identify all such protected operators: in order to have a highest weight state with only A_1, B_1 , the $SU(2) \times SU(2)$ representation must be $(\Lambda_A, \Lambda_B) = ([n], [n])$, where Λ 's are single-row. This is analogous to half-BPS operators in \mathbb{C}^3 having $\Lambda = [n]$. Then $R_1 = R_2$ can be anything, but are forced to be equal, in order to have $[n]$ in their product. Thus we have a class of operators in the chiral ring labelled by $R \vdash n$ for any n as in Figure 30.

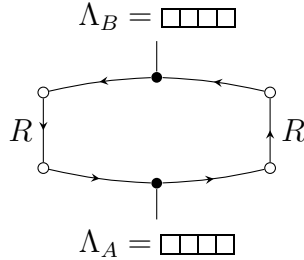


Figure 30: Protected representation

The highest weight operator in this representation can be expressed as

$$\mathcal{O}_C(R) = \frac{1}{n!} \sum_{\sigma} \chi_R(\sigma) \text{tr}_{V_N^{\otimes n}}(\sigma (A_1 B_1)^{\otimes n}) \quad (6.32)$$

7 The case with fundamental matter

In this section we sketch how our techniques can be extended to quivers involving fundamental and anti-fundamental matter. These are represented by different kind of nodes, with only incoming or only outgoing arrows.

The simplest example is SQCD. The counting of chiral operators has been studied in connection with the moduli space for SQCD in papers [79–82]. These papers have made a connection between Schur polynomials and this counting. Here we will construct a basis for these operators which diagonalizes the (Zamolodchikov) inner product given by the 2-point functions in the free field theory at finite N . The enumeration of states in the basis will agree with the previous counting results.

Consider $U(N)$ gauge theory with M chiral multiplets in a fundamental representation (quarks) and M in anti-fundamental (anti-quarks), the quiver is shown in Figure 31. Gauge

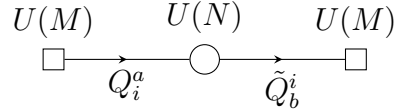


Figure 31: SQCD quiver for gauge group $U(N)$, M quarks Q_i^a and M antiquarks \tilde{Q}_b^i

invariant operators can be written like in analogy with (3.30), but now with open flavour indices

$$\begin{aligned} \mathcal{O}(\sigma, \vec{a}, \vec{b}) &= (Q_{j_1}^{a_1} \cdots Q_{j_n}^{a_n})(\delta_{i_{\sigma(1)}}^{j_1} \cdots \delta_{i_{\sigma(n)}}^{j_n})(\tilde{Q}_{b_1}^{i_1} \cdots \tilde{Q}_{b_n}^{i_n}) \\ &\equiv \vec{a} \rightarrow \boxed{Q^{\otimes n}} \rightarrow \boxed{\sigma} \rightarrow \boxed{\tilde{Q}^{\otimes n}} \rightarrow \vec{b} \end{aligned} \quad (7.1)$$

We observe, as in (3.36), there is an invariance

$$\mathcal{O}(\gamma_1 \sigma \gamma_2; \vec{a}, \vec{b}) = \mathcal{O}(\sigma; \gamma_1(\vec{a}), \gamma_2^{-1}(\vec{b})), \quad \gamma_1, \gamma_2 \in S_M \quad (7.2)$$

Define the Fourier transform and use the constraint

$$\begin{aligned} \mathcal{O}_{ij;M_S,M_T;kl}^{R,S,T} &= \sum_{\sigma \in S_n} d_R D_{ij}^R(\sigma) C_{\vec{a}}^{S,M_S,k} C_{T,M_T,l}^{\vec{b}} \mathcal{O}(\sigma; \vec{a}, \vec{b}) \\ &= \frac{1}{n!^2} \sum_{\gamma_1, \gamma_2, \sigma} D_{ij}^R(\gamma_1 \sigma \gamma_2) C_{\gamma_1(\vec{a})}^{S,M_S,k} C_{T,M_T,l}^{\gamma_2^{-1}(\vec{b})} \mathcal{O}(\sigma; \vec{a}, \vec{b}) \\ &= \frac{1}{n!^2} \sum_{\gamma_1, \gamma_2, \sigma} D_{kk'}^S(\gamma_1) D_{l'l}^T(\gamma_2) D_{ij}^R(\gamma_1 \sigma \gamma_2) C_{\vec{a}}^{S,M_S,k'} C_{T,M_T,l'}^{\vec{b}} \mathcal{O}(\sigma; \vec{a}, \vec{b}) \\ &= \delta_{R,S} \delta_{R,T} \delta_{ik} \delta_{jl} \mathcal{O}_{k'l';M_S,M_T;k'l'}^{R,S,T} \end{aligned} \quad (7.3)$$

This means that we can define

$$\mathcal{O}_{M_R, M'_R}^R = \sum_{i,j} \mathcal{O}_{ij;M_R, M'_R;ij}^{R,R,R} \quad (7.4)$$

which solve the constraint. Since the representation R of S_n comes from matrix elements of a permutation which permutes indices i_1, \dots, i_M which range over $1 \dots N$, there is a cutoff $l(R) \leq N$. Anti-symmetrizations of more than N copies of such indices always give zero.

Note the labelling of the operators follows the split-node quiver pattern, shown in Figure 32, the new ingredient is the open lines carrying flavour indices. In this simple case the branching nodes causes all irreps to be the same, but it is easy to see, how to generalize this to more complicated quivers, with non-trivial branchings.

$$\mathcal{O}_{M_R, M'_R}^R \quad \sim \quad M_R \xrightarrow{R} \circ \xrightarrow{R} \circ \xrightarrow{R} \tilde{M}_R$$

Figure 32: Labelled split-node SQCD quiver, with flavour state labels M_R, \tilde{M}_R

This has implications for counting. Let $\mathcal{N}(n_1, \dots, n_M; \tilde{n}_1, \dots, \tilde{n}_M)$ be the number of states with n_i copies of Q_i and \tilde{n}_i copies of \tilde{Q}_i . They diagonalize the generators of two copies of $U(M)$ which are $H_i \equiv \sum_{a=1}^N Q_i^a \frac{\partial}{\partial Q_i^a}$ and $\tilde{H}_i \equiv \sum_{a=1}^N \tilde{Q}_i^a \frac{\partial}{\partial \tilde{Q}_i^a}$. The generating function for these numbers can be defined as

$$\mathcal{N}(t_1, \dots, t_M; \tilde{t}_1, \dots, \tilde{t}_M) = \sum_{n_i, \tilde{n}_i} \mathcal{N}(n_1, \dots, n_M; \tilde{n}_1, \dots, \tilde{n}_M) t_1^{n_1} t_2^{n_2} \dots t_M^{n_M} \tilde{t}_1^{\tilde{n}_1} \tilde{t}_2^{\tilde{n}_2} \dots \tilde{t}_M^{\tilde{n}_M} \quad (7.5)$$

where the powers of t_i, \tilde{t}_i give the eigenvalues of H_i, \tilde{H}_i . This can be expressed in terms of the characters of $U(M) \times U(M)$

$$\chi_S(\vec{t}) = tr_S \prod_i t_i^{H_i} \quad \chi_T(\vec{\tilde{t}}) = tr_T \prod_i \tilde{t}_i^{\tilde{H}_i} \quad (7.6)$$

So the counting function is

$$\mathcal{N}(t_1, \dots, t_M; \tilde{t}_1, \dots, \tilde{t}_M) = \sum_{S, T} M(S, T) \chi_S(t_1, \dots, t_M) \chi_T(\tilde{t}_1, \dots, \tilde{t}_M) \quad (7.7)$$

where $M(S, T)$ is the number of times irreps $S \times T$ of $U(M) \times U(M)$ appear in the space of chiral operators. According to (7.4), we have $M(S, T) = \delta_{S, T}$ when $l(S) = l(T) \leq N$ and zero otherwise. So we conclude that

$$\mathcal{N}(t_1, \dots, t_M; \tilde{t}_1, \dots, \tilde{t}_M) = \sum_{\substack{S \in \text{Rep}(U(M)) \\ l(S) \leq N}} \chi_S(\vec{t}) \chi_S(\vec{\tilde{t}}) \quad (7.8)$$

When $M < N$, the $l(S) \leq N$ constraint is automatically satisfied by irreps of $U(M)$ so we have

$$\mathcal{N}(t_1, \dots, t_M; \tilde{t}_1, \dots, \tilde{t}_M) = \sum_{S \in \text{Rep}(U(M))} \chi_S(\vec{t}) \chi_S(\vec{\tilde{t}}) = \prod_{i,j=1}^M \frac{1}{(1 - t_i \tilde{t}_j)} \quad (7.9)$$

In the last line, we used the Cauchy-Littlewood formula. See similar discussion in [82] and earlier papers [79–81].

Now we will see that the Fourier basis diagonalizes the two point function in the free theory

$$\langle Q_i^a Q_j^{b\dagger} \rangle = \delta^{ab} \delta_{ij}, \quad \langle \tilde{Q}_a^i \tilde{Q}_b^{j\dagger} \rangle = \delta_{ab} \delta^{ij} \quad (7.10)$$

The first steps are written diagrammatically as:

$$\begin{aligned} \langle O_{M_R, M'_R}^R O_{M_S, M'_S}^{\dagger S} \rangle &= D_{i_1 j_1}^R(\sigma_1) D_{i_2 j_2}^S(\sigma_2) \left\langle \begin{array}{c} R, M_R, j_1 \quad S, M_S, i_2 \\ \downarrow \circ \quad \uparrow \circ \\ \boxed{Q^{\otimes n}} \quad \boxed{Q^{\dagger \otimes n}} \\ \downarrow \quad \uparrow \\ \boxed{\sigma_1} \quad \boxed{\sigma_2} \\ \downarrow \quad \uparrow \\ \boxed{\tilde{Q}^{\otimes n}} \quad \boxed{\tilde{Q}^{\dagger \otimes n}} \\ \downarrow \circ \quad \uparrow \circ \\ R, M'_R, i_1 \quad S, M'_S, j_2 \end{array} \right\rangle \\ &= \sum_{\gamma_1, \gamma_2} D_{i_1 j_1}^R(\sigma_1) D_{i_2 j_2}^S(\sigma_2) \left\langle \begin{array}{c} R, M_R, j_1 \quad S, M_S, i_2 \\ \downarrow \circ \quad \uparrow \circ \\ \boxed{\gamma_1} \\ \downarrow \quad \uparrow \\ \begin{array}{ccc} & \boxed{\gamma_1^{-1}} & \\ \boxed{\sigma_1} \leftarrow & & \rightarrow \boxed{\sigma_2} \\ & \boxed{\gamma_2^{-1}} & \\ \leftarrow \boxed{\sigma_1} & & \boxed{\sigma_2} \rightarrow \end{array} \\ \downarrow \quad \uparrow \\ \boxed{\gamma_2} \\ \downarrow \circ \quad \uparrow \circ \\ R, M'_R, i_1 \quad S, M'_S, j_2 \end{array} \right\rangle \end{aligned} \quad (7.11)$$

This leads to

$$\begin{aligned} \langle O_{M_R, M'_R}^R O_{M_S, M'_S}^{\dagger S} \rangle &= \sum_{\gamma_1, \gamma_2} \delta_{R, S} \delta_{M_R, M_S} \delta_{M'_R, M'_S} D_{j_1 i_2}^R(\gamma_1) D_{j_2 i_1}^R(\gamma_2) D_{i_1 j_1}^R(\sigma_1) D_{i_2 j_2}^S(\sigma_2) \\ &\quad \times \sum_T \text{Dim} T \chi_T(\sigma_1 \gamma_2^{-1} \sigma_2 \gamma_1^{-1}) \end{aligned} \quad (7.12)$$

Expanding the character in terms of matrix elements, and using orthogonality of elements gives

$$\frac{(n!)^4 \text{Dim} R}{d_R^2} \delta^{R,S} \delta_{M_R, M'_S} \delta_{M_S, M'_R} \quad (7.13)$$

This shows that the basis is orthogonal. The Clebsch's $C_{\vec{a}}^{R, M_R, i}$ can be written by labelling the states M_R using the numbers n_i of the different flavours of Q , along with branching coefficients for the decomposition of the representation R of S_n to the invariant representation of $\prod_i S_{n_i}$ (as we have done elsewhere).

8 Discussion and future avenues

8.1 IR fixed point

Let us discuss in some more detail the RG flow of the conifold theory (see [83] for a good review). The superpotential is

$$W = h (\text{tr}(A_1 B_1 A_2 B_2) - \text{tr}(A_1 B_2 A_2 B_1)) \quad (8.1)$$

where we have reinstated the coupling constant h . Let us define a dimensionless coupling constant $\eta = h\mu$, with energy scale μ . The dimensionless couplings of the theory are then (g_1, g_2, η) , where (g_1, g_2) are the gauge couplings of the two group factors. We focus on the case where $g_1 = g_2 \equiv g$.

The theory is asymptotically free, so perturbatively g increases in the IR. The coupling η classically scales like μ and vanishes in the IR, corresponding to the fact that W is classically irrelevant. The full non-perturbative RG flow diagram, however, looks like in Figure 33. There is a line of fixed points in the (g, η) plane, which originates at the $(g, \eta) = (g_*, 0)$ point and extends up towards the strongly coupled regime. This means the theory in the IR has a marginal coupling, which controls the position on the fixed line. In the context of AdS/CFT correspondence this marginal coupling is related to α' in the bulk, and the supergravity regime corresponds to strong coupling, that is, being far up along the line.

Note there is also a trivial free fixed point, disconnected from the line, at $(g, \eta) = (0, 0)$. Let us focus on the RG flow from this UV fixed point $(0, 0)$ to the IR fixed point $(g_*, 0)$. The theory in the IR is a strongly coupled CFT, but with zero superpotential. This fixed point is similar to the usual Seiberg fixed point in a $N_f = 2N_c$ SQCD, and is qualitatively

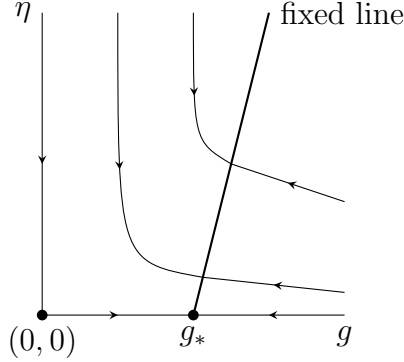


Figure 33: RG flow diagram of the conifold theory

different from the rest of the fixed line. With $W = 0$ the F-terms vanish, and the chiral ring is much larger compared to $\eta \neq 0$ theory.

Our main observation here, is that many of the results in this paper regarding “free” theory are valid not only in the UV free fixed point, but also in the IR interacting fixed point g_* . Consider the basis of operators $\mathcal{O}(\mathbf{L})$ or $\mathcal{O}(\mathbf{K})$. Part of the motivation for this particular basis is that it diagonalizes the free field metric (3.53), valid in the UV. This will get modified along the flow, and $\mathcal{O}(\mathbf{L})$ will likely no longer be orthogonal in the IR, using the CFT two-point function. However, it is known that chiral ring itself is not changed along the flow [84], so our basis will still be a *complete linearly independent finite N basis* for the chiral ring in the IR. From this perspective, the free two-point function could be seen as a particular inner product on the chiral ring states, which allows to solve the finite N constraints. Therefore, one of the key results of our paper, the chiral ring structure constants of the “free” operators (4.9) and (4.25), which depend only on the holomorphic information and not on the two-point function, are valid in the interacting fixed point g_* .

8.2 Directions for the future

We outline some applications, extensions and questions arising from this work.

- The counting formula 2.39 which we derived for quivers describing general bifundamental fields (including adjoints) should admit a generalization to the case with arbitrary number of fundamentals as well as bi-fundamentals. A derivation following the methods here should be possible. Some external nodes of the quiver will have only incoming arrows or outgoing arrows. The counting by splitting the internal nodes and associating Young diagrams to all the edges, and Littlewood-Richardson

coefficients to the nodes, should continue to work. The construction of orthogonal operators should proceed by similar methods, with quiver characters having permutations inserted between splittings of the internal nodes, and branching coefficients at vertices. A first step focusing on SQCD has been taken in Section 7.

- We have considered the 2-point functions and multiplication of operators constructed from scalar bi-fundamentals. In the case of $\mathcal{N} = 1$ SUSY, the results for fermions in a chiral multiplet can be obtained by applying the supersymmetry algebra. Deriving the formulae for the case of fermionic operators directly from the Wick contractions would be interesting, with applicability extending to non-supersymmetric theories such as those that play a role in dimensional deconstruction [85].
- The counting and chiral ring structure constants have been computed for standard quiver theories. It will be interesting to see how far we can apply the present methods to compute these quantities in theories described by generalized quivers [86].
- Generalize the present results to the case where the $U(N_a)$ gauge groups are replaced by other classical groups. An immediate question is to extend the discussion to include baryonic vertices which are important for $SU(N_a)$ gauge groups. For the one-matrix problem, corresponding to the quiver with one node and one edge, there has been progress on the $O(N)$ case [87, 88].
- The appearance of emergent Riemann surfaces in connection with gauge theory here is reminiscent of [86, 89]. The present story involves correlators (of arbitrarily high dimension operators) at a fixed point of moduli space without vevs being turned on, while the one of [86, 89] is looking at the non-perturbative moduli space of vacua and the 6D origin of 4D theories. In the present story, we encounter sums over covers of the Riemann surface, while [86] involves a distinguished covering of the UV curve by the IR curve. Despite these differences, it is tempting to ask if there is some unified story that explains these two appearances of Riemann surfaces correlated with gauge group and matter content.
- The association of Young diagrams to quiver gauge theory data we have encountered here is also reminiscent of the topological vertex [90]. For quiver theories arising from branes at toric singularities, the latter uses toric diagrams of the CY which appears in the moduli space of the gauge theory at non-zero superpotential. Our constructions have been in the limit of vanishing superpotential. Further work along the lines of Section 6 may help in exploring the relation of the present constructions to [90].

- Our results are relevant for free quiver gauge theories in any dimension. As such they are also relevant to matrix models and matrix quantum mechanics, associated with quivers. This type of quantum mechanics has been useful in the context of black holes in $N = 2$ compactifications (e.g. [91]). It would be interesting to explore potential applications of the quiver characters and S_n TFTs we find here in this black hole context [91].
- The focus in this paper has been on explicit computations at the free field point, of quantities such as the CFT inner product and fusion coefficients. In cases with enough supersymmetry, there are differential equations on the moduli space of CFTs for the inner product [92]. The free field results can serve as boundary conditions for solving these equations.
- The constraints on the permutations σ_a define a double coset, although we have not used this language. This double coset is

$$\prod_a \left(\left(\prod_{b,\alpha} S_{n_{ba;\alpha}} \times \prod_{b,\alpha} S_{n_{ab;\alpha}} \right) \setminus (S_{n_a} \times S_{n_a}) / \text{Diag}(S_{n_a}) \right) \quad (8.2)$$

Double cosets are known to admit products. It would be interesting to investigate the meaning of these products in the context of the present gauge theory applications.

Acknowledgements

We are grateful to Diego Rodriguez-Gomez for very helpful discussions and collaboration in the early stages of this work. We thank Ofer Aharony, Robert de Mello Koch, David Garner, Ami Hanany, Rodolfo Russo, Gabriele Travaglini, Brian Wecht for discussions. We are grateful to the Isaac Newton Institute, Cambridge and the Institute for Advanced Study, Princeton for hospitality where part of this work was done. SR is supported by STFC Grant ST/J000469/1, String theory, gauge theory, and duality. JP is supported by a Queen Mary, University of London studentship.

A Symmetric group formulae

A.1 General

$R \vdash n$ will denote a Young diagram with n boxes, associated with an irreducible representation (irrep) of S_n . A Young diagram R is also associated with an irrep of $U(N)$, when the length of the first column $l(R)$ obeys the constraint $l(R) \leq N$. $\text{Dim}_N(R)$ denotes the dimension of $U(N)$ irrep R . $d(R)$ is the dimension of S_n irrep R .

$$\text{Dim}_N(R) = \frac{f_N(R)}{h(R)}, \quad d(R) = \frac{n!}{h(R)} \quad (\text{A.1})$$

$\text{Dim}_N(R)$ is the dimension of $U(N)$ irrep R . $d(R)$ is the dimension of S_n irrep R . $f_N(R)$ is the (N -dependent) product of weights of boxes in the Young diagram. $h(R)$ is the product of hook lengths. Describing the boxes of a Young diagram with coordinates (i, j) running along rows and columns respectively, with r_i being the row lengths and c_j the column lengths

$$\begin{aligned} f_N(R) &= \prod_{i,j} (N - i + j) \\ h(R) &= \prod_{i,j} (r_i + c_j - i - j + 1) \end{aligned} \quad (\text{A.2})$$

The Kronecker Delta over the symmetric group $\delta(\sigma)$, defined to be 1 if the argument is 1 and zero otherwise. It is also defined, by linearity, over formal sums of group elements with complex coefficients (the group algebra) by picking the coefficient of the identity permutation. It has an expansion in characters. There is a related character orthogonality relation, obtained by summing over irreps

$$\sum_{R \vdash n} \frac{d(R)}{n!} \chi_R(\sigma) = \delta(\sigma) \quad (\text{A.3})$$

$$\sum_{R \vdash n} \chi_R(\sigma) \chi_R(\tau) = \sum_{\gamma \in S_n} \delta(\gamma \sigma \gamma^{-1} \tau^{-1}) \quad (\text{A.4})$$

The characters are traces of matrix elements $\chi_R(\sigma) = \sum_i D_{ii}^R(\sigma)$. The matrix elements

satisfy $D_{ij}^R(\sigma) = D_{ji}^R(\sigma^{-1})$). Orthogonality relations from summing over σ are

$$\sum_{\sigma \in S_n} D_{ij}^R(\sigma) D_{kl}^S(\sigma) = \frac{n!}{d(R)} \delta_{RS} \delta_{ik} \delta_{jl} \quad (\text{A.5})$$

$$\sum_{\sigma \in S_n} \chi_R(\sigma) \chi_S(\sigma\tau) = \frac{n!}{d(R)} \delta_{RS} \chi_R(\tau) \quad (\text{A.6})$$

$$\sum_{\sigma \in S_n} \chi_R(\sigma) \chi_S(\sigma) = n! \delta_{RS} \quad (\text{A.7})$$

$$\sum_{\sigma \in S_n} D_{ij}^R(\sigma) N^{c(\sigma)} = \delta_{ij} f_N(R) \quad (\text{A.8})$$

$$\sum_{\sigma \in S_n} \chi_R(\sigma) N^{c(\sigma)} = d(R) f_N(R) = n! \text{Dim}_N(R) \quad (\text{A.9})$$

$$\sum_{\sigma \in S_n} \text{tr} \left(P_{R \rightarrow \mathbf{r}}^{\nu^-, \nu^+} D^R(\sigma) \right) N^{c(\sigma)} = \delta^{\nu^- \nu^+} d(\mathbf{r}) f_N(R) \quad (\text{A.10})$$

The last equation involves generalized projectors (intertwining operators) linking different copies (labelled by ν^+, ν^-) of the irrep \mathbf{r} of a subgroup $H \subset S_n$. We will describe these subgroup reduction in more detail in the next subsection. For derivations of the above identities, the reader may consult e.g. [93].

A.2 Branching coefficients

Consider a subgroup $H \subset S_n$. In this paper H will be of the form

$$H = S_{n_1} \times S_{n_2} \times \dots \quad (\text{A.11})$$

An irrep R of S_n can be decomposed into irreps $\mathbf{r} = (r_1, r_2, \dots)$ of H

$$V_R^{(S_n)} = \bigoplus_{\substack{r_1 \vdash n_1 \\ r_2 \vdash n_2}} V_{r_1}^{(S_{n_1})} \otimes V_{r_2}^{(S_{n_2})} \otimes V_R^{r_1 r_2} \quad (\text{A.12})$$

$$|V_R^{r_1 r_2}| = g(r_1, r_2; R)$$

The states in R are spanned by the basis $|R; \mathbf{r}, \nu, \mathbf{l}\rangle$ where \mathbf{r}, ν labels the irrep of H (ν is the multiplicity label, if \mathbf{r} appears multiple times in the decomposition), and $\mathbf{l} = (l_1, l_2, \dots)$ is a state in $\mathbf{r} = (r_1, r_2, \dots)$. Branching coefficients $B_{i \rightarrow \mathbf{l}}^{R \rightarrow \mathbf{r}, \nu}$ are defined to be the components of the vector $|R; \mathbf{r}, \nu, \mathbf{l}\rangle$ in terms of any orthogonal basis for R .

$$B_{i \rightarrow \mathbf{l}}^{R \rightarrow \mathbf{r}, \nu} = \langle R; i | R; \mathbf{r}, \nu, \mathbf{l} \rangle = \langle R; \mathbf{r}, \nu, \mathbf{l} | R; i \rangle \quad (\text{A.13})$$

Since the representations of S_n can be chosen to be real, branching coefficients are real $(B_{i \rightarrow l}^{R \rightarrow r, \nu})^* = B_{i \rightarrow l}^{R \rightarrow r, \nu}$.

The multiplicities $g(r_1, r_2; R)$ are given by the Littlewood-Richardson rule, which instructs us to put together the boxes of r_2 alongside those of r_1 , subject to some conditions (see e.g [12]). These are usually first encountered in physics in the context of irreps of $U(N)$ but the present description in terms of reduction $S_n \rightarrow H$ is related to that by Schur-Weyl duality. Some times we will informally write

$$r_1 \otimes r_2 = \bigoplus_R g(r_1, r_2; R) R \quad (\text{A.14})$$

in place of the more accurate (A.12).

We use the following diagrammatic notation for the branching coefficients

$$B_{i \rightarrow (l_1, l_2, l_3)}^{R \rightarrow (r_1, r_2, r_3), \nu} \equiv i \xrightarrow{R} \begin{array}{c} \nearrow r_1 \quad l_1 \\ \circ \quad \nu \\ \searrow r_2 \quad l_2 \\ \searrow r_3 \quad l_3 \end{array} \quad (\text{A.15})$$

Because of reality, the diagram with arrows reversed is equal.

Here we list the properties of branching coefficients in the diagrammatic notation, followed by the corresponding equations. For illustration we take the subgroup $H = S_{n_1} \times S_{n_2}$, with the generalization to more factors being straightforward.

$$\begin{array}{c} \rightarrow \boxed{\gamma_1} \nearrow r_1 \\ \rightarrow \boxed{\gamma_2} \nearrow r_2 \end{array} \begin{array}{c} \circ \\ \nu \end{array} \xrightarrow{R} = \begin{array}{c} \nearrow r_1 \\ \circ \quad \nu \\ \nearrow r_2 \end{array} \xrightarrow{R} \boxed{\gamma_1 \circ \gamma_2} \rightarrow \quad (\text{A.16})$$

$$\begin{array}{c} \nearrow r_1 \\ \circ \quad \nu \\ \nearrow r_2 \end{array} \xrightarrow{R} \begin{array}{c} \circ \quad \tilde{\nu} \\ \searrow \tilde{r}_1 \\ \searrow \tilde{r}_2 \end{array} = \begin{array}{c} \rightarrow r_1 \\ \rightarrow r_2 \end{array} \times \delta_{r_1 \tilde{r}_1} \delta_{r_2 \tilde{r}_2} \delta_{\nu \tilde{\nu}} \quad (\text{A.17})$$

$$\sum_{r_1, r_2, \nu} \begin{array}{c} \xrightarrow{R} \circ \quad \nu \\ \searrow r_1 \\ \searrow r_2 \end{array} \begin{array}{c} \circ \quad \nu \\ \nearrow r_1 \\ \nearrow r_2 \end{array} \xrightarrow{R} = \begin{array}{c} \xrightarrow{R} \end{array} \quad (\text{A.18})$$

$$\sum_{r_1, r_2, \nu} \begin{array}{c} \xrightarrow{R} \circ \quad \nu \\ \searrow r_1 \\ \searrow r_2 \end{array} \begin{array}{c} \circ \quad \nu \\ \nearrow r_1 \quad \boxed{\gamma_1} \\ \nearrow r_2 \quad \boxed{\gamma_2} \end{array} \xrightarrow{R} = \begin{array}{c} \xrightarrow{R} \boxed{\gamma_1 \circ \gamma_2} \rightarrow \end{array} \quad (\text{A.19})$$

The equations can be read off by assigning some state labels to each edge and branching coefficients for each white node. As usual with index notation, we need free indices matching on both sides of the equation for the open ends of lines, and repeated indices appearing on internal legs are assumed to be summed :

$$D_{i_1 j_1}^{r_1}(\gamma_1) D_{i_2 j_2}^{r_2}(\gamma_2) B_{k \rightarrow j_1, j_2}^{R \rightarrow (r_1 r_2), \nu} = B_{j \rightarrow i_1, i_2}^{R \rightarrow (r_1 r_2), \nu} D_{kj}^R(\gamma_1 \circ \gamma_2) \quad (\text{A.20})$$

$$B_{k \rightarrow i_1, i_2}^{R \rightarrow (r_1, r_2); \nu} B_{k \rightarrow j_1, j_2}^{R \rightarrow (\tilde{r}_1, \tilde{r}_2); \tilde{\nu}} = \delta_{i_1 j_1} \delta_{i_2 j_2} \delta_{\nu \tilde{\nu}} \delta_{r_1 \tilde{r}_1} \delta_{r_2 \tilde{r}_2} \quad (\text{A.21})$$

$$\sum_{r_1, r_2, \nu} B_{i \rightarrow k_1, k_2}^{R \rightarrow (r_1 r_2), \nu} B_{j \rightarrow k_1, k_2}^{R \rightarrow (r_1 r_2), \nu} = \delta_{ij} \quad (\text{A.22})$$

$$\sum_{r_1, r_2, \nu} B_{i \rightarrow j_1, j_2}^{R \rightarrow (r_1 r_2), \nu} D_{j_1 k_1}^{R_1}(\gamma_1) D_{j_2 k_2}^{R_2}(\gamma_2) B_{j \rightarrow k_1, k_2}^{R \rightarrow (r_1 r_2), \nu} = D_{ij}^R(\gamma_1 \circ \gamma_2) \quad (\text{A.23})$$

As an example of the generalization to $H = \times_b S_{n_b}$ with an arbitrary finite number of factors, the second equation above becomes :

$$B_{k \rightarrow \cup_b i_b}^{R \rightarrow \cup_b r_b; \nu} B_{k \rightarrow \cup_b j_b}^{R \rightarrow \cup_b \tilde{r}_b; \tilde{\nu}} = \delta_{\nu, \tilde{\nu}} \prod_b \delta_{r_b, \tilde{r}_b} \delta_{i_b j_b} \quad (\text{A.24})$$

Another useful identity is

$$\chi_R(\gamma_1 \circ \gamma_2) = \sum_{r_1, r_2} g(r_1, r_2; R) \chi_{r_1}(\gamma_1) \chi_{r_2}(\gamma_2) \quad (\text{A.25})$$

which we get by taking the trace of (A.19).

A.3 Clebsch-Gordan coefficients

The standard tensor product of S_n irreps, where we take a tensor product of two irreps R, S of S_n and then decompose into irreps T of S_n with multiplicities $C(R, S, T)$, also plays a key role in this paper.

$$V_R^{(S_n)} \otimes V_S^{(S_n)} = \bigoplus_{T \vdash n} V_T \otimes V_{RS}^T \quad (\text{A.26})$$

$$|V_{RS}^T| = C(R, S, T)$$

To distinguish the coupling of irreps (r_1, r_2, \dots) of $H = S_{n_1} \times S_{n_2} \dots$ into irreps R of S_n (with $\sum_b n_b = n$) with the present decomposition relating three irreps of S_n , the former are sometimes called outer products of symmetric group irreps. while the latter are called Kronecker products. The Kronecker products are also called inner products sometimes but we will avoid that terminology, to avoid confusion with the scalar product of states within an irrep, which we will freely call inner product.

The diagrammatic notation for the Clebsch-Gordan coefficient will be a black node:

$$S_{i_1 i_2, m}^{R_1 R_2, \Lambda \tau} = \begin{array}{c} i_1 \searrow R_1 \\ \bullet \xrightarrow{\Lambda} m \\ i_2 \nearrow R_2 \end{array} \quad \tau \quad (\text{A.27})$$

It obeys the following identities:

$$\begin{array}{c} \rightarrow \boxed{\gamma} R_1 \\ \bullet \xrightarrow{\Lambda} \\ \rightarrow \boxed{\gamma} R_2 \end{array} \tau = \begin{array}{c} R_1 \searrow \\ \bullet \xrightarrow{\Lambda} \boxed{\gamma} \rightarrow \\ R_2 \nearrow \end{array} \tau \quad (\text{A.28})$$

$$\begin{array}{c} \Lambda \rightarrow \bullet \xrightarrow{R_1} \tilde{\Lambda} \\ \tau \quad \tilde{\tau} \\ \bullet \xleftarrow{R_2} \end{array} = \begin{array}{c} \Lambda \rightarrow \end{array} \times \delta_{\Lambda \tilde{\Lambda}} \delta_{\tau \tilde{\tau}} \quad (\text{A.29})$$

$$\sum_{\Lambda, \tau} \begin{array}{c} R_1 \searrow \\ \bullet \xrightarrow{\Lambda} \bullet \xrightarrow{R_1} \\ R_2 \nearrow \end{array} \tau = \begin{array}{c} R_1 \rightarrow \\ R_2 \rightarrow \end{array} \quad (\text{A.30})$$

$$\sum_{\Lambda, \tau} \begin{array}{c} R_1 \searrow \\ \bullet \xrightarrow{\Lambda} \boxed{\gamma} \rightarrow \bullet \xrightarrow{R_1} \\ R_2 \nearrow \end{array} \tau = \begin{array}{c} R_1 \rightarrow \boxed{\gamma} \rightarrow \\ R_2 \rightarrow \boxed{\gamma} \rightarrow \end{array} \quad (\text{A.31})$$

The corresponding equations are:

$$D_{i_1 j_1}^{R_1}(\gamma) D_{i_2 j_2}^{R_2}(\gamma) S_{j_1 j_2, m}^{R_1 R_2, \Lambda \tau} = S_{i_1 i_2, l}^{R_1 R_2, \Lambda \tau} D_{lm}^{\Lambda}(\gamma) \quad (\text{A.32})$$

$$S_{i_1 i_2, l}^{R_1 R_2, \Lambda \tau} S_{i_1 i_2, m}^{R_1 R_2, \tilde{\Lambda} \tilde{\tau}} = \delta_{\Lambda \tilde{\Lambda}} \delta_{\tau \tilde{\tau}} \delta_{lm} \quad (\text{A.33})$$

$$\sum_{\Lambda, \tau} S_{i_1 i_2, m}^{R_1 R_2, \Lambda \tau} S_{j_1 j_2, m}^{R_1 R_2, \Lambda \tau} = \delta_{i_1 j_1} \delta_{i_2 j_2} \quad (\text{A.34})$$

$$\sum_{\Lambda, \tau} S_{i_1 i_2, l}^{R_1 R_2, \Lambda \tau} D_{lm}^{\Lambda}(\gamma) S_{j_1 j_2, m}^{R_1 R_2, \Lambda \tau} = D_{i_1 j_1}^{R_1}(\gamma) D_{i_2 j_2}^{R_2}(\gamma) \quad (\text{A.35})$$

A.4 Multiplicities

Here we collect identities involving multiplicities $g(r_1, r_2; R)$ and $C(R_1, R_2, \Lambda)$.

Using (A.19) and (A.17) leads to:

$$\chi_R(\sigma_1 \circ \sigma_2) = \sum_{r_1 \vdash n_1} \sum_{r_2 \vdash n_2} g(r_1, r_2; R) \chi_{r_1}(\sigma_1) \chi_{r_2}(\sigma_2) \quad (\text{A.36})$$

From this, Littlewood-Richardson multiplicity can be calculated as

$$g(r_1, r_2; R) = \frac{1}{n_1!n_2!} \sum_{\sigma_1 \in S_{n_1}} \sum_{\sigma_2 \in S_{n_2}} \chi_{r_1}(\sigma_1) \chi_{r_2}(\sigma_2) \chi_R(\sigma_1 \circ \sigma_2) \quad (\text{A.37})$$

Analogously, for Clebsch-Gordan coefficients:

$$\chi_{R_1}(\sigma) \chi_{R_2}(\sigma) = \sum_{\Lambda \vdash n} C(R_1, R_2, \Lambda) \chi_\Lambda(\sigma) \quad (\text{A.38})$$

and

$$C(R_1, R_2, \Lambda) = \frac{1}{n!} \sum_{\sigma \in S_n} \chi_{R_1}(\sigma) \chi_{R_2}(\sigma) \chi_\Lambda(\sigma) \quad (\text{A.39})$$

Combining the above we find:

$$\begin{aligned} & \frac{1}{n_1!n_2!} \sum_{\sigma_1 \in S_{n_1}} \sum_{\sigma_2 \in S_{n_2}} \chi_{R_1}(\sigma_1 \circ \sigma_2) \chi_{R_2}(\sigma_1 \circ \sigma_2) \\ &= \sum_{r_1 \vdash n_1} \sum_{r_2 \vdash n_2} g(r_1, r_2; R_1) g(r_1, r_2; R_2) \\ &= \sum_{\Lambda \vdash n} C(R_1, R_2, \Lambda) g([n_1], [n_2]; \Lambda) \end{aligned} \quad (\text{A.40})$$

where $[n_1]$ and $[n_2]$ are trivial representations for the corresponding groups, arising from $\frac{1}{n_1!n_2!} \sum_{\sigma_1, \sigma_2} \chi_\Lambda(\sigma_1 \circ \sigma_2)$.

B Quiver characters

B.1 Symmetric group characters

The usual symmetric group characters $\chi_R(\sigma) \equiv \text{tr}(D^R(\sigma))$ obey the following identities

$$\chi_R(\sigma) = \chi_R(\sigma^{-1}) \quad (\text{B.1})$$

$$\chi_R(\sigma) = \chi_R(\gamma \sigma \gamma^{-1}) \quad (\text{B.2})$$

$$\frac{1}{n!} \sum_{\sigma \in S_n} \chi_R(\sigma) \chi_S(\sigma) = \delta_{RS} \quad (\text{B.3})$$

$$\sum_{R \vdash n} \chi_R(\sigma) \chi_R(\tau) = \sum_{\gamma \in S_n} \delta(\sigma \gamma \tau \gamma^{-1}) \quad (\text{B.4})$$

They could be summarized as: invariance under inversion (B.1); invariance under conjugation (B.2); orthogonality in representation labels (B.3); orthogonality in conjugacy classes (B.4). There is also a useful generalization of (B.3)

$$\frac{1}{n!} \sum_{\sigma \in S_n} \chi_R(\sigma) \chi_S(\sigma\tau) = \delta_{RS} \frac{\chi_R(\tau)}{d(R)} \quad (\text{B.5})$$

B.2 Restricted quiver characters

Restricted quiver character is defined as

$$\chi_Q(\mathbf{L}, \boldsymbol{\sigma}) = \prod_a D_{i_a j_a}^{R_a}(\sigma_a) B_{j_a \rightarrow \bigcup_{b,\alpha} l_{ab;\alpha}}^{R_a \rightarrow \bigcup_{b,\alpha} r_{ab;\alpha}, \nu_a^-} B_{i_a \rightarrow \bigcup_{b,\alpha} l_{ba;\alpha}}^{R_a \rightarrow \bigcup_{b,\alpha} r_{ba;\alpha}, \nu_a^+} \quad (\text{B.6})$$

with

$$\mathbf{L} \equiv \{R_a, r_{ab;\alpha}, \nu_a^-, \nu_a^+\}, \quad \boldsymbol{\sigma} \equiv \{\sigma_a\} \quad (\text{B.7})$$

Diagrammatically, for the case \mathbb{C}^3/Z_2 ,

$$\chi_{\mathbb{C}^3/Z_2}(\mathbf{L}, \boldsymbol{\sigma}) = \begin{array}{c} \begin{array}{ccc} \nu_1^+ & \xleftarrow{r_{21;2}} & \nu_2^- \\ \downarrow R_1 & \xleftarrow{r_{21;1}} & \downarrow \\ \boxed{\sigma_1} & & \boxed{\sigma_2} \\ \downarrow & \xrightarrow{r_{12;1}} & \downarrow R_2 \\ \nu_1^- & \xrightarrow{r_{12;2}} & \nu_2^+ \end{array} \\ \begin{array}{ccc} \curvearrowleft r_{11} & & \curvearrowright r_{22} \end{array} \end{array} \quad (\text{B.8})$$

Note that for the case of a trivial quiver with a single node and a single field, the quiver character is precisely the symmetric group character.

They obey analogous identities to (B.1), (B.2), (B.3), (B.4):

$$\chi_Q(\mathbf{L}, \boldsymbol{\sigma}) = \chi_Q(\mathbf{L}, \boldsymbol{\sigma}^{-1}) \quad (\text{B.9})$$

$$\chi_Q(\mathbf{L}, \boldsymbol{\sigma}) = \chi_Q(\mathbf{L}, \text{Adj}_{\boldsymbol{\gamma}}(\boldsymbol{\sigma})) \quad (\text{B.10})$$

$$\frac{1}{\prod_a n_a!} \sum_{\boldsymbol{\sigma}} \frac{\prod_a d(R_a)}{\prod_{a,b,\alpha} d(r_{ab;\alpha})} \chi_Q(\mathbf{L}, \boldsymbol{\sigma}) \chi_Q(\tilde{\mathbf{L}}, \boldsymbol{\sigma}) = \delta_{\mathbf{R}\tilde{\mathbf{R}}} \delta_{\mathbf{r}\tilde{\mathbf{r}}} \delta_{\nu^+ \tilde{\nu}^+} \delta_{\nu^- \tilde{\nu}^-} \quad (\text{B.11})$$

$$\sum_{\mathbf{L}} \frac{\prod_a d(R_a)}{\prod_{a,b,\alpha} d(r_{ab;\alpha})} \chi_Q(\mathbf{L}, \boldsymbol{\sigma}) \chi_Q(\mathbf{L}, \boldsymbol{\tau}) = \frac{\prod_a n_a!}{\prod_{a,b,\alpha} n_{ab;\alpha}!} \sum_{\boldsymbol{\gamma}} \prod_a \delta(\text{Adj}_{\boldsymbol{\gamma}}(\sigma_a) \tau_a^{-1}) \quad (\text{B.12})$$

For the proofs see Appendix D.2.

The generalization of (B.5) is

$$\sum_{\sigma} \chi_Q(\mathbf{L}, \tau \sigma) \chi_Q(\tilde{\mathbf{L}}, \sigma) = \delta_{\mathbf{R}\tilde{\mathbf{R}}} \delta_{\mathbf{r}\tilde{\mathbf{r}}} \delta_{\nu^-\tilde{\nu}^-} \prod_a \frac{n_a!}{d(R_a)} \text{tr} \left(D^{R_a}(\tau_a) P_{R_a \rightarrow \bigcup_{b,\alpha} r_{ba;\alpha}}^{\nu_a^+ \tilde{\nu}_a^+} \right) \quad (\text{B.13})$$

where

$$(P_{R_a \rightarrow \bigcup_{b,\alpha} r_{ba;\alpha}}^{\nu_a^+ \tilde{\nu}_a^+})_{i_a \tilde{i}_a} \equiv B_{i_a \rightarrow \bigcup_{b,\alpha} l_{ba;\alpha}}^{R_a \rightarrow \bigcup_{b,\alpha} r_{ba;\alpha}, \nu_a^+} B_{\tilde{i}_a \rightarrow \bigcup_{b,\alpha} l_{ba;\alpha}}^{R_a \rightarrow \bigcup_{b,\alpha} r_{ba;\alpha}, \tilde{\nu}_a^+} \quad (\text{B.14})$$

B.3 Covariant quiver characters

The covariant quiver characters are defined as

$$\chi_Q(\mathbf{K}, \sigma) = \left(\prod_a D_{i_a j_a}^{R_a}(\sigma_a) B_{j_a \rightarrow \bigcup_b l_{ab}^-}^{R_a \rightarrow \bigcup_b s_{ab}^-, \nu_a^-} B_{i_a \rightarrow \bigcup_b l_{ba}^+}^{R_a \rightarrow \bigcup_b s_{ba}^+, \nu_a^+} \right) \left(\prod_{a,b} B_{l_{ab}}^{\Lambda_{ab} \rightarrow [\mathbf{n}_{ab}], \beta_{ab}} S_{l_{ab}^+ l_{ab}^-, l_{ab}}^{s_{ab}^+ s_{ab}^-, \Lambda_{ab} \tau_{ab}} \right) \quad (\text{B.15})$$

with

$$\mathbf{K} = \{R_a, s_{ab}^+, s_{ab}^-, \nu_a^+, \nu_a^-, \Lambda_{ab}, \tau_{ab}, n_{ab;\alpha}, \beta_{ab}\}, \quad \sigma = \{\sigma_a\} \quad (\text{B.16})$$

Diagrammatically, for the $\mathbb{C}^3/\mathbb{Z}_2$ case,

$$\chi_{\mathbb{C}^3/\mathbb{Z}_2}(\mathbf{K}, \sigma) = \quad (\text{B.17})$$

They obey identities:

$$\chi_Q(\mathbf{K}, \sigma) = \chi_Q(\mathbf{K}, \sigma^{-1}) \quad (\text{B.18})$$

$$\chi_Q(\mathbf{K}, \sigma) = \chi_Q(\mathbf{K}, \text{Adj}_{\gamma}(\sigma)) \quad (\text{B.19})$$

$$\frac{1}{\prod_a n_a!} \sum_{\sigma} \left(\prod_a d(R_a) \right) \chi_Q(\mathbf{K}, \sigma) \chi_Q(\tilde{\mathbf{K}}, \sigma) = \delta_{\mathbf{K}\tilde{\mathbf{K}}} \quad (\text{B.20})$$

$$\sum_{\mathbf{K}} \left(\prod_a d(R_a) \right) \chi_Q(\mathbf{K}, \sigma) \chi_Q(\mathbf{K}, \tau) = \frac{\prod_a n_a!}{\prod_{a,b,\alpha} n_{ab;\alpha}!} \sum_{\gamma} \prod_a \delta(\text{Adj}_{\gamma}(\sigma_a) \tau_a^{-1}) \quad (\text{B.21})$$

And

$$\begin{aligned} \sum_{\sigma} \chi_Q(\mathbf{K}, \tau\sigma) \chi_Q(\tilde{\mathbf{K}}, \sigma) &= \delta_{\mathbf{R}\tilde{\mathbf{R}}} \delta_{\mathbf{s}-\tilde{\mathbf{s}}} \delta_{\mathbf{v}-\tilde{\mathbf{v}}} \\ &\times \prod_a \left(\frac{n_a!}{d(R_a)} D_{i_a \tilde{i}_a}^{R_a}(\tau_a) B_{i_a \rightarrow \bigcup_b l_{ba}}^{R_a \rightarrow \bigcup_b s_{ba}^+, \nu_a^+} B_{\tilde{i}_a \rightarrow \bigcup_b \tilde{l}_{ba}}^{R_a \rightarrow \bigcup_b \tilde{s}_{ba}^+, \tilde{\nu}_a^+} \prod_b S_{l_{ba} k_{ba}}^{s_{ba}^+ s_{ba}^-; \Lambda_{ba} \tau_{ba} \beta_{ba} \mathbf{n}_{ba}} S_{\tilde{l}_{ba} k_{ba}}^{\tilde{s}_{ba}^+ s_{ba}^-; \tilde{\Lambda}_{ba} \tilde{\tau}_{ba} \tilde{\beta}_{ba} \mathbf{n}_{ba}} \right) \end{aligned} \quad (\text{B.22})$$

$$\sum_{\sigma, \tau} \chi_Q(\mathbf{K}, \tau\sigma) \chi_Q(\tilde{\mathbf{K}}, \sigma) \prod_a N^{c(\tau_a)} = \delta_{\mathbf{K}\tilde{\mathbf{K}}} \prod_a \frac{n_a!}{d(R_a)} f_N(R_a) \quad (\text{B.23})$$

C General basis from invariance

Here we want to show how solving the invariance (3.36)

$$\mathcal{O}_Q(\mathbf{n}, \sigma) = \mathcal{O}_Q(\mathbf{n}, \text{Adj}_{\gamma}(\sigma)) \quad (\text{C.1})$$

naturally leads to the complete bases (3.48)

$$\mathcal{O}_Q(\mathbf{L}) = \frac{1}{\prod n_a!} \sqrt{\frac{\prod d(R_a)}{\prod d(r_{ab; \alpha})}} \sum_{\sigma} \chi_Q(\mathbf{L}, \sigma) \mathcal{O}_Q(\mathbf{n}, \sigma) \quad (\text{C.2})$$

and (3.59)

$$\mathcal{O}_Q(\mathbf{K}) = \frac{\sqrt{\prod d(R_a)}}{\prod n_a!} \sum_{\sigma} \chi_Q(\mathbf{K}, \sigma) \mathcal{O}_Q(\mathbf{n}, \sigma) \quad (\text{C.3})$$

C.1 Review of \mathbb{C}

First, let us start with the familiar example of half-BPS operators. Those are described by a trivial quiver \mathbb{C} , with single node and single field Φ_{11} . The operators obey invariance

$$\mathcal{O}_{\mathbb{C}}(\sigma) = \mathcal{O}_{\mathbb{C}}(\gamma\sigma\gamma^{-1}), \quad \gamma \in S_n \quad (\text{C.4})$$

We want to express this as a projection to the invariant subspace

$$\mathcal{O}_{\mathbb{C}}(\sigma) = \frac{1}{n!} \sum_{\gamma \in S_n} \mathcal{O}_{\mathbb{C}}(\gamma\sigma\gamma^{-1}) = \sum_{\rho \in S_n} \left(\frac{1}{n!} \sum_{\gamma \in S_n} \delta(\gamma\sigma\gamma^{-1}\rho^{-1}) \right) \mathcal{O}_{\mathbb{C}}(\rho) \quad (\text{C.5})$$

Now

$$P(\sigma, \rho) = \frac{1}{n!} \sum_{\gamma \in S_n} \delta(\gamma\sigma\gamma^{-1}\rho^{-1}) \quad (\text{C.6})$$

is a projector, and we want to find the explicit basis that it projects to. That amounts to being able to write $P(\sigma, \rho) = \sum_L \Psi_L(\sigma) \Psi_L^*(\rho)$ for some labels L and wavefunctions $\Psi_L(\sigma)$. In order to do that, we rewrite $\delta(\sigma)$ using (A.3)

$$\begin{aligned} P(\sigma, \rho) &= \sum_{R \vdash n} \frac{d(R)}{(n!)^2} \sum_{\gamma} \chi_R(\gamma \sigma \gamma^{-1} \rho^{-1}) \\ &= \sum_{R \vdash n} \frac{d(R)}{(n!)^2} \sum_{\gamma} D_{ij}^R(\gamma) D_{jk}^R(\sigma) D_{kl}^R(\gamma^{-1}) D_{li}^R(\rho^{-1}) \end{aligned} \quad (\text{C.7})$$

This allows us to perform γ sum using (A.5), resulting in

$$P(\sigma, \rho) = \frac{1}{n!} \sum_{R \vdash n} \chi_R(\sigma) \chi_R(\rho) \quad (\text{C.8})$$

which is the desired explicit form for the projector. It leads to the complete basis (up to normalization, chosen for convenience) – Schur polynomial basis

$$\mathcal{O}_{\mathbb{C}}(R) = \frac{1}{n!} \sum_{\sigma} \chi_R(\sigma) \mathcal{O}_{\mathbb{C}}(\sigma) \quad (\text{C.9})$$

C.2 Review of \mathbb{C}^3

Now let us see how the same procedure is applied to \mathbb{C}^3 . The operators are invariant under (3.8)

$$\mathcal{O}_{\mathbb{C}^3}(\mathbf{n}, \gamma \sigma \gamma^{-1}) = \mathcal{O}_{\mathbb{C}^3}(\mathbf{n}, \sigma), \quad \gamma \in S_{n_1} \times S_{n_2} \times S_{n_3} \equiv H \subset S_n \quad (\text{C.10})$$

This leads to a projection

$$\mathcal{O}_{\mathbb{C}^3}(\mathbf{n}, \sigma) = \sum_{\rho \in S_n} P(\sigma, \rho) \mathcal{O}_{\mathbb{C}^3}(\mathbf{n}, \rho) \quad (\text{C.11})$$

with

$$P(\sigma, \rho) = \frac{1}{|H|} \sum_{\gamma \in H} \delta(\gamma \sigma \gamma^{-1} \rho^{-1}) \quad (\text{C.12})$$

Again introducing sum over R we get the same as (C.7)

$$P(\sigma, \rho) = \sum_{R \vdash n} \frac{d(R)}{|H| n!} \sum_{\gamma \in H} D_{ij}^R(\gamma) D_{jk}^R(\sigma) D_{km}^R(\gamma^{-1}) D_{mi}^R(\rho^{-1}) \quad (\text{C.13})$$

with a key difference that now the sum

$$\sum_{\gamma \in S_{n_1} \times S_{n_2} \times S_{n_3}} D_{ij}^R(\gamma) D_{km}^R(\gamma^{-1}) \quad (\text{C.14})$$

is only over the subgroup of S_n .

There are two ways to evaluate (C.14), eventually leading to the two different bases (3.9) and (3.20). For the first one, we introduce explicit representations for the subgroup $S_{n_1} \times S_{n_2} \times S_{n_3}$ by inserting a delta function as a sum over projectors (3.16)

$$\delta_{ij} = \sum_{r_1, r_2, r_3, \nu} (P_{R \rightarrow r_1, r_2, r_3}^{\nu, \nu})_{ij} = \sum_{r_1, r_2, r_3, \nu} B_{i \rightarrow \mathbf{l}}^{R \rightarrow \mathbf{r}, \nu} B_{j \rightarrow \mathbf{l}}^{R \rightarrow \mathbf{r}, \nu} \quad (\text{C.15})$$

When $\gamma \in S_{n_1} \times S_{n_2} \times S_{n_3}$, $D^R(\gamma)$ can be moved through the branching coefficients, which allows us to express

$$D_{ij}^R(\gamma_1 \circ \gamma_2 \circ \gamma_3) = \sum_{r_1, r_2, r_3, \nu} B_{i \rightarrow \mathbf{l}}^{R \rightarrow \mathbf{r}, \nu} D_{l_1 \tilde{l}_1}^{r_1}(\gamma_1) D_{l_2 \tilde{l}_2}^{r_2}(\gamma_2) D_{l_3 \tilde{l}_3}^{r_3}(\gamma_3) B_{j \rightarrow \tilde{\mathbf{l}}}^{R \rightarrow \mathbf{r}, \nu} \quad (\text{C.16})$$

Applying this to both terms in (C.14) we get

$$\begin{aligned} \sum_{\gamma \in H} D_{ij}^R(\gamma) D_{km}^R(\gamma^{-1}) &= \sum_{\mathbf{r}^+, \nu^+} \sum_{\mathbf{r}^-, \nu^-} \sum_{\gamma_1, \gamma_2, \gamma_3} B_{i \rightarrow \mathbf{l}^+}^{R \rightarrow \mathbf{r}^+, \nu^+} D_{l_1^+ \tilde{l}_1^+}^{r_1^+}(\gamma_1) D_{l_2^+ \tilde{l}_2^+}^{r_2^+}(\gamma_2) D_{l_3^+ \tilde{l}_3^+}^{r_3^+}(\gamma_3) B_{j \rightarrow \tilde{\mathbf{l}}^+}^{R \rightarrow \mathbf{r}^+, \nu^+} \\ &\quad \times B_{k \rightarrow \mathbf{l}^-}^{R \rightarrow \mathbf{r}^-, \nu^-} D_{l_1^- \tilde{l}_1^-}^{r_1^-}(\gamma_1^{-1}) D_{l_2^- \tilde{l}_2^-}^{r_2^-}(\gamma_2^{-1}) D_{l_3^- \tilde{l}_3^-}^{r_3^-}(\gamma_3^{-1}) B_{m \rightarrow \tilde{\mathbf{l}}^-}^{R \rightarrow \mathbf{r}^-, \nu^-} \end{aligned} \quad (\text{C.17})$$

Now the $\gamma_1, \gamma_2, \gamma_3$ sums give $(\delta_{l_1^+ \tilde{l}_1^-}^{r_1^+ r_1^-} \delta_{l_1^- \tilde{l}_1^+}^{r_1^- r_1^+})$ etc, which reconnect the branching coefficients. The final answer for (C.14) is thus

$$\begin{aligned} \sum_{\gamma \in H} D_{ij}^R(\gamma) D_{km}^R(\gamma^{-1}) &= \sum_{\mathbf{r}, \nu^+, \nu^-} \frac{n_1! n_2! n_3!}{d(r_1) d(r_2) d(r_3)} B_{m \rightarrow \mathbf{l}}^{R \rightarrow \mathbf{r}, \nu^-} B_{i \rightarrow \mathbf{l}}^{R \rightarrow \mathbf{r}, \nu^+} B_{k \rightarrow \tilde{\mathbf{l}}}^{R \rightarrow \mathbf{r}, \nu^-} B_{j \rightarrow \tilde{\mathbf{l}}}^{R \rightarrow \mathbf{r}, \nu^+} \\ &= \sum_{\mathbf{r}, \nu^+, \nu^-} \frac{n_1! n_2! n_3!}{d(r_1) d(r_2) d(r_3)} (P_{R \rightarrow \mathbf{r}}^{\nu^-, \nu^+})_{mi} (P_{R \rightarrow \mathbf{r}}^{\nu^-, \nu^+})_{kj} \end{aligned} \quad (\text{C.18})$$

The projector (C.13) is thus

$$P(\sigma, \rho) = \frac{1}{n!} \sum_{R, \mathbf{r}, \nu^+, \nu^-} \frac{d(R)}{d(r_1) d(r_2) d(r_3)} \text{tr}(P_{R \rightarrow \mathbf{r}}^{\nu^-, \nu^+} D^R(\sigma)) \text{tr}(P_{R \rightarrow \mathbf{r}}^{\nu^-, \nu^+} D^R(\rho)) \quad (\text{C.19})$$

This is again of the form $\sum_L \Psi_L(\sigma) \Psi_L^*(\rho)$, with labels $\mathbf{L} = \{R, r_1, r_2, r_3, \nu^+, \nu^-\}$, thus we conclude that the complete basis is (3.9)

$$\mathcal{O}_{\mathbb{C}^3}(\mathbf{L}) \sim \sum_{\sigma} \text{tr}(P_{R \rightarrow \mathbf{r}}^{\nu^-, \nu^+} D^R(\sigma)) \mathcal{O}_{\mathbb{C}^3}(\mathbf{n}, \sigma) \quad (\text{C.20})$$

up to a normalization coefficient.

An alternative way to evaluate the sum (C.14) is to observe that $D_{ij}^R(\gamma)D_{mk}^R(\gamma)$ is a representation matrix of γ in the tensor product $R \otimes R$ rep. We can decompose this into irreps using S_n Clebsch-Gordan coefficients

$$D_{ij}^R(\gamma)D_{mk}^R(\gamma) = \sum_{\Lambda, \tau} D_{il}^\Lambda(\gamma) S_{im, l}^{RR, \Lambda\tau} S_{jk, \tilde{l}}^{RR, \Lambda\tau} \quad (C.21)$$

Now the γ only appears in a single $D(\gamma)$, and the sum over $\gamma \in S_{n_1} \times S_{n_2} \times S_{n_3}$ is simply a projection to invariants under the subgroup

$$\sum_{\gamma \in S_{n_1} \times S_{n_2} \times S_{n_3}} D_{il}^\Lambda(\gamma) = n_1!n_2!n_3! \sum_{\beta=1}^{g([\mathbf{n}]; \Lambda)} B_l^{\Lambda \rightarrow [\mathbf{n}], \beta} B_{\tilde{l}}^{\Lambda \rightarrow [\mathbf{n}], \beta} \quad (C.22)$$

The branching coefficients have the same meaning as before: $[\mathbf{n}]$ denotes three single-row Young diagrams of length n_1, n_2, n_3 , which is the trivial one-dimensional representation of $S_{n_1} \times S_{n_2} \times S_{n_3}$. Since it is one-dimensional, we suppress the index for it. β is the multiplicity for how many times $[\mathbf{n}]$ appears in Λ . Branching coefficient $B_l^{\Lambda \rightarrow [\mathbf{n}], \beta}$ itself is a vector in Λ , which is invariant under $S_{n_1} \times S_{n_2} \times S_{n_3}$, labelled by β . Note the number of invariants is $g([n_1], [n_2], [n_3]; \Lambda)$, that is, how many ways there are to combine three single-row diagrams into Λ using Littlewood-Richardson rule. It vanishes if Λ has more than three rows, so we have a constraint

$$l(\Lambda) \leq 3 \quad (C.23)$$

Λ is a representation of the global symmetry $U(3)$. The full sum (C.14) is thus

$$\sum_{\gamma \in H} D_{ij}^R(\gamma) D_{km}^R(\gamma^{-1}) = n_1!n_2!n_3! \sum_{\Lambda, \tau, \beta} \left(B_l^{\Lambda \rightarrow [\mathbf{n}], \beta} S_{im, l}^{RR, \Lambda\tau} \right) \left(B_{\tilde{l}}^{\Lambda \rightarrow [\mathbf{n}], \beta} S_{jk, \tilde{l}}^{RR, \Lambda\tau} \right) \quad (C.24)$$

and the projector (C.13) evaluates to

$$P(\sigma, \rho) = \sum_{R, \Lambda, \tau, \beta} \frac{d(R)}{n!} \left(B_l^{\Lambda \rightarrow [\mathbf{n}], \beta} S_{im, l}^{RR, \Lambda\tau} D_{im}^R(\rho) \right) \left(B_{\tilde{l}}^{\Lambda \rightarrow [\mathbf{n}], \beta} S_{jk, \tilde{l}}^{RR, \Lambda\tau} D_{jk}^R(\sigma) \right) \quad (C.25)$$

This leads to the basis (3.20)

$$\mathcal{O}(\mathbf{K}) \sim \sum_{\sigma \in S_n} B_m^{\Lambda \rightarrow [\mathbf{n}], \beta} S_{ij, m}^{RR, \Lambda\tau} D_{ij}^R(\sigma) \mathcal{O}(\mathbf{n}, \sigma) \quad (C.26)$$

up to normalization.

C.3 General quiver

Now let us extend this derivation for a general quiver. We need to solve the invariance (3.36)

$$\mathcal{O}_Q(\mathbf{n}, \boldsymbol{\sigma}) = \mathcal{O}_Q(\mathbf{n}, \text{Adj}_\gamma(\boldsymbol{\sigma})) \quad (\text{C.27})$$

that is, to evaluate the projector

$$\begin{aligned} P(\boldsymbol{\sigma}, \boldsymbol{\rho}) &= \frac{1}{|H|} \sum_{\gamma \in H} \delta(\text{Adj}_\gamma(\boldsymbol{\sigma}) \boldsymbol{\rho}^{-1}) \\ &= \frac{1}{|H|} \sum_{\gamma \in H} \prod_a \delta(\text{Adj}_\gamma(\sigma_a) \rho_a^{-1}) \end{aligned} \quad (\text{C.28})$$

in analogy with (C.12). The invariance group is

$$H = \bigotimes_{a,b,\alpha} S_{n_{ab;\alpha}}, \quad |H| = \prod_{a,b,\alpha} n_{ab;\alpha}! \quad (\text{C.29})$$

Note beforehand, that $\chi_Q(\mathbf{L}, \boldsymbol{\sigma})$ obeys exactly the required identity (B.12), which allows to write (C.28) like $\sum_{\mathbf{L}} \chi_Q(\mathbf{L}, \boldsymbol{\sigma}) \chi_Q(\mathbf{L}, \boldsymbol{\rho})$, leading to the $\mathcal{O}_Q(\mathbf{L})$ basis. The same is true of $\chi_Q(\mathbf{K}, \boldsymbol{\sigma})$, which obeys (B.21), leading to $\mathcal{O}_Q(\mathbf{K})$ basis. The purpose here, however, is to constructively *derive* $\chi_Q(\mathbf{L}, \boldsymbol{\sigma})$ and $\chi_Q(\mathbf{K}, \boldsymbol{\sigma})$ as the basis diagonalizing $P(\boldsymbol{\sigma}, \boldsymbol{\rho})$.

Like before, we expand the deltas in terms of characters

$$\begin{aligned} P(\boldsymbol{\sigma}, \boldsymbol{\rho}) &= \frac{1}{|H|} \sum_{\mathbf{R}} \sum_{\gamma \in H} \prod_a \frac{d(R_a)}{n_a!} \chi_{R_a}(\text{Adj}_\gamma(\sigma_a) \rho_a^{-1}) \\ &= \frac{1}{|H|} \sum_{\mathbf{R}} \sum_{\gamma \in H} \prod_a \frac{d(R_a)}{n_a!} D_{i_a j_a}^{R_a}(\otimes_{b,\alpha} \gamma_{ba;\alpha}) D_{j_a k_a}^{R_a}(\sigma_a) D_{k_a m_a}^{R_a}(\otimes_{b,\alpha} \gamma_{ab;\alpha}^{-1}) D_{m_a i_a}^{R_a}(\rho_a^{-1}) \end{aligned} \quad (\text{C.30})$$

The question is, again, how to perform the $\gamma_{ab;\alpha}$ sum

$$\sum_{\gamma \in H} \prod_a D_{i_a j_a}^{R_a}(\otimes_{b,\alpha} \gamma_{ba;\alpha}) D_{j_a k_a}^{R_a}(\otimes_{b,\alpha} \gamma_{ab;\alpha}^{-1}) \quad (\text{C.31})$$

Note each $\gamma_{ab;\alpha}$ and $\gamma_{ab;\alpha}^{-1}$ occurs exactly once.

One way, in analogy to the restricted Schur basis, is to insert the branching coefficients around γ 's:

$$D_{i_a j_a}^{R_a}(\otimes_{b,\alpha} \gamma_{ba;\alpha}) = \sum_{\bigcup_{b,\alpha} r_{ba;\alpha}} \sum_{\nu} B_{i_a \rightarrow \bigcup_{b,\alpha} l_{ba;\alpha}}^{R_a \rightarrow \bigcup_{b,\alpha} r_{ba;\alpha}, \nu_a} B_{j_a \rightarrow \bigcup_{b,\alpha} \tilde{l}_{ba;\alpha}}^{R_a \rightarrow \bigcup_{b,\alpha} r_{ba;\alpha}, \nu_a} \prod_{b,\alpha} D_{l_{ba;\alpha} \tilde{l}_{ba;\alpha}}^{r_{ba;\alpha}}(\gamma_{ba;\alpha}) \quad (\text{C.32})$$

Replacing all $D(\gamma)$ and $D(\gamma^{-1})$ we get analogous expansion to (C.17), which allows us to perform $\gamma_{ab;\alpha}$ sums. They generate delta functions which contract the branching coefficients in analogy to (C.17) as follows:

$$\begin{aligned} & \sum_{\gamma \in H} \prod_a D_{i_a j_a}^{R_a}(\otimes_{b,\alpha} \gamma_{ba;\alpha}) D_{k_a m_a}^{R_a}(\otimes_{b,\alpha} \gamma_{ab;\alpha}^{-1}) \\ &= \sum_{\{r_{ab;\alpha}\}} \sum_{\{\nu_a^+\}} \sum_{\{\nu_a^-\}} \frac{\prod n_{ab;\alpha}!}{\prod d(r_{ab;\alpha})} \prod_a \left(B_{m_a \rightarrow \cup_{b,\alpha} l_{ab;\alpha}}^{R_a \rightarrow \cup_{b,\alpha} r_{ab;\alpha}, \nu_a^-} B_{i_a \rightarrow \cup_{b,\alpha} l_{ba;\alpha}}^{R_a \rightarrow \cup_{b,\alpha} r_{ba;\alpha}, \nu_a^+} \right) \\ & \quad \times \left(B_{k_a \rightarrow \cup_{b,\alpha} \tilde{l}_{ab;\alpha}}^{R_a \rightarrow \cup_{b,\alpha} r_{ab;\alpha}, \nu_a^-} B_{j_a \rightarrow \cup_{b,\alpha} \tilde{l}_{ba;\alpha}}^{R_a \rightarrow \cup_{b,\alpha} r_{ba;\alpha}, \nu_a^+} \right) \end{aligned} \quad (C.33)$$

This leads to

$$P(\boldsymbol{\sigma}, \boldsymbol{\rho}) = \frac{1}{\prod n_a!} \sum_{\mathbf{R}, \mathbf{r}, \nu^+, \nu^-} \frac{\prod d(R_a)}{\prod d(r_{ab;\alpha})} \chi_Q(\mathbf{L}, \boldsymbol{\sigma}) \chi_Q(\mathbf{L}, \boldsymbol{\rho}) \quad (C.34)$$

with $\chi_Q(\mathbf{L}, \boldsymbol{\sigma})$ defined as in (3.47) and thus the basis

$$\mathcal{O}_Q(\mathbf{L}) = \frac{1}{\prod n_a!} \sqrt{\frac{\prod d(R_a)}{\prod d(r_{ab;\alpha})}} \sum_{\boldsymbol{\sigma}} \chi_Q(\mathbf{L}, \boldsymbol{\sigma}) \mathcal{O}_Q(\boldsymbol{\sigma}). \quad (C.35)$$

An alternative way of evaluating (C.31) is to use Clebsch-Gordan coefficients, leading to the covariant basis. In order to apply (C.24) we need a term $D(\gamma)D(\gamma^{-1})$ with γ in some subgroup of S_n . In general, however, (C.31) does not have that form, because $D(\otimes_{b,\alpha} \gamma_{ba;\alpha})$ contains permutations corresponding to fields incoming to a , and $D(\otimes_{b,\alpha} \gamma_{ab;\alpha}^{-1})$ contains outgoing. Therefore, first we have to insert branching coefficients to separate fields between different quiver nodes

$$\begin{aligned} & \sum_{\gamma \in H} \prod_a D_{i_a j_a}^{R_a}(\otimes_{b,\alpha} \gamma_{ba;\alpha}) D_{k_a m_a}^{R_a}(\otimes_{b,\alpha} \gamma_{ab;\alpha}^{-1}) \\ &= \sum_{\gamma \in H} \prod_a \left(\sum_{\cup_b s_{ba}^+} \sum_{\nu_a^+} B_{i_a \rightarrow \cup_b l_{ba}^+}^{R_a \rightarrow \cup_b s_{ba}^+, \nu_a^+} B_{j_a \rightarrow \cup_b \tilde{l}_{ba}^+}^{R_a \rightarrow \cup_b s_{ba}^+, \nu_a^+} \prod_b D_{l_{ba}^+ \tilde{l}_{ba}^+}^{s_{ba}^+}(\otimes_{\alpha} \gamma_{ba;\alpha}) \right) \\ & \quad \times \left(\sum_{\cup_b s_{ab}^-} \sum_{\nu_a^-} B_{k_a \rightarrow \cup_b l_{ab}^-}^{R_a \rightarrow \cup_b s_{ab}^-, \nu_a^-} B_{m_a \rightarrow \cup_b \tilde{l}_{ab}^-}^{R_a \rightarrow \cup_b s_{ab}^-, \nu_a^-} \prod_b D_{l_{ab}^- \tilde{l}_{ab}^-}^{s_{ab}^-}(\otimes_{\alpha} \gamma_{ab;\alpha}^{-1}) \right) \end{aligned} \quad (C.36)$$

Now for each ordered pair of quiver nodes (a, b) , where we have M_{ab} fields labelled by α , we can apply (C.24)

$$\begin{aligned} & \sum_{\cup_{\alpha} \gamma_{ab;\alpha}} D_{l_{ab}^+ \tilde{l}_{ab}^+}^{s_{ab}^+}(\otimes_{\alpha} \gamma_{ab;\alpha}) D_{l_{ab}^- \tilde{l}_{ab}^-}^{s_{ab}^-}(\otimes_{\alpha} \gamma_{ab;\alpha}^{-1}) \\ &= \left(\prod_{\alpha} n_{ab;\alpha}! \right) \sum_{\Lambda_{ab}, \tau_{ab}, \beta_{ab}} \left(B_{l_{ab}^+}^{\Lambda_{ab} \rightarrow [\mathbf{n}_{ab}], \beta_{ab}} S_{l_{ab}^+ \tilde{l}_{ab}^+, l_{ab}^+}^{s_{ab}^+, s_{ab}^-, \Lambda \tau_{ab}} \right) \left(B_{\tilde{l}_{ab}^-}^{\Lambda_{ab} \rightarrow [\mathbf{n}_{ab}], \beta_{ab}} S_{\tilde{l}_{ab}^- l_{ab}^-, \tilde{l}_{ab}^-}^{s_{ab}^+, s_{ab}^-, \Lambda \tau_{ab}} \right) \end{aligned} \quad (C.37)$$

Note that the effect on (C.36) is to reconnect l_{ab}^+ with \tilde{l}_{ab}^- via the Clebsch-Gordan coefficient $S_{l_{ab}^+ \tilde{l}_{ab}^-, l_{ab}}^{s_{ab}^+ s_{ab}^-, \Lambda \tau_{ab}}$, and the same for \tilde{l}_{ab}^+ with l_{ab}^- . This produces the right structure where the branching coefficients factor into two quivers. The end result, putting everything back into (C.30) is

$$P(\boldsymbol{\sigma}, \boldsymbol{\rho}) = \frac{1}{\prod n_a!} \sum_{\mathbf{K}} \left(\prod_a d(R_a) \right) \chi_Q(\mathbf{K}, \boldsymbol{\sigma}) \chi_Q(\mathbf{K}, \boldsymbol{\rho}) \quad (\text{C.38})$$

where the label \mathbf{K} includes

$$\mathbf{K} = \{R_a, s_{ab}^+, s_{ab}^-, \nu_a^+, \nu_a^-, \Lambda_{ab}, \tau_{ab}, \beta_{ab}, n_{ab; \alpha}\} \quad (\text{C.39})$$

and $\chi_Q(\mathbf{K}, \boldsymbol{\sigma})$ is as in (3.60). The basis is then

$$\mathcal{O}_Q(\mathbf{K}) = \frac{\sqrt{\prod d(R_a)}}{\prod n_a!} \sum_{\boldsymbol{\sigma}} \chi_Q(\mathbf{K}, \boldsymbol{\sigma}) \mathcal{O}_Q(\mathbf{n}, \boldsymbol{\sigma}) \quad (\text{C.40})$$

D Proofs

D.1 Proof of large N counting

We need to do some sums over R_a, S_{ab}^\pm in order to arrive at the (2.29) starting from (2.28). We apply the identity

$$\sum_{R \vdash n} \chi_R(\sigma_1) \chi_R(\sigma_2) = \sum_{\gamma \in S_n} \delta(\gamma \sigma_1 \gamma^{-1} \sigma_2) \quad (\text{D.1})$$

to the quantity $\mathcal{N}(\{t_{ab; \alpha}\}; \{M_{ab}\})$ in (2.29) to obtain

$$\begin{aligned} & \mathcal{N}(\{t_{ab; \alpha}\}, \{M_{ab}\}) \\ &= \sum_{R_a \vdash n_a} \sum_{\Lambda_{ab} \vdash n_{ab}} \sum_{S_{ab}^\pm \vdash n_{ab}} \sum_{\{\sigma_{ab}^+ \in S_{n_{ab}}\}} \sum_{\{\sigma_{ab}^- \in S_{n_{ab}}\}} \prod_a \chi_{R_a}(\overset{\circ}{\prod}_b \sigma_{ba}^+) \chi_{R_a}(\overset{\circ}{\prod}_b \sigma_{ba}^-) \\ & \quad \prod_{a,b} \frac{\chi_{S_{ab}^+}(\sigma_{ab}^+)}{n_{ab}!} \frac{\chi_{S_{ab}^-}(\sigma_{ab}^-)}{n_{ab}!} \chi_{S_{ab}^+}(\tau_{ab}) \chi_{S_{ab}^-}(\tau_{ab}) \chi_{\Lambda_{ab}}(\tau_{ab}) \chi_{\Lambda_{ab}}(\mathbb{T}_{ab}) \\ &= \prod_a \sum_{\gamma_{ab}^\pm \vdash S_{n_{ab}}} \delta_{S_{n_{ab}}} \left(\prod_b \sigma_{ba}^+ \cdot \mu_a \cdot \overset{\circ}{\prod}_b \sigma_{ab}^- \cdot \mu_a^{-1} \right) \\ & \quad \prod_{a,b} \frac{1}{(n_{ab}!)^2} \delta_{S_{n_{ab}}} (\gamma_{ab}^+ \sigma_{ab}^+ (\gamma_{ab}^+)^{-1} \tau_{ab}) \delta_{S_{n_{ab}}} (\gamma_{ab}^- \sigma_{ab}^- (\gamma_{ab}^-)^{-1} \tau_{ab}) \text{tr}(\mathbb{T}_{ab} \tau_{ab}) \end{aligned} \quad (\text{D.2})$$

We can use the delta functions to solve for τ_{ab} as $\gamma_{ab}^+(\sigma_{ab}^+)^{-1}(\gamma_{ab}^+)^{-1}$). There is the invariance

$$\text{tr}(\mathbb{T}_{ab}\gamma_{ab}^+(\sigma_{ab}^+)^{-1}(\gamma_{ab}^+)^{-1}) = \text{tr}(\mathbb{T}_{ab}(\sigma_{ab}^+)^{-1}) \quad (\text{D.3})$$

of the trace in $V_{M_{ab}}^{\otimes n_{ab}}$. The sum over γ_{ab}^- is invariant under left multiplication by $(\gamma_{ab}^+)^{-1}$. Hence we obtain

$$\begin{aligned} \mathcal{N}(\{t_{ab;\alpha}\}; \{M_{ab}\}) &= \prod_a \sum_{\gamma_a} \delta_{S_{n_a}} \left(\overset{\circ}{\prod}_a \sigma_{ba}^+ \cdot \gamma_a \cdot \overset{\circ}{\prod}_a \sigma_{ba}^- \cdot \gamma_a^{-1} \right) \\ &\quad \prod_{a,b} \frac{1}{n_{ab}!} \sum_{\gamma_{ab}^-} \delta_{S_{n_{ab}}} (\gamma_{ab}^- \sigma_{ab}^- (\gamma_{ab}^-)^{-1} (\sigma_{ab}^+)^{-1}) \text{tr}(\mathbb{T}_{ab}(\sigma_{ab}^+)^{-1}) \end{aligned} \quad (\text{D.4})$$

Now we can solve for σ_{ab}^- , use invariance of the trace under conjugation of \mathbb{T}_{ab} by γ_{ab}^- , as well as invariance of the sums over $\gamma_a \in S_{n_a}$ under right multiplication by $\gamma_{ab}^- \in S_{n_{ab}} \subset S_{n_a}$ to arrive at

$$\mathcal{N}(\{t_{ab;\alpha}\}; \{M_{ab}\}) = \prod_a \sum_{\gamma_a} \delta_{S_{n_a}} \left(\prod_b \sigma_{ab}^+ \cdot \gamma_a \cdot \prod_b \sigma_{ab}^+ \cdot \gamma_a^{-1} \right) \prod_{a,b} \text{tr}(\mathbb{T}_{ab}(\sigma_{ab}^+)^{-1}) \quad (\text{D.5})$$

Renaming $\sigma_{ab}^+ \rightarrow \sigma_{ab}$ we arrive at (2.29)

D.2 Proofs of quiver character identities

Here we prove the identities (B.10), (B.11), (B.12), (B.13) obeyed by the restricted quiver characters $\chi_Q(\mathbf{L}, \boldsymbol{\sigma})$.

Invariance of $\chi_Q(\mathbf{L}, \boldsymbol{\sigma})$

Here we show that restricted quiver characters $\chi_Q(\mathbf{L}, \boldsymbol{\sigma})$ obey (B.10), invariance under $\boldsymbol{\sigma} \rightarrow \text{Adj}_\gamma(\boldsymbol{\sigma})$.

It is easiest to see from a diagram. For example, if we take simplified version of (B.8)

with only single flavor, we have:

$$\begin{aligned}
\chi_Q(\mathbf{L}, \text{Adj}_\gamma(\boldsymbol{\sigma})) &\sim r_{11} \text{ (diagram 1) } = r_{11} \text{ (diagram 2) } \\
&= \chi_Q(\mathbf{L}, \boldsymbol{\sigma})
\end{aligned} \tag{D.6}$$

The diagrams represent the same quantity in two different ways. Diagram 1 is a square with vertices ν_1^+ (top-left), ν_2^- (top-right), ν_1^- (bottom-left), and ν_2^+ (bottom-right). The edges are labeled r_{21} (top), r_{12} (bottom), r_{11} (left), and r_{22} (right). Inside the square, there are four boxes: top-left $\gamma_{11} \circ \gamma_{21}$, top-right $\gamma_{22}^{-1} \circ \gamma_{21}^{-1}$, bottom-left $\gamma_{11}^{-1} \circ \gamma_{12}^{-1}$, and bottom-right $\gamma_{22} \circ \gamma_{12}$. Arrows labeled R_1 and R_2 connect the vertices to the boxes, and arrows labeled σ_1 and σ_2 connect the boxes. Diagram 2 is a similar square but with the boxes arranged differently, reflecting the same underlying structure after a series of transformations.

This follows from the property (A.16) of the branching coefficients, which allows to pull γ 's through and cancel with each other

This procedure can be written explicitly for the general case (3.47):

$$\begin{aligned}
\chi_Q(\mathbf{L}, \text{Adj}_\gamma(\boldsymbol{\sigma})) &= \prod_a D_{i_a i'_a}^{R_a}(\otimes_{b,\alpha} \gamma_{ba;\alpha}) D_{i'_a j'_a}^{R_a}(\sigma_a) D_{j'_a j_a}^{R_a}(\otimes_{b,\alpha} \gamma_{ab;\alpha}^{-1}) \\
&\quad \times B_{i_a \rightarrow \cup_{b,\alpha} l_{ba;\alpha}}^{R_a \rightarrow \cup_{b,\alpha} r_{ba;\alpha}, \nu_a^+} B_{j_a \rightarrow \cup_{b,\alpha} l_{ab;\alpha}}^{R_a \rightarrow \cup_{b,\alpha} r_{ab;\alpha}, \nu_a^-} \\
&= \prod_a D_{i_a j_a}^{R_a}(\sigma_a) B_{i_a \rightarrow \cup_{b,\alpha} l'_{ba;\alpha}}^{R_a \rightarrow \cup_{b,\alpha} r_{ba;\alpha}, \nu_a^+} B_{j_a \rightarrow \cup_{b,\alpha} l''_{ab;\alpha}}^{R_a \rightarrow \cup_{b,\alpha} r_{ab;\alpha}, \nu_a^-} \\
&\quad \times \left(\prod_{b,\alpha} D_{l_{ba;\alpha} l'_{ba;\alpha}}^{r_{ba;\alpha}}(\gamma_{ba;\alpha}) \right) \left(\prod_{b,\alpha} D_{l''_{ab;\alpha} l_{ab;\alpha}}^{r_{ab;\alpha}}(\gamma_{ab;\alpha}^{-1}) \right) \\
&= \prod_a D_{i_a j_a}^{R_a}(\sigma_a) B_{i_a \rightarrow \cup_{b,\alpha} l'_{ba;\alpha}}^{R_a \rightarrow \cup_{b,\alpha} r_{ba;\alpha}, \nu_a^+} B_{j_a \rightarrow \cup_{b,\alpha} l''_{ab;\alpha}}^{R_a \rightarrow \cup_{b,\alpha} r_{ab;\alpha}, \nu_a^-} \\
&\quad \prod_{a,b,\alpha} D_{l_{ab;\alpha} l'_{ab;\alpha}}^{r_{ab;\alpha}}(\gamma_{ab;\alpha}) D_{l''_{ab;\alpha} l_{ab;\alpha}}^{r_{ab;\alpha}}(\gamma_{ab;\alpha}^{-1}) \\
&= \prod_a D_{i_a j_a}^{R_a}(\sigma_a) B_{i_a \rightarrow \cup_{b,\alpha} l_{ba;\alpha}}^{R_a \rightarrow \cup_{b,\alpha} r_{ba;\alpha}, \nu_a^+} B_{j_a \rightarrow \cup_{b,\alpha} l_{ab;\alpha}}^{R_a \rightarrow \cup_{b,\alpha} r_{ab;\alpha}, \nu_a^-} \\
&= \chi_Q(\mathbf{L}, \boldsymbol{\sigma})
\end{aligned} \tag{D.7}$$

Proof of orthogonality in \mathbf{L} of $\chi_Q(\mathbf{L}, \boldsymbol{\sigma})$

Here we will prove (B.13), of which (B.11) is a special case. Expanding the definition

of $\chi_Q(\mathbf{L}, \boldsymbol{\sigma})$:

$$\begin{aligned} \sum_{\tilde{\boldsymbol{\sigma}}} \chi_Q(\mathbf{L}, \boldsymbol{\sigma} \tilde{\boldsymbol{\sigma}}) \chi_Q(\tilde{\mathbf{L}}, \tilde{\boldsymbol{\sigma}}) &= \sum_{\tilde{\boldsymbol{\sigma}}} \prod_a D_{i_a \tilde{j}_a}^{R_a}(\sigma_a \tilde{\sigma}_a) D_{\tilde{i}_a \tilde{j}_a}^{\tilde{R}_a}(\tilde{\sigma}_a) \\ &\times B_{i_a \rightarrow \bigcup_{b,\alpha} l_{ba;\alpha}}^{R_a \rightarrow \bigcup_{b,\alpha} r_{ba;\alpha}, \nu_a^+} B_{j_a \rightarrow \bigcup_{b,\alpha} l_{ab;\alpha}}^{R_a \rightarrow \bigcup_{b,\alpha} r_{ab;\alpha}, \nu_a^-} B_{\tilde{i}_a \rightarrow \bigcup_{b,\alpha} \tilde{l}_{ba;\alpha}}^{\tilde{R}_a \rightarrow \bigcup_{b,\alpha} \tilde{r}_{ba;\alpha}, \tilde{\nu}_a^+} B_{\tilde{j}_a \rightarrow \bigcup_{b,\alpha} \tilde{l}_{ab;\alpha}}^{\tilde{R}_a \rightarrow \bigcup_{b,\alpha} \tilde{r}_{ab;\alpha}, \tilde{\nu}_a^-} \end{aligned} \quad (\text{D.8})$$

We apply identity (A.5) to do the sum in each product term

$$\sum_{\tilde{\sigma}_a} D_{i_a \tilde{j}_a}^{R_a}(\sigma_a \tilde{\sigma}_a) D_{\tilde{i}_a \tilde{j}_a}^{\tilde{R}_a}(\tilde{\sigma}_a) = \frac{n_a!}{d(R_a)} \delta_{R_a \tilde{R}_a} D_{i_a \tilde{i}_a}^{R_a}(\sigma_a) \delta_{j_a \tilde{j}_a} \quad (\text{D.9})$$

Now contract a pair of branching coefficients with $\delta_{j_a \tilde{j}_a}$, applying (A.17)

$$B_{j_a \rightarrow \bigcup_{b,\alpha} l_{ab;\alpha}}^{R_a \rightarrow \bigcup_{b,\alpha} r_{ab;\alpha}, \nu_a^-} B_{j_a \rightarrow \bigcup_{b,\alpha} \tilde{l}_{ab;\alpha}}^{R_a \rightarrow \bigcup_{b,\alpha} \tilde{r}_{ab;\alpha}, \tilde{\nu}_a^-} = \delta_{\nu_a^- \tilde{\nu}_a^-} \prod_{b,\alpha} \delta_{r_{ab;\alpha} \tilde{r}_{ab;\alpha}} \delta_{l_{ab;\alpha} \tilde{l}_{ab;\alpha}} \quad (\text{D.10})$$

Since this appears in (D.8) under \prod_a , we effectively get a delta on all $\nu_a^-, r_{ab;\alpha}, l_{ab;\alpha}$. So the sum is

$$\sum_{\tilde{\boldsymbol{\sigma}}} \chi_Q(\mathbf{L}, \boldsymbol{\sigma} \tilde{\boldsymbol{\sigma}}) \chi_Q(\tilde{\mathbf{L}}, \tilde{\boldsymbol{\sigma}}) = \delta_{\mathbf{R} \tilde{\mathbf{R}}} \delta_{\mathbf{r} \tilde{\mathbf{r}}} \delta_{\boldsymbol{\nu}^- \tilde{\boldsymbol{\nu}}^-} \prod_a \frac{n_a!}{d(R_a)} D_{i_a \tilde{i}_a}^{R_a}(\sigma_a) B_{i_a \rightarrow \bigcup_{b,\alpha} l_{ba;\alpha}}^{R_a \rightarrow \bigcup_{b,\alpha} r_{ba;\alpha}, \nu_a^+} B_{\tilde{i}_a \rightarrow \bigcup_{b,\alpha} l_{ba;\alpha}}^{R_a \rightarrow \bigcup_{b,\alpha} r_{ba;\alpha}, \nu_a^+} \quad (\text{D.11})$$

which is (B.13).

Proof of orthogonality in $\boldsymbol{\sigma}$ conjugacy class of $\chi_Q(\mathbf{L}, \boldsymbol{\sigma})$

Here we show (B.12).

Consider the product of quiver characters $\chi_Q(\mathbf{L}, \boldsymbol{\sigma}) \chi_Q(\mathbf{L}, \boldsymbol{\tau})$:

$$\begin{aligned} \chi_Q(\mathbf{L}, \boldsymbol{\sigma}) \chi_Q(\mathbf{L}, \boldsymbol{\tau}) &= \prod_a D_{i_a \tilde{j}_a}^{R_a}(\sigma_a) B_{j_a \rightarrow \bigcup_{b,\alpha} l_{ab;\alpha}}^{R_a \rightarrow \bigcup_{b,\alpha} r_{ab;\alpha}, \nu_a^-} B_{i_a \rightarrow \bigcup_{b,\alpha} l_{ba;\alpha}}^{R_a \rightarrow \bigcup_{b,\alpha} r_{ba;\alpha}, \nu_a^+} D_{\tilde{j}_a \tilde{i}_a}^{R_a}(\tau_a^{-1}) B_{\tilde{j}_a \rightarrow \bigcup_{b,\alpha} \tilde{l}_{ab;\alpha}}^{\tilde{R}_a \rightarrow \bigcup_{b,\alpha} \tilde{r}_{ab;\alpha}, \tilde{\nu}_a^-} B_{\tilde{i}_a \rightarrow \bigcup_{b,\alpha} \tilde{l}_{ba;\alpha}}^{\tilde{R}_a \rightarrow \bigcup_{b,\alpha} \tilde{r}_{ba;\alpha}, \tilde{\nu}_a^+} \end{aligned} \quad (\text{D.12})$$

We flipped $D_{ij}^R(\tau) = D_{ji}^R(\tau^{-1})$ in the second character for later convenience. Each index $l_{ab;\alpha}$ appears once in a branching coefficient with ν^+ and once with ν^- , which are contracted together (and same for $\tilde{l}_{ab;\alpha}$). Next we “reconnect” the branching coefficients by inserting

$$\delta_{i_{ab;\alpha} j_{ab;\alpha}} \delta_{\tilde{i}_{ab;\alpha} \tilde{j}_{ab;\alpha}} = \frac{d(r_{ab;\alpha})}{n_{ab;\alpha}!} \sum_{\gamma_{ab;\alpha}} D_{i_{ab;\alpha} i_{ab;\alpha}}^{r_{ab;\alpha}}(\gamma_{ab;\alpha}) D_{j_{ab;\alpha} j_{ab;\alpha}}^{r_{ab;\alpha}}(\gamma_{ab;\alpha}^{-1}) \quad (\text{D.13})$$

for each $l_{ab;\alpha}, \tilde{l}_{ab;\alpha}$:

$$\begin{aligned}
& \chi_Q(\mathbf{L}, \boldsymbol{\sigma}) \chi_Q(\mathbf{L}, \boldsymbol{\tau}) \\
&= \prod_a D_{i_a j_a}^{R_a}(\sigma_a) B_{j_a \rightarrow \bigcup_{b,\alpha} j_{ab;\alpha}}^{R_a \rightarrow \bigcup_{b,\alpha} r_{ab;\alpha}, \nu_a^-} B_{i_a \rightarrow \bigcup_{b,\alpha} i_{ba;\alpha}}^{R_a \rightarrow \bigcup_{b,\alpha} r_{ba;\alpha}, \nu_a^+} D_{\tilde{j}_a \tilde{i}_a}^{R_a}(\tau_a^{-1}) B_{\tilde{j}_a \rightarrow \bigcup_{b,\alpha} \tilde{j}_{ab;\alpha}}^{R_a \rightarrow \bigcup_{b,\alpha} r_{ab;\alpha}, \nu_a^-} B_{\tilde{i}_a \rightarrow \bigcup_{b,\alpha} \tilde{i}_{ba;\alpha}}^{R_a \rightarrow \bigcup_{b,\alpha} r_{ba;\alpha}, \nu_a^+} \\
&\quad \times \left(\prod_{a,b,\alpha} \frac{d(r_{ab;\alpha})}{n_{ab;\alpha}!} \sum_{\gamma_{ab;\alpha}} D_{i_{ab;\alpha} i_{ab;\alpha}}^{r_{ab;\alpha}}(\gamma_{ab;\alpha}) D_{j_{ab;\alpha} \tilde{j}_{ab;\alpha}}^{r_{ab;\alpha}}(\gamma_{ab;\alpha}^{-1}) \right)
\end{aligned} \tag{D.14}$$

After this, $i_{ba;\alpha}, \tilde{i}_{ba;\alpha}$ appear in a matrix element of $\gamma_{ba;\alpha}$, hence they link, via branching coefficients, to σ_a, τ_a^{-1} . Likewise $j_{ba;\alpha}, \tilde{j}_{ba;\alpha}$ appear in a matrix element of $(\gamma_{ba;\alpha})^{-1}$ and, via branching coefficients, link σ_b, τ_b^{-1} . This reconnection step can be understood diagrammatically, for each $r_{ab;\alpha}$:

$$\begin{aligned}
& \begin{array}{c} \sigma_a \xrightarrow{R_a} \nu_a^- \xrightarrow{r_{ab;\alpha}} \nu_b^+ \xrightarrow{R_a} \sigma_b \\ \tau_a^{-1} \xleftarrow{R_a} \nu_a^- \xleftarrow{r_{ab;\alpha}} \nu_b^+ \xleftarrow{R_a} \tau_b^{-1} \end{array} = \frac{d(r_{ab;\alpha})}{n_{ab;\alpha}!} \sum_{\gamma} \begin{array}{c} \sigma_a \xrightarrow{R_a} \nu_a^- \xrightarrow{r_{ab;\alpha}} \boxed{\gamma^{-1}} \xrightarrow{r_{ab;\alpha}} \boxed{\gamma} \xrightarrow{r_{ab;\alpha}} \nu_b^+ \xrightarrow{R_a} \sigma_b \\ \tau_a^{-1} \xleftarrow{R_a} \nu_a^- \xleftarrow{r_{ab;\alpha}} \boxed{\gamma} \xleftarrow{r_{ab;\alpha}} \boxed{\gamma^{-1}} \xleftarrow{r_{ab;\alpha}} \nu_b^+ \xleftarrow{R_a} \tau_b^{-1} \end{array}
\end{aligned} \tag{D.15}$$

Performing reconnection for all legs, the group factors disconnect into pieces like

$$\begin{array}{c}
r_{b1a;\alpha} \curvearrowright \boxed{\gamma_{b1a;\alpha}} \curvearrowleft r_{b2a;\alpha} \\
\nu_a^+ \curvearrowleft \boxed{\gamma_{b2a;\alpha}} \curvearrowright \nu_a^+ \\
\sigma_a \xrightarrow{R_a} \nu_a^- \curvearrowleft \boxed{\gamma_{ab3;\alpha}^{-1}} \curvearrowright r_{ab3;\alpha} \\
\nu_a^- \curvearrowleft \boxed{\gamma_{ab4;\alpha}^{-1}} \curvearrowright r_{ab4;\alpha} \curvearrowright \tau_a^{-1} \xleftarrow{R_a} \nu_a^+
\end{array} \tag{D.16}$$

Here $r_{b1a;\alpha}, r_{b2a;\alpha}$ represent fields incoming to a , and $r_{ab3;\alpha}, r_{ab4;\alpha}$ represent fields outgoing from a . The full expression (D.14) is just a product of such factors over a .

We can move $D(\gamma)$ and $D(\gamma^{-1})$ through branching coefficients next to $D(\sigma)$

$$\begin{aligned}
& \chi_Q(\mathbf{L}, \boldsymbol{\sigma}) \chi_Q(\mathbf{L}, \boldsymbol{\tau}) \\
&= \frac{\prod d(r_{ab;\alpha})}{\prod n_{ab;\alpha}!} \sum_{\gamma} \prod_a D_{i_a j_a}^{R_a} ((\otimes_{b,\alpha} \gamma_{ba;\alpha}) \sigma_a (\otimes_{b,\alpha} \gamma_{ab;\alpha}^{-1})) D_{\tilde{j}_a \tilde{i}_a}^{R_a} (\tau_a^{-1}) \\
&\quad \times B_{j_a \rightarrow \bigcup_{b,\alpha} j_{ab;\alpha}}^{R_a \rightarrow \bigcup_{b,\alpha} r_{ab;\alpha}, \nu_a^-} B_{\tilde{j}_a \rightarrow \bigcup_{b,\alpha} j_{ab;\alpha}}^{R_a \rightarrow \bigcup_{b,\alpha} r_{ab;\alpha}, \nu_a^-} B_{\tilde{i}_a \rightarrow \bigcup_{b,\alpha} i_{ba;\alpha}}^{R_a \rightarrow \bigcup_{b,\alpha} r_{ba;\alpha}, \nu_a^+} B_{i_a \rightarrow \bigcup_{b,\alpha} i_{ba;\alpha}}^{R_a \rightarrow \bigcup_{b,\alpha} r_{ba;\alpha}, \nu_a^+}
\end{aligned} \tag{D.17}$$

Now the branching coefficients are contracted in a way to make projectors, which we can sum over, using (A.18)

$$\sum_{\{r_{ab,\alpha}\}, \nu_a^-} B_{j_a \rightarrow \bigcup_{b,\alpha} j_{ab;\alpha}}^{R_a \rightarrow \bigcup_{b,\alpha} r_{ab;\alpha}, \nu_a^-} B_{\tilde{j}_a \rightarrow \bigcup_{b,\alpha} j_{ab;\alpha}}^{R_a \rightarrow \bigcup_{b,\alpha} r_{ab;\alpha}, \nu_a^-} = \sum_{r_{ab,\alpha}, \nu_a^-} P_{j_a \tilde{j}_a}^{R_a \rightarrow \bigcup_{b,\alpha} r_{ab;\alpha}, \nu_a^-} = \delta_{j_a \tilde{j}_a} \tag{D.18}$$

Performing this for both pairs of branching coefficients we arrive at

$$\sum_{\mathbf{L}} \frac{\prod n_{ab;\alpha}!}{\prod d(r_{ab;\alpha})} \chi_Q(\mathbf{L}, \boldsymbol{\sigma}) \chi_Q(\mathbf{L}, \boldsymbol{\tau}) = \sum_{R_a} \sum_{\gamma} \prod_a \chi_{R_a} ((\otimes_{b,\alpha} \gamma_{ba;\alpha}) \sigma_a (\otimes_{b,\alpha} \gamma_{ab;\alpha}^{-1}) \tau_a^{-1}) \tag{D.19}$$

Finally, the sum over R_a can be done for each group factor using (A.3), if we include a factor $\frac{d(R_a)}{n_a!}$

$$\begin{aligned}
\sum_{\mathbf{L}} \frac{\prod n_{ab;\alpha}!}{\prod d(r_{ab;\alpha})} \frac{\prod d(R_a)}{\prod n_a!} \chi_Q(\mathbf{L}, \boldsymbol{\sigma}) \chi_Q(\mathbf{L}, \boldsymbol{\tau}) &= \sum_{\gamma} \prod_a \sum_{R_a} \frac{\prod d(R_a)}{\prod n_a!} \chi_{R_a} ((\otimes_{b,\alpha} \gamma_{ba;\alpha}) \sigma_a (\otimes_{b,\alpha} \gamma_{ab;\alpha}^{-1}) \tau_a^{-1}) \\
&= \sum_{\gamma} \prod_a \delta((\otimes_{b,\alpha} \gamma_{ba;\alpha}) \sigma_a (\otimes_{b,\alpha} \gamma_{ab;\alpha}^{-1}) \tau_a^{-1})
\end{aligned} \tag{D.20}$$

Thus we arrive at (B.12).

D.3 Derivation of two-point function

Here we show (3.54), the two-point function of operators $\mathcal{O}_Q(\mathbf{n}, \boldsymbol{\sigma})$ defined in (3.31), which is used to show the orthogonality of restricted basis in Section 3.3.

The conjugated operator is:

$$\begin{aligned}
\mathcal{O}_Q(\mathbf{n}, \boldsymbol{\sigma})^\dagger &= \prod_{a,b,\alpha} \left(\bar{\Phi}_{ab;\alpha}^{\otimes n_{ab;\alpha}} \right)_{\mathbf{J}_{ab;\alpha}}^{\mathbf{I}_{ab;\alpha}} \prod_a (\sigma_a)_{\bigcup_{b,\alpha} \mathbf{I}_{ab;\alpha}}^{\bigcup_{b,\alpha} \mathbf{J}_{ba;\alpha}} \\
&= \prod_{a,b,\alpha} \left(\Phi_{ab;\alpha}^{\dagger \otimes n_{ab;\alpha}} \right)_{\mathbf{I}_{ab;\alpha}}^{\mathbf{J}_{ab;\alpha}} \prod_a (\sigma_a^{-1})_{\bigcup_{b,\alpha} \mathbf{J}_{ba;\alpha}}^{\bigcup_{b,\alpha} \mathbf{I}_{ab;\alpha}}
\end{aligned} \tag{D.21}$$

In the first line, since \mathcal{O}_Q is a scalar, conjugation is simply a complex conjugation of the fields $\bar{\Phi}$. In the second line we convert it to Hermitian conjugate by transposing both $(\bar{\Phi})_j^i = (\Phi^\dagger)_i^j$ and $(\sigma)_j^i = (\sigma^{-1})_i^j$. The appearance of σ^{-1} indicates reversal of cyclic order, so that e.g. $\text{tr}(XYZ)^\dagger = \text{tr}(Z^\dagger Y^\dagger X^\dagger)$. The two point function for two fields is

$$\left\langle (\Phi_{ab;\alpha})_j^i (\Phi_{ab}^{\dagger\alpha})_l^k \right\rangle = \delta_l^i \delta_j^k \quad (\text{D.22})$$

The Wick contraction between $n_{ab;\alpha}$ fields generate

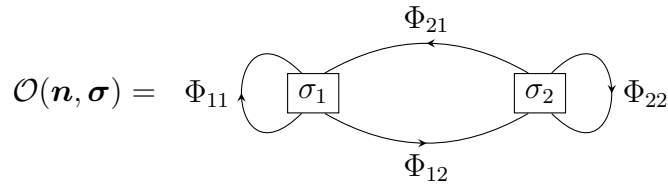
$$\left\langle \left(\Phi_{ab;\alpha}^{\otimes n_{ab;\alpha}} \right)_{J_{ab;\alpha}}^{I_{ab;\alpha}} \left(\Phi_{ab;\alpha}^{\dagger \otimes n_{ab;\alpha}} \right)_{\tilde{I}_{ab;\alpha}}^{\tilde{J}_{ab;\alpha}} \right\rangle = \sum_{\gamma \in S_{n_{ab;\alpha}}} \delta_{\tilde{I}_{ab;\alpha}}^{\gamma(I_{ab;\alpha})} \delta_{\gamma(J_{ab;\alpha})}^{\tilde{J}_{ab;\alpha}} = \sum_{\gamma \in S_{n_{ab;\alpha}}} (\gamma^{-1})_{\tilde{I}_{ab;\alpha}}^{I_{ab;\alpha}} (\gamma)_{J_{ab;\alpha}}^{\tilde{J}_{ab;\alpha}} \quad (\text{D.23})$$

So the two point function, combining (3.31), (D.21) and (D.23):

$$\begin{aligned} \langle \mathcal{O}_Q(\mathbf{n}, \sigma) \mathcal{O}_Q(\mathbf{n}, \tilde{\sigma})^\dagger \rangle &= \sum_{\gamma} \prod_{a,b,\alpha} (\gamma_{ab;\alpha}^{-1})_{\tilde{I}_{ab;\alpha}}^{I_{ab;\alpha}} (\gamma_{ab;\alpha})_{J_{ab;\alpha}}^{\tilde{J}_{ab;\alpha}} \prod_a (\sigma_a)_{\bigcup_{b,\alpha} I_{ab;\alpha}}^{\bigcup_{b,\alpha} J_{ba;\alpha}} (\tilde{\sigma}_a^{-1})_{\bigcup_{b,\alpha} \tilde{I}_{ba;\alpha}}^{\bigcup_{b,\alpha} \tilde{J}_{ba;\alpha}} \\ &= \sum_{\gamma} \prod_a \text{tr} (\sigma_a (\otimes_{b,\alpha} \gamma_{ab;\alpha}^{-1}) \tilde{\sigma}_a^{-1} (\otimes_{b,\alpha} \gamma_{ba;\alpha})) \\ &\equiv \sum_{\gamma} \prod_a \text{tr} (\text{Adj}_{\gamma}(\sigma_a) \tilde{\sigma}_a^{-1}) \end{aligned} \quad (\text{D.24})$$

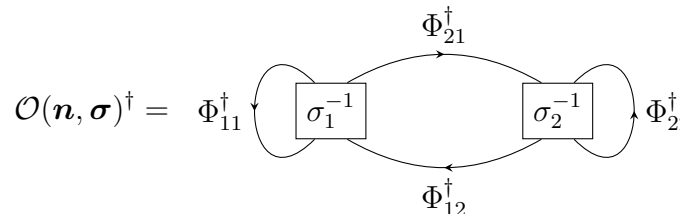
which gives (3.54).

This calculation can also be understood diagrammatically. As an example let us take a simplified $\mathbb{C}^3/\mathbb{Z}_2$ quiver, with only a single flavor of Φ_{12} and Φ_{21}



$$\mathcal{O}(\mathbf{n}, \sigma) = \quad \text{Diagram} \quad (\text{D.25})$$

Conjugate operator (D.21) is represented by



$$\mathcal{O}(\mathbf{n}, \sigma)^\dagger = \quad \text{Diagram} \quad (\text{D.26})$$

Our convention is that outgoing arrow corresponds to lower index, and incoming to upper index, so the reversed arrows indicate transposed indices in the second line of (D.21). The Wick contraction between blocks of conjugate fields (D.23) is, diagrammatically

$$\left\langle \left(\Phi_{ab;\alpha} \right)^{\otimes n} \left(\Phi_{ab}^{\dagger\alpha} \right)^{\otimes n} \right\rangle = \sum_{\gamma \in S_n} \begin{array}{c} \downarrow \\ \boxed{\gamma^{-1}} \\ \uparrow \end{array} \begin{array}{c} \downarrow \\ \boxed{\gamma} \\ \uparrow \end{array} \quad (D.27)$$

Applying this rule to the product of diagrams (D.25) and (D.26) we find

$$\langle \mathcal{O}(\mathbf{n}, \boldsymbol{\sigma}) \mathcal{O}(\mathbf{n}, \tilde{\boldsymbol{\sigma}})^\dagger \rangle = \sum_{\gamma} \begin{array}{c} \sigma_1 \\ \gamma_{21} \quad \gamma_{11} \quad \gamma_{11}^{-1} \quad \gamma_{12}^{-1} \\ \tilde{\sigma}_1^{-1} \end{array} \begin{array}{c} \sigma_2 \\ \gamma_{12} \quad \gamma_{22} \quad \gamma_{22}^{-1} \quad \gamma_{21}^{-1} \\ \tilde{\sigma}_2^{-1} \end{array} \quad (D.28)$$

It is easy to see that in general quivers will break up into separate factors for each group, with σ_a and $\tilde{\sigma}_a^{-1}$ connected by $\gamma_{ab;\alpha}^{-1}$ and $\gamma_{ba;\alpha}$. This reproduces (D.24).

D.4 Derivation of chiral ring structure constants

Here we explain the formulae corresponding to the diagrammatic derivation of (4.11) given in section 4.1.

We can write (4.8) as

$$\begin{aligned} G(\mathbf{L}^{(1)}, \mathbf{L}^{(2)}; \mathbf{L}^{(3)}) &= \tilde{f}_{\mathbf{L}^{(1)}\mathbf{L}^{(2)}}^{\mathbf{L}^{(3)}} \frac{1}{\prod_a n_a^{(1)}! n_a^{(2)}!} \sum_{\boldsymbol{\sigma}^{(1)}, \boldsymbol{\sigma}^{(2)}} \prod_a \left(\prod_{p=1}^3 B_{i_a^{(p)} \rightarrow \cup_{b,\alpha} r_{ba;\alpha}}^{R_a^{(p)}} \right) \left(\prod_{p=1}^3 B_{i_a^{(p)} \rightarrow \cup_{b,\alpha} l_{ab}^{(p)\alpha}}^{R_a^{(p)}} \right) \\ &\quad \times D_{i_a^{(1)} j_a^{(1)}}^{R_a^{(1)}}(\sigma_a^{(1)}) D_{i_a^{(2)} j_a^{(2)}}^{R_a^{(2)}}(\sigma_a^{(2)}) D_{i_a^{(3)} j_a^{(2)}}^{R_a^{(3)}}(\sigma_a^{(1)} \circ \sigma_a^{(2)}) \\ &= \tilde{f}_{\mathbf{L}^{(1)}\mathbf{L}^{(2)}}^{\mathbf{L}^{(3)}} \frac{1}{\prod_a n_a^{(1)}! n_a^{(2)}!} \sum_{\boldsymbol{\sigma}^{(1)}, \boldsymbol{\sigma}^{(2)}} \prod_a \left(\prod_{p=1}^3 B_{i_a^{(p)} \rightarrow \cup_{b,\alpha} r_{ba;\alpha}}^{R_a^{(p)}} \right) \left(\prod_{p=1}^3 B_{i_a^{(p)} \rightarrow \cup_{b,\alpha} l_{ab}^{(p)\alpha}}^{R_a^{(p)}} \right) \\ &\quad \times D_{i_a^{(1)} j_a^{(1)}}^{R_a^{(1)}}(\sigma_a^{(1)}) D_{i_a^{(2)} j_a^{(2)}}^{R_a^{(2)}}(\sigma_a^{(2)}) D_{j_a^{(3)} i_a^{(3)}}^{R_a^{(3)}}((\sigma_a^{(1)})^{-1} \circ (\sigma_a^{(2)})^{-1}) \end{aligned} \quad (D.29)$$

Next we do the sum over the $\sigma_a^{(1)}, \sigma_a^{(2)}$, expressing the answer in terms of branching coefficients as in (4.17).

$$\begin{aligned}
& \sum_{\sigma^{(1)} \in S_{n^{(1)}}} \sum_{\sigma^{(2)} \in S_{n^{(2)}}} D_{i_1 j_1}^{R^{(1)}}(\sigma^{(1)}) D_{i_2 j_2}^{R^{(2)}}(\sigma^{(2)}) D_{i_3 j_3}^{R^{(3)}}(\sigma^{(1)} \circ \sigma^{(2)}) \\
&= \sum_{\sigma^{(1)}, \sigma^{(2)}} \sum_{S^{(1)}, S^{(2)}} \sum_{\nu} D_{i_1 j_1}^{R^{(1)}}(\sigma^{(1)}) D_{i_2 j_2}^{R^{(2)}}(\sigma^{(2)}) B_{i_3 \rightarrow k_1, k_2}^{R^{(3)} \rightarrow S^{(1)}, S^{(2)}; \nu} D_{k_1 m_1}^{S^{(1)}}(\sigma^{(1)}) D_{k_2 m_2}^{S^{(2)}}(\sigma^{(2)}) B_{j_3 \rightarrow m_1, m_2}^{R^{(3)} \rightarrow S^{(1)}, S^{(2)}; \nu} \\
&= \sum_{S^{(1)}, S^{(2)}} \sum_{\nu} \frac{n^{(1)}!}{d(R^{(1)})} \frac{n^{(2)}!}{d(R^{(2)})} \delta_{R^{(1)}, S^{(1)}} \delta_{R^{(2)}, S^{(2)}} \delta_{i_1 k_1} \delta_{j_1 m_1} \delta_{i_2 k_2} \delta_{j_2 m_2} B_{i_3 \rightarrow k_1, k_2}^{R^{(3)} \rightarrow S^{(1)}, S^{(2)}; \nu} B_{j_3 \rightarrow m_1, m_2}^{R^{(3)} \rightarrow S^{(1)}, S^{(2)}; \nu} \\
&= \frac{n^{(1)}!}{d(R^{(1)})} \frac{n^{(2)}!}{d(R^{(2)})} \sum_{\nu} B_{i_3 \rightarrow i_1, i_2}^{R^{(3)} \rightarrow R^{(1)}, R^{(2)}; \nu} B_{j_3 \rightarrow j_1, j_2}^{R^{(3)} \rightarrow S^{(1)}, S^{(2)}; \nu}
\end{aligned} \tag{D.30}$$

Applying this at each node, gives two extra branching coefficients at each node of the quiver Q , leading to:

$$\begin{aligned}
G(\mathbf{L}^{(1)}, \mathbf{L}^{(2)}; \mathbf{L}^{(3)}) &= \frac{\tilde{f}_{\mathbf{L}^{(1)} \mathbf{L}^{(2)}}^{\mathbf{L}^{(3)}}}{\prod_a d(R_a^{(1)}) d(R_a^{(2)})} \sum_{\{\nu_a\}} \\
& \prod_a B_{i_a^{(1)} \rightarrow \cup_{b, \alpha} r_{ba; \alpha}^{(1)}; \nu_a^{(1)+}}^{R_a^{(1)} \rightarrow \cup_{b, \alpha} r_{ba; \alpha}^{(1)}; \nu_a^{(1)+}} B_{i_a^{(2)} \rightarrow \cup_{b, \alpha} r_{ba; \alpha}^{(2)}; \nu_a^{(2)+}}^{R_a^{(2)} \rightarrow \cup_{b, \alpha} r_{ba; \alpha}^{(2)}; \nu_a^{(2)+}} B_{i_a^{(3)} \rightarrow i_a^{(1)}, i_a^{(2)}}^{R_a^{(3)} \rightarrow R_a^{(1)}, R_a^{(2)}; \nu_a^+} B_{i_a^{(3)} \rightarrow \cup_{b, \alpha} l_{ba; \alpha}^{(3)}; \nu_a^{(3)+}}^{R_a^{(3)} \rightarrow \cup_{b, \alpha} l_{ba; \alpha}^{(3)}; \nu_a^{(3)+}} \\
& \times B_{j_a^{(3)} \rightarrow \cup_{b, \alpha} l_{ab; \alpha}^{(3)}; \nu_a^{(3)-}}^{R_a^{(3)} \rightarrow \cup_{b, \alpha} l_{ab; \alpha}^{(3)}; \nu_a^{(3)-}} B_{j_a^{(3)} \rightarrow j_a^{(1)}, j_a^{(2)}}^{R_a^{(3)} \rightarrow R_a^{(1)}, R_a^{(2)}; \nu_a^-} B_{j_a^{(1)} \rightarrow \cup_{b, \alpha} r_{ab; \alpha}^{(1)}; \nu_a^{(1)-}}^{R_a^{(1)} \rightarrow \cup_{b, \alpha} r_{ab; \alpha}^{(1)}; \nu_a^{(1)-}} B_{j_a^{(2)} \rightarrow \cup_{b, \alpha} r_{ab; \alpha}^{(2)}; \nu_a^{(2)-}}^{R_a^{(2)} \rightarrow \cup_{b, \alpha} r_{ab; \alpha}^{(2)}; \nu_a^{(2)-}} \\
&= \frac{\tilde{f}_{\mathbf{L}^{(1)} \mathbf{L}^{(2)}}^{\mathbf{L}^{(3)}}}{\prod_a d(R_a^{(1)}) d(R_a^{(2)})} \sum_{\{\nu_a\}} \prod_a B_{i_a^{(3)} \rightarrow i_a^{(1)}, i_a^{(2)}}^{R_a^{(3)} \rightarrow R_a^{(1)}, R_a^{(2)}; \nu_a^+} B_{j_a^{(3)} \rightarrow j_a^{(1)}, j_a^{(2)}}^{R_a^{(3)} \rightarrow R_a^{(1)}, R_a^{(2)}; \nu_a^-} \\
& \left(\prod_{p=1}^3 B_{i_a^{(p)} \rightarrow \cup_{b, \alpha} r_{ba; \alpha}^{(p)\alpha}; \nu_a^{(p)+}}^{R_a^{(p)} \rightarrow \cup_{b, \alpha} r_{ba; \alpha}^{(p)\alpha}; \nu_a^{(p)+}} \right) \left(\prod_{p=1}^3 B_{j_a^{(p)} \rightarrow \cup_{b, \alpha} l_{ab; \alpha}^{(p)\alpha}}^{R_a^{(p)} \rightarrow \cup_{b, \alpha} l_{ab; \alpha}^{(p)\alpha}; \nu_a^{(p)-}} \right)
\end{aligned} \tag{D.31}$$

The label ν_a is summed over the Littlewood-Richardson multiplicity $g(R_a^{(1)}, R_a^{(2)}; R_a^{(3)})$ for the reduction of the irrep $R_a^{(3)}$ of $S_{n_a^{(3)}}$ to irrep $R^{(1)} \otimes R_a^{(2)}$ of $S_{n_a^{(1)}} \times S_{n_a^{(2)}}$. By Schur-Weyl duality, this is also the multiplicity of the $U(N_a)$ representation $R_a^{(3)}$ in the tensor product of $R_a^{(1)} \otimes R_a^{(2)}$.

The next step is to exploit the invariance, under the action of $\times_{a, b, \alpha} S_{n_{ab; \alpha}^{(1)}} \times S_{n_{ab; \alpha}^{(2)}}$, of the branching coefficients in (D.31) labeled by $\nu_a^{(1)-}, \nu_a^{(2)-}, \nu_a^{(3)-}$ (we could equally well have

chosen to work with the $\nu_a^{(1)+}, \nu_a^{(2)+}, \nu_a^{(3)+}$ as indicated in (4.19).

$$\begin{aligned}
G(\mathbf{L}^{(1)}, \mathbf{L}^{(2)}; \mathbf{L}^{(3)}) &= \tilde{f}_{\mathbf{L}^{(1)}\mathbf{L}^{(2)}}^{\mathbf{L}^{(3)}} \frac{1}{\prod_a d(R_a^{(1)})d(R_a^{(2)})} \frac{1}{\prod_{a,b,\alpha} n_{ab;\alpha}^{(1)}! n_{ab;\alpha}^{(2)}!} \sum_{\{\nu_a\}} \sum_{\gamma_{ab;\alpha}^{(1)}, \gamma_{ab;\alpha}^{(2)}} \\
&\prod_a B_{i_a^{(3)} \rightarrow i_a^{(1)}, i_a^{(2)}}^{R_a^{(3)} \rightarrow R_a^{(1)}, R_a^{(2)}; \nu_a^+} B_{j_a^{(3)} \rightarrow j_a^{(1)}, j_a^{(2)}}^{R_a^{(3)} \rightarrow R_a^{(1)}, R_a^{(2)}; \nu_a^-} \left(\prod_{p=1}^3 B_{i_a^{(p)} \rightarrow \cup_{b,\alpha} r_{ba}^{(p)\alpha}}^{R_a^{(p)} \rightarrow \cup_{b,\alpha} r_{ba}^{(p)\alpha}; \nu_a^{(p)+}} \right) \\
&\left(\prod_{a,b,\alpha} D_{k_{ab;\alpha}^{(1)} l_{ab;\alpha}^{(1)}}^{r_{ab}^{(1)\alpha}} (\gamma_{ab}^{(1)\alpha}) D_{k_{ab;\alpha}^{(2)} l_{ab;\alpha}^{(2)}}^{r_{ab}^{(2)\alpha}} (\gamma_{ab}^{(2)\alpha}) D_{k_{ab;\alpha}^{(3)} l_{ab;\alpha}^{(3)}}^{r_{ab}^{(3)\alpha}} ((\gamma_{ab}^{(1)\alpha})^{-1} \circ (\gamma_{ab}^{(2)\alpha})^{-1}) \prod_{p=1}^3 B_{j_a^{(3)} \rightarrow \cup_{b,\alpha} k_{ab}^{(p)\alpha}}^{R_a^{(p)} \rightarrow \cup_{b,\alpha} r_{ba}^{(p)\alpha}; \nu_a^{(3)-}} \right)
\end{aligned} \tag{D.32}$$

Now we do the sum over the permutations $\{\gamma_{ab;\alpha}^{(1)}, \gamma_{ab;\alpha}^{(2)}\}$ which introduces branching coefficients for $r_{ab;\alpha}^{(3)} \rightarrow r_{ab;\alpha}^{(1)} \otimes r_{ab;\alpha}^{(2)}$

$$\begin{aligned}
G(\mathbf{L}^{(1)}, \mathbf{L}^{(2)}; \mathbf{L}^{(3)}) &= \tilde{f}_{\mathbf{L}^{(1)}\mathbf{L}^{(2)}}^{\mathbf{L}^{(3)}} \frac{1}{\prod_a d(R_a^{(1)})d(R_a^{(2)})} \frac{1}{\prod_{a,b,\alpha} d(r_{ab;\alpha}^{(1)})d(r_{ab;\alpha}^{(2)})} \\
&\sum_{\{\nu_a, \nu_{ab;\alpha}\}} \prod_a \left(B_{i_a^{(3)} \rightarrow i_a^{(1)}, i_a^{(2)}}^{R_a^{(3)} \rightarrow R_a^{(1)}, R_a^{(2)}; \nu_a^+} B_{j_a^{(3)} \rightarrow j_a^{(1)}, j_a^{(2)}}^{R_a^{(3)} \rightarrow R_a^{(1)}, R_a^{(2)}; \nu_a^-} \right) \\
&\prod_a \left(\prod_{p=1}^3 B_{i_a^{(p)} \rightarrow \cup_{b,\alpha} r_{ba}^{(p)\alpha}}^{R_a^{(p)} \rightarrow \cup_{b,\alpha} r_{ba}^{(p)\alpha}; \nu_a^{(p)+}} \right) \left(\prod_{p=1}^3 B_{j_a^{(p)} \rightarrow \cup_{b,\alpha} k_{ab}^{(p)\alpha}}^{R_a^{(p)} \rightarrow \cup_{b,\alpha} r_{ba}^{(p)\alpha}; \nu_a^{(p)-}} \right) \\
&\prod_{a,b,\alpha} B_{l_{ab;\alpha}^{(3)} \rightarrow l_{ab;\alpha}^{(1)}, l_{ab;\alpha}^{(2)}}^{r_{ab;\alpha}^{(3)} \rightarrow r_{ab;\alpha}^{(1)}, r_{ab;\alpha}^{(2)}; \nu_{ab;\alpha}} B_{k_{ab;\alpha}^{(3)} \rightarrow k_{ab;\alpha}^{(1)}, k_{ab;\alpha}^{(2)}}^{r_{ab;\alpha}^{(3)} \rightarrow r_{ab;\alpha}^{(1)}, r_{ab;\alpha}^{(2)}; \nu_{ab;\alpha}}
\end{aligned} \tag{D.33}$$

We now see that there is a factorization between state indices for Young diagrams associated branching coefficients carrying ν^- indices and those for Young diagrams associated branching coefficients carrying ν^+ indices, which corresponds to the factorized form in the diagram (4.9)

$$\begin{aligned}
G(\mathbf{L}^{(1)}, \mathbf{L}^{(2)}; \mathbf{L}^{(3)}) &= \tilde{f}_{\mathbf{L}^{(1)}\mathbf{L}^{(2)}}^{\mathbf{L}^{(3)}} \frac{1}{\prod_a d(R_a^{(1)})d(R_a^{(2)})} \frac{1}{\prod_{a,b,\alpha} d(r_{ab;\alpha}^{(1)})d(r_{ab;\alpha}^{(2)})} \\
&\sum_{\{\nu_a, \nu_{ab;\alpha}\}} \prod_a \left(B_{i_a^{(3)} \rightarrow i_a^{(1)}, i_a^{(2)}}^{R_a^{(3)} \rightarrow R_a^{(1)}, R_a^{(2)}; \nu_a^+} \prod_{p=1}^3 B_{i_a^{(p)} \rightarrow \cup_{b,\alpha} r_{ba}^{(p)\alpha}}^{R_a^{(p)} \rightarrow \cup_{b,\alpha} r_{ba}^{(p)\alpha}; \nu_a^{(p)+}} \prod_{b,\alpha} B_{l_{ab;\alpha}^{(3)} \rightarrow l_{ab;\alpha}^{(1)}, l_{ab;\alpha}^{(2)}}^{r_{ab;\alpha}^{(3)} \rightarrow r_{ab;\alpha}^{(1)}, r_{ab;\alpha}^{(2)}; \nu_{ab;\alpha}} \right) \\
&\prod_a \left(B_{j_a^{(3)} \rightarrow j_a^{(1)}, j_a^{(2)}}^{R_a^{(3)} \rightarrow R_a^{(1)}, R_a^{(2)}; \nu_a^-} \prod_{p=1}^3 B_{j_a^{(p)} \rightarrow \cup_{b,\alpha} k_{ab}^{(p)\alpha}}^{R_a^{(p)} \rightarrow \cup_{b,\alpha} r_{ba}^{(p)\alpha}; \nu_a^{(p)-}} \prod_{b,\alpha} B_{k_{ab;\alpha}^{(3)} \rightarrow k_{ab;\alpha}^{(1)}, k_{ab;\alpha}^{(2)}}^{r_{ab;\alpha}^{(3)} \rightarrow r_{ab;\alpha}^{(1)}, r_{ab;\alpha}^{(2)}; \nu_{ab;\alpha}} \right)
\end{aligned} \tag{D.34}$$

This is the factorized result, where we have a factor for each gauge group, and for each gauge group there is a factorization separating the ν^+ branching coefficients from the ν^-

branching coefficients. The close connection between the final formula and the diagrammatic moves means that we can interpret the process of constructing the final answer diagrammatically. Start with the original quiver and modify it to produce the split-node version with R_a lines joining the plus and minus nodes. Now cut this split-node quiver along all the edges, thus separating it into a collection of nodes labelled ν_a^+, ν_a^- . The ν_a^+ nodes have a collection of directed lines carrying labels $R_a, r_{ba;\alpha}$. The ν_a^- nodes have outgoing directed lines labeled $R_a, r_{ab;\alpha}$. Doing this cutting procedure for the three labelled quivers, to produce nodes $(\nu_a^{(I)+}, \nu_a^{(I)-})$ (for $I = 1, 2, 3$) with dangling lines labeled $R_a^{(I)}, r_{ba}^{(I)\alpha}$. Link up the nodes $\nu_a^{(I)+}$ using new nodes μ_a^+ for $(R_a^{(1)}, R_a^{(2)}) \rightarrow R_a^{(3)}$, and new nodes $\mu_{ab;\alpha}$ for the $r_{ba;\alpha}^{(1)}, r_{ba;\alpha}^{(2)} \rightarrow r_{ba;\alpha}^{(3)}$. This gives a graph for each gauge group labelled a , with nodes labelled by $\{\cup_I \nu_a^{(I)+}, \mu_a, \mu_{ab;\alpha}\}$. Repeating the same procedure for the minus nodes gives another set of graphs for each gauge group, with nodes labeled $\{\cup_I \nu_a^{(I)-}, \mu_a, \mu_{ba;\alpha}\}$. So the result for the chiral ring structure constants can be obtained by cutting and gluing of the split-node quivers labeled $\mathbf{L}_1, \mathbf{L}_2, \mathbf{L}_3$. This is an illustration of the power of quivers as calculators.

D.5 Finite N chiral ring with superpotential, using explicit operators

Here we confirm the expected dimension from (6.24) using the explicit description of operators in V_N, V_F . The space V_N (6.7) is spanned by the operators, where any R_a is taller than N . For our choice of charges there are three such operators (using the restricted Schur basis):

$$\begin{aligned}
V_N &= \{O_1, O_2, O_3\} \\
O_1 &\equiv \mathcal{O}(R_1 = [1^{N+1}], R_2 = [1^{N+1}]; \mathbf{r}) \\
O_2 &\equiv \mathcal{O}(R_1 = [1^{N+1}], R_2 = [2, 1^{N-1}]; \mathbf{r}) \\
O_3 &\equiv \mathcal{O}(R_1 = [2, 1^{N-1}], R_2 = [1^{N+1}]; \mathbf{r})
\end{aligned} \tag{D.35}$$

with $r_{A_1} = [1], r_{B_1} = [1], r_{A_2} = [1^N], r_{B_2} = [1^N]$ for all three.

A convenient way to characterize V_F is as the kernel

$$V_F = \text{Ker}(\mathcal{P}) \tag{D.36}$$

where \mathcal{P} is the *symmetrization operator* acting on $V^{(\infty)}$ as a linear operator. For example

$$\mathcal{P} \text{tr}(A_1 B_1 A_2 B_2) = \frac{1}{2} \text{tr}(A_1 B_1 A_2 B_2) + \frac{1}{2} \text{tr}(A_1 B_2 A_1 B_2) \tag{D.37}$$

Then V_F is the subspace of $V^{(\infty)}$ annihilated by \mathcal{P} . In order to find $V_F \cap V_N$ we need the operators annihilated by \mathcal{P} in V_N

$$V_F \cap V_N = \text{Ker}(\mathcal{P}_{V_N}) \quad (\text{D.38})$$

The action of \mathcal{P} is easily written in the product-of-traces or the permutation basis $\mathcal{O}(\sigma)$, but we have V_N in terms of the $\mathcal{O}(\mathbf{L})$ basis. In order to calculate \mathcal{P} acting on $\mathcal{O}_1, \mathcal{O}_2, \mathcal{O}_3$ we need to expand them in terms of $\mathcal{O}(\sigma)$ using the definitions (3.48). The first operator is easy, since all representations are one-dimensional and branching coefficients are trivial:

$$\mathcal{O}_1 = \frac{1}{(N+1)!^2} \sum_{\sigma_1, \sigma_2 \in S_{N+1}} (-1)^{\sigma_1 + \sigma_2} \mathcal{O}(\sigma_1, \sigma_2) \quad (\text{D.39})$$

For \mathcal{O}_2 and \mathcal{O}_3 we need the branching coefficient $B_i^{[2, 1^{N-1}] \rightarrow [1], [1^N]}$. The representation $([1], [1^N])$ of the subgroup $S_1 \times S_N$ is one-dimensional, so we do not include a label for it. Representation $[2, 1^{N-1}]$ is N -dimensional, for which we use the Young-Yamanouchi (YY) basis. The YY-basis is labelled by Young tableaux, i.e. Young diagrams with integers $\{1, \dots, N+1\}$ in the boxes. We use the convention where the numbers are decreasing along rows and down columns. For example, $[2, 1^3]$ is spanned by:

$$\left\{ \begin{array}{|c|c|} \hline 5 & 1 \\ \hline 4 & 2 \\ \hline 3 & 3 \\ \hline 2 & 4 \\ \hline \end{array}, \begin{array}{|c|c|} \hline 5 & 2 \\ \hline 4 & 3 \\ \hline 3 & 2 \\ \hline 2 & 1 \\ \hline \end{array}, \begin{array}{|c|c|} \hline 5 & 3 \\ \hline 4 & 2 \\ \hline 3 & 1 \\ \hline 2 & 4 \\ \hline \end{array}, \begin{array}{|c|c|} \hline 5 & 4 \\ \hline 4 & 3 \\ \hline 3 & 2 \\ \hline 2 & 1 \\ \hline \end{array} \right\} \quad (\text{D.40})$$

The YY-basis is particularly convenient for our purpose, because it is constructed using the decomposition $S_{N+1} \rightarrow S_1 \times S_N$. The state in $[2, 1^{N-1}]$ which transforms according to $([1], [1^N])$ of $S_1 \times S_N$ is precisely the one which has the label 1 in the second column. Thus the branching coefficient we need is simply⁴

$$B_i^{[2, 1^{N-1}] \rightarrow [1], [1^N]} = \delta(i = \begin{array}{|c|} \hline 1 \\ \hline \end{array}) \quad (\text{D.41})$$

The operator is thus

$$\begin{aligned} \mathcal{O}_2 &= \frac{\sqrt{N}}{(N+1)!^2} \sum_{\substack{\sigma_1 \in S_{N+1} \\ \sigma_2 \in S_{N+1}}} (-1)^{\sigma_1} \left\langle \begin{array}{|c|} \hline 1 \\ \hline \end{array} \middle| \sigma_2 \begin{array}{|c|} \hline 1 \\ \hline \end{array} \right\rangle \mathcal{O}(\sigma_1, \sigma_2) \\ &= \frac{\sqrt{N}}{(N+1)!^2} \sum_{\substack{\sigma_1 \in S_{N+1} \\ \sigma_2 \in S_N}} (-1)^{\sigma_1} \left(\left\langle \begin{array}{|c|} \hline 1 \\ \hline \end{array} \middle| \sigma_2 \begin{array}{|c|} \hline 1 \\ \hline \end{array} \right\rangle \mathcal{O}(\sigma_1, \sigma_2) + \sum_{k=2}^{N+1} \left\langle \begin{array}{|c|} \hline 1 \\ \hline \end{array} \middle| \sigma_2(1k) \begin{array}{|c|} \hline 1 \\ \hline \end{array} \right\rangle \mathcal{O}(\sigma_1, \sigma_2(1k)) \right) \end{aligned} \quad (\text{D.42})$$

⁴Here the diagram denotes the first column of any height, with numbers from 2 to $N+1$.

We have split the sum over $\sigma_2 \in S_{N+1}$ into a part where $\sigma_2 \in S_1 \times S_N$, and the rest, where first element gets permuted. The corresponding matrix elements are:

$$\left\langle \begin{array}{|c|} \hline \boxed{1} \\ \hline \end{array} \middle| \sigma_2 \begin{array}{|c|} \hline \boxed{1} \\ \hline \end{array} \right\rangle = (-1)^{\sigma_2}, \quad \left\langle \begin{array}{|c|} \hline \boxed{1} \\ \hline \end{array} \middle| \sigma_2(1k) \begin{array}{|c|} \hline \boxed{1} \\ \hline \end{array} \right\rangle = \frac{(-1)^{\sigma_2}}{N}, \quad (\sigma_2 \in S_1 \times S_N) \quad (\text{D.43})$$

Substituting this in (D.42):

$$\begin{aligned} \mathcal{O}_2 &= \frac{\sqrt{N}}{(N+1)!^2} \sum_{\substack{\sigma_1 \in S_{N+1} \\ \sigma_2 \in S_N}} (-1)^{\sigma_1} (-1)^{\sigma_2} \left(\mathcal{O}(\sigma_1, \sigma_2) + \frac{1}{N} \sum_{k=2}^{N+1} \mathcal{O}(\sigma_1, \sigma_2(1k)) \right) \\ &= \frac{N! \sqrt{N}}{(N+1)!^2} \sum_{\sigma \in S_{N+1}} (-1)^\sigma (\mathcal{O}(\sigma, \mathbb{I}) + \mathcal{O}(\sigma, (12))) \end{aligned} \quad (\text{D.44})$$

In the second line we performed the σ_2 sum by using invariance (3.36) to set $\mathcal{O}(\sigma_1, \sigma_2) = \mathcal{O}(\sigma_1 \sigma_2^{-1}, \mathbb{I})$ and redefining $\sigma = \sigma_1 \sigma_2^{-1}$. This is possible because σ_2 does not run over the full S_{N+1} , but only the subgroup (3.37). Also using invariance we find $\mathcal{O}(\sigma, (1k)) = \mathcal{O}((2k)\sigma(2k), (12))$, which allows to remove k dependence.

Analogously the final operator in V_N is

$$\mathcal{O}_3 = \frac{N! \sqrt{N}}{(N+1)!^2} \sum_{\sigma \in S_{N+1}} (-1)^\sigma (\mathcal{O}(\mathbb{I}, \sigma) + \mathcal{O}((12), \sigma)) \quad (\text{D.45})$$

Now, the question is, how many linear combinations of $\mathcal{O}_1, \mathcal{O}_2, \mathcal{O}_3$ are annihilated by \mathcal{P} . This will give $V_N \cap V_F$. First, observe that \mathcal{O}_1 is unchanged by the symmetrization

$$\mathcal{P} \mathcal{O}_1 = \mathcal{O}_1 \quad (\text{D.46})$$

because any permutation of A 's or B 's is already included in the sum

$$\begin{aligned} \sum_{\sigma_1, \sigma_2 \in S_{N+1}} (-1)^{\sigma_1 + \sigma_2} \mathcal{O}(\sigma_1, \sigma_2) &= \sum_{\sigma_1, \sigma_2 \in S_{N+1}} (-1)^{\sigma_1 + \sigma_2} \mathcal{O}(\sigma_1 \gamma, \gamma^{-1} \sigma_2) \\ &= \sum_{\sigma_1, \sigma_2 \in S_{N+1}} (-1)^{\sigma_1 + \sigma_2} \mathcal{O}(\gamma \sigma_1, \sigma_2 \gamma^{-1}) \end{aligned} \quad (\text{D.47})$$

so all permutations within a trace are already present. Note in (D.47) we do not use (3.36), because $\gamma \notin S_1 \times S_N$, instead we absorb γ in the sums σ_1, σ_2 . The same relationship is not obeyed by $\mathcal{O}_2, \mathcal{O}_3$, because of non-trivial σ_1, σ_2 dependence.

Now, let us deal with $\mathcal{O}_2, \mathcal{O}_3$. It is useful to separate (D.44), (D.45)

$$\begin{aligned} \mathcal{O}_2^{\mathbb{I}} &= \sum_{\sigma \in S_{N+1}} (-1)^\sigma \mathcal{O}(\sigma, \mathbb{I}), \quad \mathcal{O}_2^{(12)} = \sum_{\sigma \in S_{N+1}} (-1)^\sigma \mathcal{O}(\sigma, (12)) \\ \mathcal{O}_3^{\mathbb{I}} &= \sum_{\sigma \in S_{N+1}} (-1)^\sigma \mathcal{O}(\mathbb{I}, \sigma), \quad \mathcal{O}_3^{(12)} = \sum_{\sigma \in S_{N+1}} (-1)^\sigma \mathcal{O}((12), \sigma) \end{aligned} \quad (\text{D.48})$$

so that

$$\mathcal{O}_2 \sim \mathcal{O}_2^{\mathbb{I}} + \mathcal{O}_2^{(12)}, \quad \mathcal{O}_3 \sim \mathcal{O}_3^{\mathbb{I}} + \mathcal{O}_3^{(12)} \quad (\text{D.49})$$

We can evaluate (D.48) explicitly

$$\begin{aligned} \mathcal{O}_2^{\mathbb{I}} &= \sum_{\sigma \in S_{N+1}} (-1)^\sigma \text{tr}(\sigma(B_1 A_1) \otimes (B_2 A_2)^{\otimes N}) \\ \mathcal{O}_3^{\mathbb{I}} &= \sum_{\sigma \in S_{N+1}} (-1)^\sigma \text{tr}(\sigma(A_1 B_1) \otimes (A_2 B_2)^{\otimes N}) \\ \mathcal{O}_2^{(12)} &= - \sum_{\sigma \in S_{N+1}} (-1)^\sigma \text{tr}(\sigma(B_2 A_1) \otimes (B_1 A_2) \otimes (B_2 A_2)^{\otimes N-1}) \\ \mathcal{O}_3^{(12)} &= - \sum_{\sigma \in S_{N+1}} (-1)^\sigma \text{tr}(\sigma(A_1 B_2) \otimes (A_2 B_1) \otimes (A_2 B_2)^{\otimes N-1}) \end{aligned} \quad (\text{D.50})$$

These are “determinant-like” operators made from composites $A_i B_j$. It is easy to see that

$$\mathcal{P} \mathcal{O}_2^{\mathbb{I}} = \mathcal{P} \mathcal{O}_3^{\mathbb{I}}, \quad \mathcal{P} \mathcal{O}_2^{(12)} = \mathcal{P} \mathcal{O}_3^{(12)} \quad (\text{D.51})$$

because $\mathcal{O}_2^{\mathbb{I}}, \mathcal{O}_3^{\mathbb{I}}$ and $\mathcal{O}_2^{(12)}, \mathcal{O}_3^{(12)}$ only differ by the ordering inside the trace. This leads to

$$\mathcal{P} \mathcal{O}_2 = \mathcal{P} \mathcal{O}_3 \quad (\text{D.52})$$

Also we can check that $\mathcal{P} \mathcal{O}_2 \neq \mathcal{P} \mathcal{O}_1$ by using an example, so these are in fact two linearly independent operators spanning image of \mathcal{P} .

This leads, finally, to the single operator in the kernel

$$V_N \cap V_F = \{\mathcal{O}_2 - \mathcal{O}_3\} \quad (\text{D.53})$$

which is annihilated by \mathcal{P} . Thus we have derived the size of the interacting chiral ring (6.21) from first principles, in agreement with N -boson counting (6.17).

References

- [1] J. M. Maldacena, “The Large N limit of superconformal field theories and supergravity,” *Adv.Theor.Math.Phys.* **2** (1998) 231–252, [arXiv:hep-th/9711200](#) [hep-th] .
- [2] S. Gubser, I. R. Klebanov, and A. M. Polyakov, “Gauge theory correlators from noncritical string theory,” *Phys.Lett.* **B428** (1998) 105–114, [arXiv:hep-th/9802109](#) [hep-th] .

- [3] E. Witten, “Anti-de Sitter space and holography,” *Adv.Theor.Math.Phys.* **2** (1998) 253–291, [arXiv:hep-th/9802150](#) [hep-th] .
- [4] M. R. Douglas and G. W. Moore, “D-branes, quivers, and ALE instantons,” [arXiv:hep-th/9603167](#) [hep-th] .
- [5] J. Pasukonis and S. Ramgoolam, “From counting to construction of BPS states in N=4 SYM,” *JHEP* **1102** (2011) 078, [arXiv:1010.1683](#) [hep-th] .
- [6] R. de Mello Koch and S. Ramgoolam, “A double coset ansatz for integrability in AdS/CFT,” *JHEP* **1206** (2012) 083, [arXiv:1204.2153](#) [hep-th] .
- [7] J. McGreevy, L. Susskind, and N. Toumbas, “Invasion of the giant gravitons from Anti-de Sitter space,” *JHEP* **0006** (2000) 008, [arXiv:hep-th/0003075](#) [hep-th] .
- [8] V. Balasubramanian, M. Berkooz, A. Naqvi, and M. J. Strassler, “Giant gravitons in conformal field theory,” *JHEP* **0204** (2002) 034, [arXiv:hep-th/0107119](#) [hep-th] .
- [9] S. Corley, A. Jevicki, and S. Ramgoolam, “Exact correlators of giant gravitons from dual N=4 SYM theory,” *Adv.Theor.Math.Phys.* **5** (2002) 809–839, [arXiv:hep-th/0111222](#) [hep-th] .
- [10] H. Lin, O. Lunin, and J. M. Maldacena, “Bubbling AdS space and 1/2 BPS geometries,” *JHEP* **0410** (2004) 025, [arXiv:hep-th/0409174](#) [hep-th] .
- [11] E. D’Hoker and D. Z. Freedman, “Supersymmetric gauge theories and the AdS / CFT correspondence,” [arXiv:hep-th/0201253](#) [hep-th] .
- [12] W. Fulton and J. Harris, *Representation theory: a first course*. Springer, 1991.
- [13] A. Bissi, C. Kristjansen, D. Young, and K. Zoubos, “Holographic three-point functions of giant gravitons,” *JHEP* **1106** (2011) 085, [arXiv:1103.4079](#) [hep-th] .
- [14] P. Caputa, R. d. M. Koch, and K. Zoubos, “Extremal versus Non-Extremal Correlators with Giant Gravitons,” *JHEP* **1208** (2012) 143, [arXiv:1204.4172](#) [hep-th] .
- [15] H. Lin, “Giant gravitons and correlators,” *JHEP* **1212** (2012) 011, [arXiv:1209.6624](#) [hep-th] .

- [16] D. Berenstein, “Shape and holography: Studies of dual operators to giant gravitons,” *Nucl.Phys.* **B675** (2003) 179–204, [arXiv:hep-th/0306090 \[hep-th\]](#) ;
D. Sadri and M. Sheikh-Jabbari, “Giant hedgehogs: Spikes on giant gravitons,” *Nucl.Phys.* **B687** (2004) 161–185, [arXiv:hep-th/0312155 \[hep-th\]](#) ;
D. Berenstein, D. H. Correa, and S. E. Vazquez, “Quantizing open spin chains with variable length: An Example from giant gravitons,” *Phys.Rev.Lett.* **95** (2005) 191601, [arXiv:hep-th/0502172 \[hep-th\]](#) ;
D. Berenstein, D. H. Correa, and S. E. Vazquez, “A Study of open strings ending on giant gravitons, spin chains and integrability,” *JHEP* **0609** (2006) 065, [arXiv:hep-th/0604123 \[hep-th\]](#) ;
V. Balasubramanian, D. Berenstein, B. Feng, and M.-x. Huang, “D-branes in Yang-Mills theory and emergent gauge symmetry,” *JHEP* **0503** (2005) 006, [arXiv:hep-th/0411205 \[hep-th\]](#) ;
R. de Mello Koch, J. Smolic, and M. Smolic, “Giant Gravitons - with Strings Attached (I),” *JHEP* **0706** (2007) 074, [arXiv:hep-th/0701066 \[hep-th\]](#) ;
R. de Mello Koch, J. Smolic, and M. Smolic, “Giant Gravitons - with Strings Attached (II),” *JHEP* **0709** (2007) 049, [arXiv:hep-th/0701067 \[hep-th\]](#) ;
D. Bekker, R. de Mello Koch, and M. Stephanou, “Giant Gravitons - with Strings Attached. III,” *JHEP* **0802** (2008) 029, [arXiv:0710.5372 \[hep-th\]](#) .
- [17] J. Kinney, J. M. Maldacena, S. Minwalla, and S. Raju, “An Index for 4 dimensional super conformal theories,” *Commun.Math.Phys.* **275** (2007) 209–254, [arXiv:hep-th/0510251 \[hep-th\]](#) .
- [18] I. Biswas, D. Gaiotto, S. Lahiri, and S. Minwalla, “Supersymmetric states of N=4 Yang-Mills from giant gravitons,” *JHEP* **0712** (2007) 006, [arXiv:hep-th/0606087 \[hep-th\]](#) .
- [19] M. Bianchi, F. Dolan, P. Heslop, and H. Osborn, “N=4 superconformal characters and partition functions,” *Nucl.Phys.* **B767** (2007) 163–226, [arXiv:hep-th/0609179 \[hep-th\]](#) .
- [20] T. W. Brown, P. Heslop, and S. Ramgoolam, “Diagonal multi-matrix correlators and BPS operators in N=4 SYM,” *JHEP* **0802** (2008) 030, [arXiv:0711.0176 \[hep-th\]](#) .
- [21] T. W. Brown, P. Heslop, and S. Ramgoolam, “Diagonal free field matrix correlators, global symmetries and giant gravitons,” *JHEP* **0904** (2009) 089, [arXiv:0806.1911 \[hep-th\]](#) .

- [22] Y. Kimura and S. Ramgoolam, “Branes, anti-branes and brauer algebras in gauge-gravity duality,” *JHEP* **0711** (2007) 078, [arXiv:0709.2158 \[hep-th\]](#) .
- [23] R. Bhattacharyya, S. Collins, and R. d. M. Koch, “Exact Multi-Matrix Correlators,” *JHEP* **0803** (2008) 044, [arXiv:0801.2061 \[hep-th\]](#) .
- [24] N. Beisert, “The complete one loop dilatation operator of N=4 superYang-Mills theory,” *Nucl.Phys.* **B676** (2004) 3–42, [arXiv:hep-th/0307015 \[hep-th\]](#) .
- [25] A. V. Ryzhov, “Quarter BPS operators in N=4 SYM,” *JHEP* **0111** (2001) 046, [arXiv:hep-th/0109064 \[hep-th\]](#) .
- [26] E. D’Hoker, P. Heslop, P. Howe, and A. Ryzhov, “Systematics of quarter BPS operators in N=4 SYM,” *JHEP* **0304** (2003) 038, [arXiv:hep-th/0301104 \[hep-th\]](#) .
- [27] Y. Kimura, S. Ramgoolam, and D. Turton, “Free particles from Brauer algebras in complex matrix models,” *JHEP* **1005** (2010) 052, [arXiv:0911.4408 \[hep-th\]](#) ; Y. Kimura, “Non-holomorphic multi-matrix gauge invariant operators based on Brauer algebra,” *JHEP* **0912** (2009) 044, [arXiv:0910.2170 \[hep-th\]](#) .
- [28] Y. Kimura and S. Ramgoolam, “Enhanced symmetries of gauge theory and resolving the spectrum of local operators,” *Phys.Rev.* **D78** (2008) 126003, [arXiv:0807.3696 \[hep-th\]](#) .
- [29] Y. Kimura, “Quarter BPS classified by Brauer algebra,” *JHEP* **1005** (2010) 103, [arXiv:1002.2424 \[hep-th\]](#) ; Y. Kimura, “Correlation functions and representation bases in free N=4 Super Yang-Mills,” *Nucl.Phys.* **B865** (2012) 568–594, [arXiv:1206.4844 \[hep-th\]](#) .
- [30] Y. Kimura and H. Lin, “Young diagrams, Brauer algebras, and bubbling geometries,” *JHEP* **1201** (2012) 121, [arXiv:1109.2585 \[hep-th\]](#) .
- [31] N. Beisert, M. Bianchi, J. F. Morales, and H. Samtleben, “Higher spin symmetry and N=4 SYM,” *JHEP* **0407** (2004) 058, [arXiv:hep-th/0405057 \[hep-th\]](#) .
- [32] D. J. Gross and W. Taylor, “Two-dimensional QCD is a string theory,” *Nucl.Phys.* **B400** (1993) 181–210, [arXiv:hep-th/9301068 \[hep-th\]](#) .
- [33] T. Brown, “Complex matrix model duality,” *Phys.Rev.* **D83** (2011) 085002, [arXiv:1009.0674 \[hep-th\]](#) .

- [34] R. d. M. Koch and S. Ramgoolam, “From Matrix Models and Quantum Fields to Hurwitz Space and the absolute Galois Group,” [arXiv:1002.1634 \[hep-th\]](#) .
- [35] R. Gopakumar, “What is the Simplest Gauge-String Duality?,” [arXiv:1104.2386 \[hep-th\]](#) .
- [36] S. Kachru and E. Silverstein, “4-D conformal theories and strings on orbifolds,” *Phys.Rev.Lett.* **80** (1998) 4855–4858, [arXiv:hep-th/9802183 \[hep-th\]](#) .
- [37] S. Franco, A. Hanany, D. Martelli, J. Sparks, D. Vegh, *et al.*, “Gauge theories from toric geometry and brane tilings,” *JHEP* **0601** (2006) 128, [arXiv:hep-th/0505211 \[hep-th\]](#) ; S. Benvenuti, S. Franco, A. Hanany, D. Martelli, and J. Sparks, “An Infinite family of superconformal quiver gauge theories with Sasaki-Einstein duals,” *JHEP* **0506** (2005) 064, [arXiv:hep-th/0411264 \[hep-th\]](#) .
- [38] I. R. Klebanov and E. Witten, “Superconformal field theory on three-branes at a Calabi-Yau singularity,” *Nucl.Phys.* **B536** (1998) 199–218, [arXiv:hep-th/9807080 \[hep-th\]](#) .
- [39] O. Aharony, O. Bergman, D. L. Jafferis, and J. Maldacena, “N=6 superconformal Chern-Simons-matter theories, M2-branes and their gravity duals,” *JHEP* **0810** (2008) 091, [arXiv:0806.1218 \[hep-th\]](#) .
- [40] T. K. Dey, “Exact Large R -charge Correlators in ABJM Theory,” *JHEP* **1108** (2011) 066, [arXiv:1105.0218 \[hep-th\]](#) ; R. de Mello Koch, B. A. E. Mohammed, J. Murugan, and A. Prinsloo, “Beyond the Planar Limit in ABJM,” *JHEP* **1205** (2012) 037, [arXiv:1202.4925 \[hep-th\]](#) ; B. A. E. Mohammed, “Nonplanar Integrability and Parity in ABJ Theory,” [arXiv:1207.6948 \[hep-th\]](#) ; P. Caputa and B. A. E. Mohammed, “From Schurs to Giants in ABJ(M),” [arXiv:1210.7705 \[hep-th\]](#) ; A. Bissi, C. Kristjansen, A. Martirosyan, and M. Orselli, “On Three-point Functions in the AdS_4/CFT_3 Correspondence,” [arXiv:1211.1359 \[hep-th\]](#) .
- [41] F. Cachazo, M. R. Douglas, N. Seiberg, and E. Witten, “Chiral rings and anomalies in supersymmetric gauge theory,” *JHEP* **0212** (2002) 071, [arXiv:hep-th/0211170 \[hep-th\]](#) .
- [42] R. Dijkgraaf and C. Vafa, “A Perturbative window into nonperturbative physics,” [arXiv:hep-th/0208048 \[hep-th\]](#) .

- [43] B. Sundborg, “The Hagedorn transition, deconfinement and N=4 SYM theory,” *Nucl.Phys.* **B573** (2000) 349–363, [arXiv:hep-th/9908001](#) [hep-th] .
- [44] O. Aharony, J. Marsano, S. Minwalla, K. Papadodimas, and M. Van Raamsdonk, “The Hagedorn - deconfinement phase transition in weakly coupled large N gauge theories,” *Adv.Theor.Math.Phys.* **8** (2004) 603–696, [arXiv:hep-th/0310285](#) [hep-th] .
- [45] D. Gaiotto, L. Rastelli, and S. S. Razamat, “Bootstrapping the superconformal index with surface defects,” [arXiv:1207.3577](#) [hep-th] .
- [46] H.-C. Kim, S.-S. Kim, and K. Lee, “5-dim Superconformal Index with Enhanced En Global Symmetry,” *JHEP* **1210** (2012) 142, [arXiv:1206.6781](#) [hep-th] .
- [47] S. Collins, “Restricted Schur Polynomials and Finite N Counting,” *Phys.Rev.* **D79** (2009) 026002, [arXiv:0810.4217](#) [hep-th] .
- [48] F. Dolan, “Counting BPS operators in N=4 SYM,” *Nucl.Phys.* **B790** (2008) 432–464, [arXiv:0704.1038](#) [hep-th] .
- [49] M. R. Douglas, B. R. Greene, and D. R. Morrison, “Orbifold resolution by D-branes,” *Nucl.Phys.* **B506** (1997) 84–106, [arXiv:hep-th/9704151](#) [hep-th] .
- [50] R. Bhattacharyya, R. de Mello Koch, and M. Stephanou, “Exact Multi-Restricted Schur Polynomial Correlators,” *JHEP* **0806** (2008) 101, [arXiv:0805.3025](#) [hep-th] .
- [51] R. Dijkgraaf and E. Witten, “Topological Gauge Theories and Group Cohomology,” *Commun.Math.Phys.* **129** (1990) 393 .
- [52] A. D’Adda and P. Provero, “Two-dimensional gauge theories of the symmetric group S(n) in the large n limit,” *Commun.Math.Phys.* **245** (2004) 1–25, [arXiv:hep-th/0110243](#) [hep-th] .
- [53] S. Cordes, G. W. Moore, and S. Ramgoolam, “Lectures on 2-d Yang-Mills theory, equivariant cohomology and topological field theories,” *Nucl.Phys.Proc.Suppl.* **41** (1995) 184–244, [arXiv:hep-th/9411210](#) [hep-th] .
- [54] M. Fukuma, S. Hosono, and H. Kawai, “Lattice topological field theory in two-dimensions,” *Commun.Math.Phys.* **161** (1994) 157–176, [arXiv:hep-th/9212154](#) [hep-th] .

- [55] E. Witten, “On quantum gauge theories in two-dimensions,”
Commun.Math.Phys. **141** (1991) 153–209 .
- [56] R. de Mello Koch and S. Ramgoolam, “Strings from Feynman Graph counting :
without large N,” *Phys.Rev.* **D85** (2012) 026007, [arXiv:1110.4858 \[hep-th\]](#) .
- [57] V. Turaev, “Homotopy field theory in dimension two and group algebras,”
[arXiv:math/9910010 \[math-qa\]](#) .
- [58] G. W. Moore and G. Segal, “D-branes and K-theory in 2D topological field
theory,” [arXiv:hep-th/0609042 \[hep-th\]](#) .
- [59] P. Cameron, *Combinatorics: topics, techniques, algorithms*. Cambridge University
Press, 1994.
- [60] S. Cordes, G. W. Moore, and S. Ramgoolam, “Large N 2-D Yang-Mills theory and
topological string theory,” *Commun.Math.Phys.* **185** (1997) 543–619,
[arXiv:hep-th/9402107 \[hep-th\]](#) .
- [61] S. Ramgoolam, “Wilson loops in 2-D Yang-Mills: Euler characters and loop
equations,” *Int.J.Mod.Phys.* **A11** (1996) 3885–3933,
[arXiv:hep-th/9412110 \[hep-th\]](#) .
- [62] A. Recknagel, “Permutation branes,” *JHEP* **0304** (2003) 041,
[arXiv:hep-th/0208119 \[hep-th\]](#) .
- [63] M. Atiyah, “Topological quantum field theories,” *Inst.Hautes Etudes
Sci.Publ.Math.* **68** (1989) 175–186 .
- [64] T. Barmeier and C. Schweigert, “A Geometric Construction for Permutation
Equivariant Categories from Modular Functors,” *ArXiv e-prints* (Apr., 2010) ,
[arXiv:1004.1825 \[math.QA\]](#).
- [65] A. Davydov, L. Kong, and I. Runkel, “Field theories with defects and the centre
functor,” [arXiv:1107.0495 \[math.QA\]](#) .
- [66] A. Mironov, A. Morozov, and S. Natanzon, “A Hurwitz theory avatar of
open-closed strings,” [arXiv:1208.5057 \[hep-th\]](#) .
- [67] R. Dijkgraaf, E. P. Verlinde, and H. L. Verlinde, “Matrix string theory,”
Nucl.Phys. **B500** (1997) 43–61, [arXiv:hep-th/9703030 \[hep-th\]](#) .

- [68] M. A. Luty and W. Taylor, “Varieties of vacua in classical supersymmetric gauge theories,” *Phys.Rev.* **D53** (1996) 3399–3405, [arXiv:hep-th/9506098](#) [[hep-th](#)] .
- [69] A. Hanany and K. D. Kennaway, “Dimer models and toric diagrams,” [arXiv:hep-th/0503149](#) [[hep-th](#)] .
- [70] S. Franco, A. Hanany, K. D. Kennaway, D. Vegh, and B. Wecht, “Brane dimers and quiver gauge theories,” *JHEP* **0601** (2006) 096, [arXiv:hep-th/0504110](#) [[hep-th](#)] .
- [71] A. Butti, D. Forcella, A. Hanany, D. Vegh, and A. Zaffaroni, “Counting Chiral Operators in Quiver Gauge Theories,” *JHEP* **0711** (2007) 092, [arXiv:0705.2771](#) [[hep-th](#)] .
- [72] S. Benvenuti, B. Feng, A. Hanany, and Y.-H. He, “Counting BPS Operators in Gauge Theories: Quivers, Syzygies and Plethystics,” *JHEP* **0711** (2007) 050, [arXiv:hep-th/0608050](#) [[hep-th](#)] .
- [73] C. E. Beasley, “BPS branes from baryons,” *JHEP* **0211** (2002) 015, [arXiv:hep-th/0207125](#) [[hep-th](#)] .
- [74] A. Butti, D. Forcella, and A. Zaffaroni, “Counting BPS baryonic operators in CFTs with Sasaki-Einstein duals,” *JHEP* **0706** (2007) 069, [arXiv:hep-th/0611229](#) [[hep-th](#)] .
- [75] D. Forcella, A. Hanany, and A. Zaffaroni, “Baryonic Generating Functions,” *JHEP* **0712** (2007) 022, [arXiv:hep-th/0701236](#) [[HEP-TH](#)] .
- [76] A. Butti, D. Forcella, A. Hanany, D. Vegh, and A. Zaffaroni, “Counting Chiral Operators in Quiver Gauge Theories,” *JHEP* **0711** (2007) 092, [arXiv:0705.2771](#) [[hep-th](#)] .
- [77] D. Giovannoni, J. Murugan, and A. Prinsloo, “The Giant graviton on $AdS_4 \times CP^3$ - another step towards the emergence of geometry,” *JHEP* **1112** (2011) 003, [arXiv:1108.3084](#) [[hep-th](#)] ; A. Hamilton, J. Murugan, and A. Prinsloo, “Lessons from giant gravitons on $AdS_5 \times T^{1,1}$,” *JHEP* **1006** (2010) 017, [arXiv:1001.2306](#) [[hep-th](#)] ; A. Hamilton, J. Murugan, A. Prinsloo, and M. Strydom, “A Note on dual giant gravitons in $AdS(4) \times CP^{*3}$,” *JHEP* **0904** (2009) 132, [arXiv:0901.0009](#) [[hep-th](#)] .

- [78] A. Mikhailov, “Giant gravitons from holomorphic surfaces,” *JHEP* **0011** (2000) 027, [arXiv:hep-th/0010206](#) [hep-th] .
- [79] Y. Chen and N. Mekareeya, “The Hilbert series of U/SU SQCD and Toeplitz Determinants,” *Nucl.Phys.* **B850** (2011) 553–593, [arXiv:1104.2045](#) [hep-th] .
- [80] A. Hanany and N. Mekareeya, “Counting Gauge Invariant Operators in SQCD with Classical Gauge Groups,” *JHEP* **0810** (2008) 012, [arXiv:0805.3728](#) [hep-th] .
- [81] J. Gray, A. Hanany, Y.-H. He, V. Jejjala, and N. Mekareeya, “SQCD: A Geometric Apercu,” *JHEP* **0805** (2008) 099, [arXiv:0803.4257](#) [hep-th] .
- [82] N. Jokela, M. Jarvinen, and E. Keski-Vakkuri, “New results for the SQCD Hilbert series,” *JHEP* **1203** (2012) 048, [arXiv:1112.5454](#) [hep-th] .
- [83] M. J. Strassler, “The Duality cascade,” [arXiv:hep-th/0505153](#) [hep-th] .
- [84] F. Cachazo, N. Seiberg, and E. Witten, “Chiral rings and phases of supersymmetric gauge theories,” *JHEP* **0304** (2003) 018, [arXiv:hep-th/0303207](#) [hep-th] .
- [85] N. Arkani-Hamed, A. G. Cohen, and H. Georgi, “(De)constructing dimensions,” *Phys.Rev.Lett.* **86** (2001) 4757–4761, [arXiv:hep-th/0104005](#) [hep-th] .
- [86] D. Gaiotto, “N=2 dualities,” *JHEP* **1208** (2012) 034, [arXiv:0904.2715](#) [hep-th] .
- [87] O. Aharony, Y. E. Antebi, M. Berkooz, and R. Fishman, “‘Holey sheets’: Pfaffians and subdeterminants as D-brane operators in large N gauge theories,” *JHEP* **0212** (2002) 069, [arXiv:hep-th/0211152](#) [hep-th] .
- [88] P. Caputa, R. d. M. Koch, and P. Diaz, “A basis for large operators in N=4 SYM with orthogonal gauge group,” [arXiv:1301.1560](#) [hep-th] .
- [89] E. Witten, “Solutions of four-dimensional field theories via M theory,” *Nucl.Phys.* **B500** (1997) 3–42, [arXiv:hep-th/9703166](#) [hep-th] .
- [90] M. Aganagic, A. Klemm, M. Marino, and C. Vafa, “The Topological vertex,” *Commun.Math.Phys.* **254** (2005) 425–478, [arXiv:hep-th/0305132](#) [hep-th] .
- [91] I. Bena, M. Berkooz, J. de Boer, S. El-Showk, and D. Van den Bleeken, “Scaling BPS Solutions and pure-Higgs States,” *JHEP* **1211** (2012) 171, [arXiv:1205.5023](#) [hep-th] .

- [92] K. Papadodimas, “Topological Anti-Topological Fusion in Four-Dimensional Superconformal Field Theories,” *JHEP* **1008** (2010) 118, [arXiv:0910.4963 \[hep-th\]](#) .
- [93] M. Hamermesh, *Group theory and its application to physical problems*. Dover publications, 1989.